Increased Order in Single Molecule Magnets

Zane Farrow

Chemistry – Institute of Fundamental Sciences

Massey University

Masters Thesis under the supervision of Associate Professor Gareth J. Rowlands.

2018

Abstract

Single Molecule Magnets (SMMs) show promise in advancing computer technology and our understanding of quantum behaviours, however we first have to understand how to successfully synthesize ligand systems that allow them to perform at viable temperatures. As such, my project explored the synthesis of new ligand systems for potential SMMs based on [2.2]paracyclophane and pyrazine. These structures were chosen to be a synthetic backbone for the synthesis of new ligands for potential SMMs formation due to their structural and electronic properties. Attempts were undertaken to form complexes with these ligands and grow crystals suitable for X-ray crystallography.

In this project three new ligand systems were synthesized and characterized, one with a [2.2]paracyclophane backbone (**L_1**) and two containing a pyrazine bridging group (**L_2** and **L_3**). Complexations with a variety of metals were undertaken with all three ligands, unfortunately crystals of sufficient quality for single crystal X-ray diffraction experiments were not obtained. In total 8 new compounds were synthesized and a novel route for the synthesis of 4-(benzylamino)[2.2]PC was developed during this project.

Acknowledgements

I would like to thank my family and friends for supporting me through this project, my colleagues for support, assistance and wonderful baking, and in particular my supervisor Associate Professor Gareth J. Rowlands for his knowledge, patience, and support. I would also like to acknowledge Associate Professor Paul Plieger, Tyson Dais, and Sidney Woodhouse for their screening of crystals.

Table of Contents

Abbreviations

[2.2]PC	[2.2]Paracyclophane
AC	Alternating Current
Ac	Acetyl
BINAP	2,2’-Bis(diphenylphosphino)-1,1’-binapthyl
Bn	Benzyl
dba	Dibenzylideneacetone
DC	Direct Current
DCM	Dichloromethane
DMF	Dimethylformamide
DMSO	Dimethyl sulfoxide
EDTA	Ethylenediaminetetraacetic acid
Et	Ethyl
H	External magnetic field
K	Kelvin
m-CPBA	*meta*-Chloroperoxybenzoic acid
Me	Methyl
NBS	*N*-Bromosuccinimide
NMR	Nuclear Magnetic Resonance
Ph	Phenyl
QTM	Quantum Tunnelling of Magnetism
RT	Room Temperature
S	Spin state
sao	Salicylaldoxime
SMM	Single Molecule Magnets
T	Tesla
T_B	Blocking temperature

THF	Tetrahydrofuran
TLC	Thin Layer Chromatography
Ts	4-toluenesulfonyl
U_{eff}	Thermal barrier
X_m”	Out-of-phase component

1. Introduction

1.1 Single Molecule Magnets

Magnetism is a physical phenomena that allows for certain substances to be attracted to or repelled from each other. The most common examples of magnetism in everyday life come from ferromagnetic materials, which are strongly attracted to magnetic fields and themselves can be made into permanent magnets. This magnetism is due to Weiss domains, which are three-dimensional regions within the material that have the spins of the many atoms/molecules aligned. Altering these magnetic domains has an energy cost, which results in the magnetism being retained in the material long after the field that applied the magnetism has been removed.[1] This period of the magnetism is known as magnetic hysteresis.

Single molecule magnets (SMMs) differ from traditional magnets because each individual molecule has its own domain. While there are no domain walls, each molecule is magnetically isolated and does not interact with its neighbours. This allows them to have magnetic hysteresis and therefore retention of magnetism, meaning they have potential applications in many fields. Currently the highest temperature that a SMM has been shown to exhibit magnetic hysteresis is 60 K (-213 °C), with the majority of SMMs only exhibiting hysteresis below 15 K.[2-4] For SMMs to be useful they would have to be able to exhibit hysteresis at temperatures at that of liquid nitrogen or higher (>77 K or -196 °C), therefore allowing them to be used in fields such as exploring quantum phenomena and increasing magnetic based storage density.[2,5-6]

The first SMM discovered was a $[Mn_{12}O_{12}(OAc)_{16}(H_2O)_4]$ complex in 1993, commonly referred to as Mn_{12}, with an effective temperature of around 4 K.[7] Since this discovery many researchers have been working on developing new and better SMMs that encompass different metals, ligand groups, and metal ratios.[1-3] The first SMMs were made with transition metals, such as Mn, Fe, and Ni, however lanthanides are also used in making SMMs and in general have higher effective temperatures, such as a dysprosium SMM with a hysteresis temperature of 21 K or the recently developed dysprosocenium SMM (dysprosium sandwiched between two aromatic rings) with hysteresis present at 60 K (Figure 1).[2,4] Part of the reason for

lanthanides forming more effective SMMs is that the interaction with the magnetic fields and their outer electrons causes a splitting of orbits, resulting in multiplets that are well separated in energy, allowing for a high spin state to be achieved.

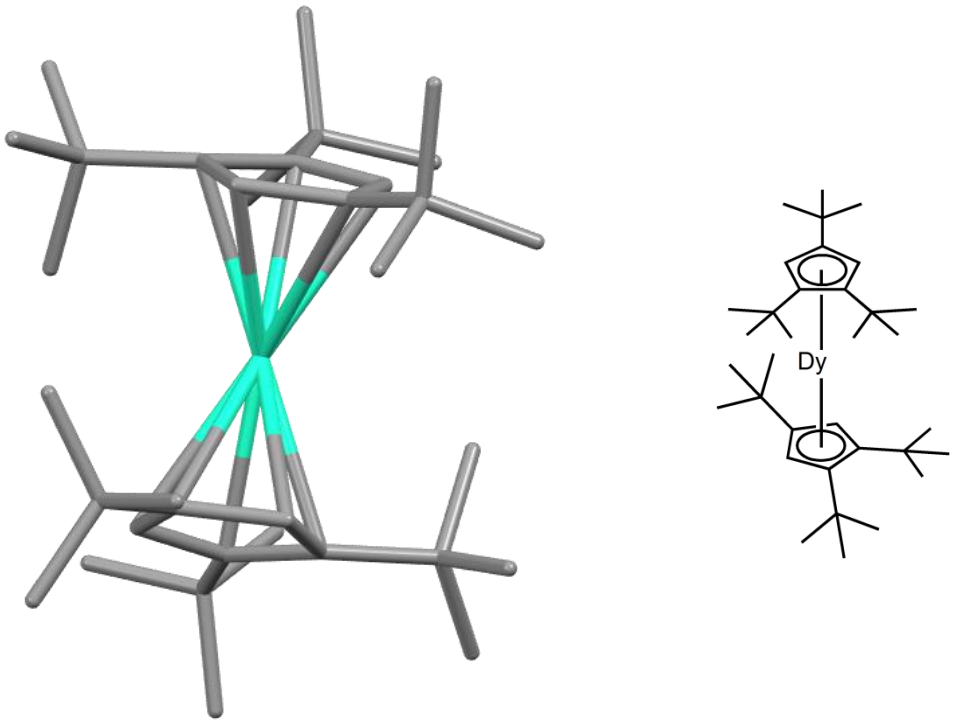

Figure 1. Left: X-ray crystal image of the dysprosocenium SMM. Right: Structure of the Dy SMM. Dy = cyan, C = grey. Hydrogens omitted for clarity.

For a complex to exhibit SMM behaviour, there are a number of requirements that must be met. The most important of these requirements is that the complex must have a spin state, *S*, that is non-zero.[1] The value of *S* is determined by the number of unpaired electrons in the metal orbitals. A molecule will have a spin state of zero if all the orbitals are full, causing it to be diamagnetic. Having ferromagnetically coupled ions in a molecule, such as the Mn^{IV} ions in the Mn_{12} complex, increases the spin state of the molecule. Another important requirement is that the molecules must be isolated from each other in the solid state, otherwise traditional bulk magnetic behaviour may occur. This isolation is generally achieved by having bulky organic groups on the periphery of the complex, such as *tert*-butyl groups. An example of such a molecule is the dysprosocenium molecule shown in Figure 1. However, there are other ways of isolating the molecules, such as in the Mn_{12} complex where the Mn^{IV} cluster was effectively isolated by the Mn^{III} ions around them as well as their bridging acetate ligands that face outwards. Figure 2 shows a schematic view of the

Mn_{12} metal cluster. Both of these requirements mean that careful molecule design is necessary to develop effective SMMs that may have hysteresis at temperatures high enough for them to have practical applications.

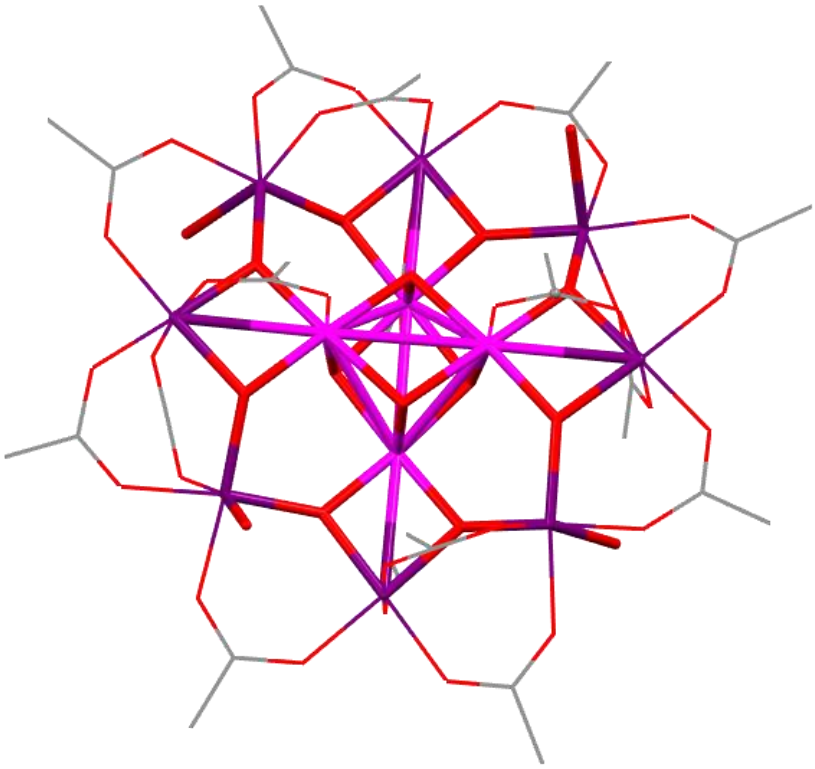

Figure 2. X-ray crystal structure of the Mn_{12} complex. The 4 interior Mn ions in the cubic shape are Mn^{IV} ions while the exterior Mn ions are Mn^{III}.[7] Mn^{IV} = magenta, Mn^{III} = purple, O = red, C = grey. Hydrogens omitted and ligands made thinner for clarity.

Being able to measure magnetic hysteresis is important, as this property determines if a molecule is a SMM. To measure hysteresis, the molecule is subjected to an external magnetic field (*H*), which is increased to a high value (+*H*), typically around 7 T, in an attempt to fully saturate the magnetism of the molecule. The external magnetic field is then cycled from +*H* to –*H* at a range of low temperatures, and the results plotted to determine if a hysteresis loop is present. If there is a hysteresis loop, such as that shown in Figure 3, then the complex has an energy barrier to magnetic reversal (within the scan rate used). The temperature at which the hysteresis loop opens is known as the blocking temperature (T_B), however due to the dependence on the scan rate for the value of T_B it can be difficult to compare the T_B values for different SMMs. In Figure 3 you can see that the hysteresis loop opens at 14 K under a scan rate of 0.9 mT s^{-1} for a $\{[(Me_3Si)_2N](THF)Tb\}_2$ complex.[3] However, it is not uncommon for a complex's magnetism to not become fully

saturated, particularly in complexes that have anisotropic ions. If this occurs then magnetic hysteresis cannot be used to determine if the complex is a SMM. In these cases other evidence is required to prove the existence of a SMM.

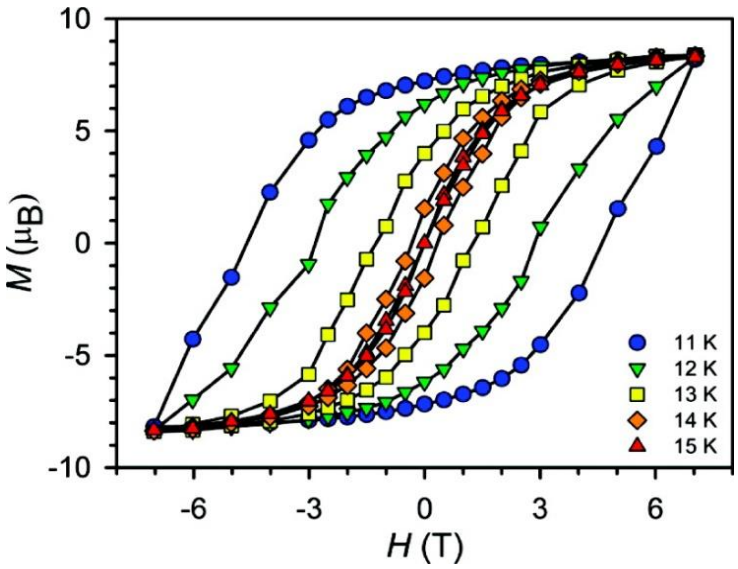

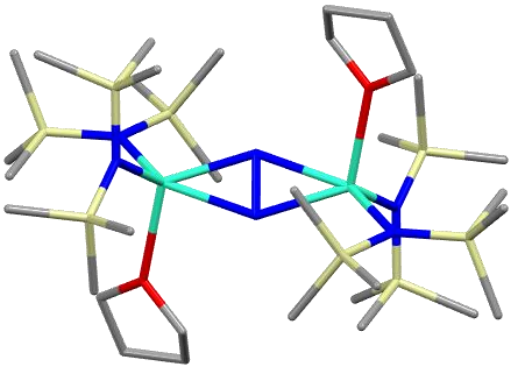

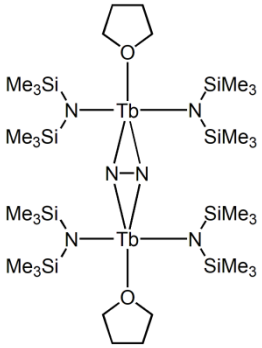

Figure 3. Top: Hysteresis loop measurements of the $\{[(Me_3Si)_2N]_2(THF)Tb_2\}(\mu\text{-}\eta^2\text{:}\eta^2\text{-}N_2)^-$ complex showing the hysteresis loop opening at 14 K (obtained from J. Am. Chem. Soc., **2011**, 133, 14236-14239). Bottom Left: X-ray crystal image of the $\{[(Me_3Si)_2N]_2(THF)Tb_2\}(\mu\text{-}\eta^2\text{:}\eta^2\text{-}N_2)^-$ complex. Bottom Right: Structure of Tb_2 complex. Tb = cyan, N = blue, O = red, Si = cream, C = grey. Hydrogens omitted for clarity.

A second method to determine if the complex is a SMM is to see if it has a magnetic susceptibility to an alternating current (AC) field. If there is a delay between the change of the magnetic field and the magnetic direction of the complex, known as an out-of-phase component (χ_m"), then this supports the claim of a complex being a SMM. However this is only secondary evidence and is not sufficient to prove a complex is a SMM. The value of χ_m" is dependent on both the frequency of the AC

field and the temperature at which the experiment is run. The T_B can be read directly off the plot of χ_m" vs T, as shown in Figure 4 where a $[Dy_4K_2O(O^tBu)_{12}]$ complex (Figure 5) was measured in an AC field of 0.55 Oe at a range of frequencies from 0.5 Hz to 1.2 kHz.[8] At high frequencies this complex showed two peaks at 30 and 47 K.

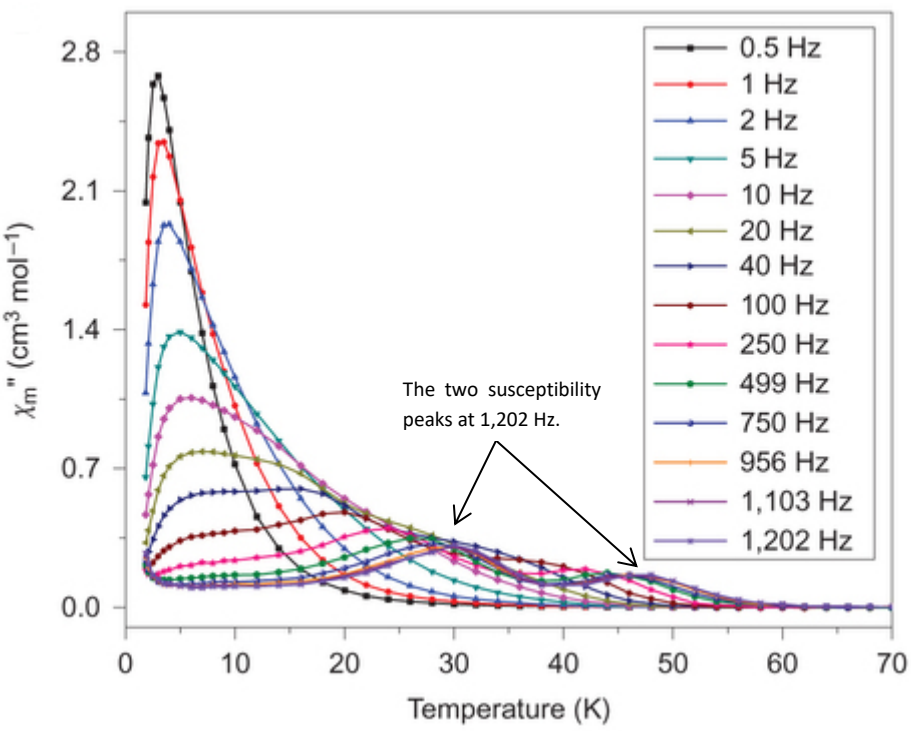

Figure 4. Top: Magnetic susceptibility of a $[Dy_4K_2O(O^tBu)_{12}]$ complex at a range of frequencies from 0.5 Hz to 1.2 kHz.

Magnetic anisotropy is the directional dependence of the material's magnetic properties, and having high anisotropy is one of the factors that contribute to having an effective SMM. There has been debate in the literature on whether having a large *S* value or a high anisotropic value is of greater importance in producing a SMM with a large thermal barrier (U_{eff}), with current theory favouring a higher anisotropy over a high *S* value. One such example of this is in the $[Mn^{III}_6O_2(C_7H_7NO_2)_6(O_2CPh)_2(EtOH)_4]$ complex of Milios *et al*., which at the time of discovery had the highest U_{eff} of any SMM developed.[9] This complex only had a *S* value of 12, compared to other Mn complexes in the literature that have *S* values up to $^{83}/_2$, yet because of a large anisotropic value it has a U_{eff} of 60 cm^{-1}. The complex with the *S* value of $^{83}/_2$, $[Mn^{III}_{12}Mn^{II}_7(\mu_4\text{-}O)_8(\mu_3,\eta^1\text{-}N_3)_8(C_9H_{12}O_3)_{12}(MeCN)_6]Cl_2$,

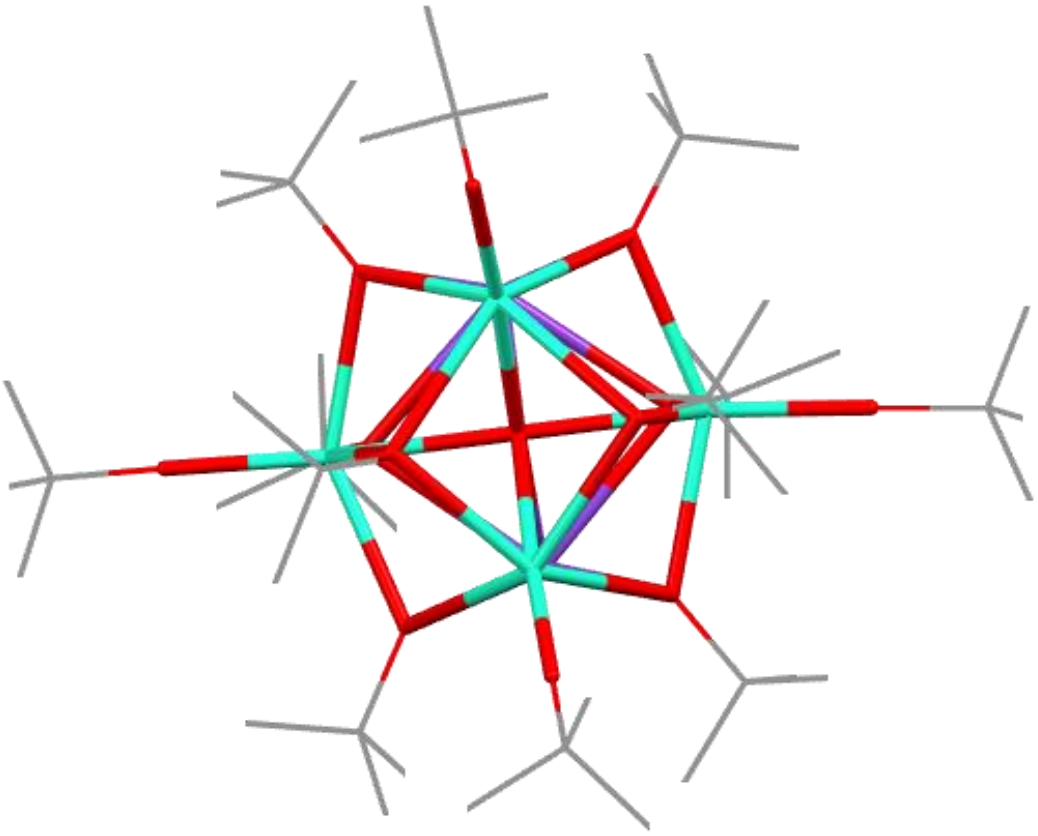

Figure 5. X-ray structure of the $[Dy_4K_2O(O^tBu)_{12}]$ complex. Dy = cyan, O = red, K = purple, C = grey. Hydrogens omitted and ligands made thinner for clarity.

shown in Figure 6, does not exhibit SMM behaviour as it does not exhibit slow relaxation of the magnetism. This is due to an almost complete lack of anisotropy at such a high value of *S*.[10] Results such as these show that having a reasonable anisotropic value is needed for SMM behaviour to be exhibited, and supports the importance of a high anisotropic value over a large spin state.

An effective SMM needs a large thermal barrier, established by the need to be able to use them at or above the temperature of liquid nitrogen. Another requirement for a usable SMM is that it displays no quantum tunnelling of magnetism (QTM). QTM is a process in which the spin sublevels that are separated by the energy barrier can transition through the barrier with little energy loss. This process occurs in many SMMs at low temperatures (>10 K), and provides a pathway for magnetic relaxation that circumvents the thermal barrier. This relaxation reduces the effective energy barrier, in some cases dropping it to nearly zero, and results in a rapid loss of the magnetism. Only SMMs that do not exhibit QTM, or in which it has been

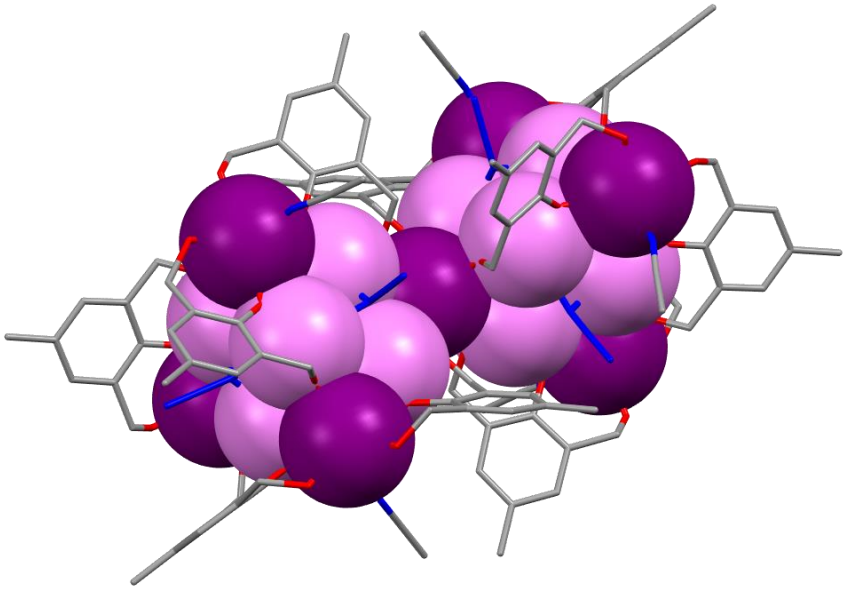

Figure 6. X-ray structure of the $[Mn^{III}_{12}Mn^{II}_{7}(\mu_4\text{-}O)_8(\mu_3,\eta^1\text{-}N_3)_8(C_9H_{12}O_3)_{12}(MeCN)_6]Cl_2$ complex. Mn^{III} = violet Mn^{II} = purple, O = red, N = blue, C = grey. Hydrogens omitted, ligands made thinner for clarity, and metal atoms expanded.

suppressed, show practical lifetimes of magnetism, showing that QTM needs to be suppressed in SMMs that do exhibit it to get molecules that may be of practical use.[1] QTM can be suppressed by an external DC field, as shown in the paper by Zhang *et al*., however structural methods to suppress QTM have yet to be developed.[1,11] Understanding the cause of QTM and being able to develop complexes that do not exhibit this phenomenon is of large importance.

One factor that comes up repeatedly in the formation of SMMs with high energy barriers is that the geometry of the molecule differs from the optimal geometry.[1,8-9,12-13] Optimal geometry refers to the preferred angles of the bonds, and it is the distortion of the ligand-metal bonds which results in the higher energy barriers. Geometries which are significantly different to the optimal geometry are normally a result of steric or ring strain in the system. Having a distorted geometry can also help to lower the ability of the complex to exhibit QTM, as complexes with a symmetry of C_3 or higher have been shown to exhibit unquenchable QTM.[1] It has been postulated that having bulky peripheral substituents, such as a *tert*-butyl groups, can also assist with SMM behaviour by assisting in isolating the molecules from each other.[12] One example of this was shown by a heteroleptic double-decker $[Tb^{III}(Pc)(Pc')]$ compound, which had the highest energy barrier reported in the

literature in 2013 (Figure 7).[12] Peripheral substituents such as *tert*-butyl and *tert*-butylphenoxy groups can also behave as electron donating moieties, and therefore help to stabilize the complex. Ganivet *et al.* observed that when these electron donating groups were added to the periphery of homoleptic [$Tb^{III}(Pc)_2$] complexes, the coordination between the lanthanide ion and the organic ligand was distorted.[12]

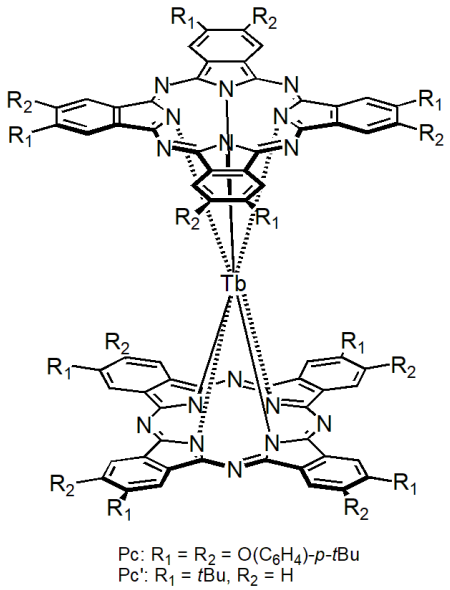

Figure 7. Structure of the Pc ligands that form the $Tb^{III}(Pc)(Pc')$ complex. They form an 8-coordinate complex with the Tb ion in a double-decker structure.[12]

Milios *et al.* showed that small changes to the structure of a ligand could result in a large difference to the overall geometry of the complex and that this could greatly increase the energy barrier and decrease the relaxation time of the complex (Figure 8).[9] This was achieved by changing the bridging ligand between the Mn^{III} ions from a 2-hydroxybenzaldehyde oximato group to the bulkier 2-hydroxyphenylpropanone oximato group, resulting in a large change to the structure of the core of the complex. The oximato bonding angles between the Mn^{III} ions went from being relatively straight to having a torsion angle of 36.5°. Changing the benzoate in the outer ligand system to 3,5-dimethylbenzoate resulted in an even higher torsion angle of 39.1°. This distortion to the core of the molecule resulted in the complex displaying a higher energy barrier than any previously discovered Mn complex (U_{eff} = 60 cm^{-1}) while also having a slow relaxation time. It is clear that many complexes will need to be studied in order to optimize SMMs properties to allow practical applications.

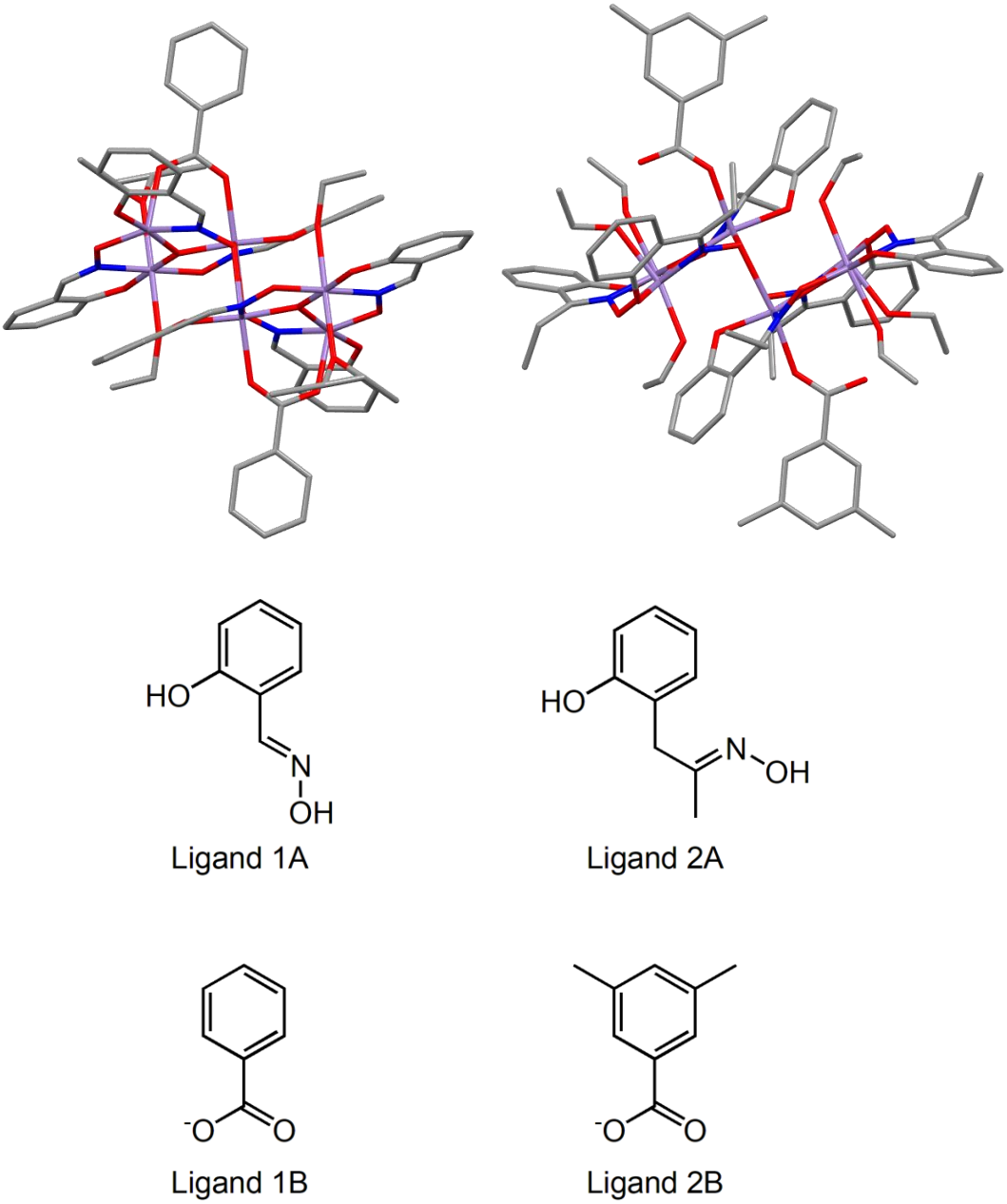

Figure 8. Top Left: Mn_6 complex with simple ligands. Top Right: Mn_6 complex with bulkier ligands. Middle: Original (left) and modified (right) oxime ligand. Bottom: Original (left) and modified (right) benzoate ligand. Note the altered geometry of the metal centres. Mn = purple, N = blue, O = red, C = grey. Hydrogens omitted for clarity.

A combined 3*d*-4*f* SMM complex with two Fe^{II} ions and one Dy^{III} ion was made by Liu *et al.* in 2014, and this complex showed the highest energy barrier so far exhibited by any 3*d*-4*f* SMM.[13] This complex used two identical ligands to bind the three metals together in a Fe^{II}–Dy^{III}–Fe^{II} pattern (Figure 9), however the geometries of the two Fe^{II} ions are not identical. One Fe^{II} ion exhibited distorted octahedral geometry while the other one exhibited distorted trigonal prismatic geometry. The

Dy^{III} ion exhibits distorted pentagonal bipyramid geometry. The distortion in the geometry for the Fe^{II} centres means that the degeneracy of the ground state energy levels is removed, and the asymmetry between the two Fe^{II} centres results in different electronic states to each other. This complex has a large anisotropy value of 319 cm^{-1}, and slow relaxation of magnetism is shown in the absence of a DC field, meaning that QTM in the molecule is highly suppressed.

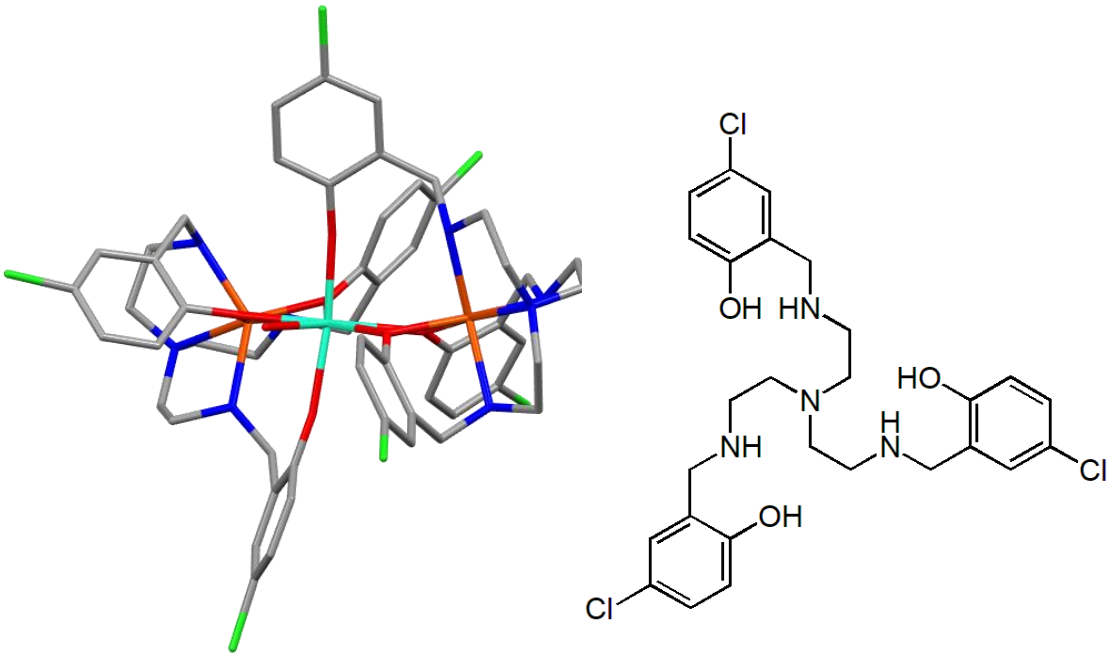

Figure 9. Left: The X-ray structure of the combined 3*d*-4*f* complex. Note the difference in geometry for the two Fe^{II} centres as well as the distorted binding angle to the Dy^{III} ion. Right: The ligand used to make the complex. Dy = cyan, Fe = orange, N = blue, Cl = green, O = red, C = grey. Hydrogens omitted for clarity.

There are no set rules for creating SMMs, and many different combinations of metals and ligand systems can be used to make them with a variety of results. The best results have come from using bulky ligands that keep the individual complexes from having magnetic interactions with each other, while also causing the metal binding geometries to be distorted. Due to this, ligand design for potential SMMs should be focused on achieving these goals. A combined ligand system of salicylaldoxime and [2.2]paracyclophane has the ability to provide both the requisite separation and to cause distorted geometries.

1.2 Salicylaldoximes

The focus of this project was on ligand design for potential SMMs, in particular using a salicylaldoxime group for the metal binding site. Salicylaldoxime (abbreviated to sao in formula) has an established history as a chelating ligand, having first been used to bind to metals in 1930 by Ephraim.[14] Within a few years X-ray structures were reported of Ni^{II}, Pd^{II} and Pt^{II} complexes of salicylaldoxime,[15] and it has been shown in recent literature to be able to bind to anions both broadly and selectively.[16-19] Salicylaldoxime has three potential binding sites; the nitrogen and oxygen of the oxime, and the phenol. Not all of them have to be involved in coordination and the oxygen of the oxime can remain free. This flexibility allows a range of metals to bind to the ligand and a variety of structural shapes including boxes and helicates to be formed, such as those shown in Figure 10.

The first manganese cluster made with salicylaldoxime was $Mn^{III}_6O_2(O_2CH_3)_2(sao)_6(EtOH)_4$, and this had two stacked triangles bridged by the oximato groups of the salicylaldoxime.[20] The two triangles were connected by two oxime groups, to give a distorted octahedral geometry for four of the Mn^{III} ions, while the two Mn^{III} ions on the periphery have a distorted square-pyramidal geometry (Figure 11). $S = 4$ for this complex, with each triangle unit having a value of $S = 2$. The U_{eff} value was measured to be 19.5 cm^{-1}, however hysteresis was not observed for this complex. Derivatives of the salicylaldoxime were made, where the oximic carbon atom was derivatised to have a Me, Et or Ph group coming off it. These changes 'twisted' the Mn–O–N–Mn moiety, increasing the torsion angles significantly. The complex made with the Et derivative ($[Mn_6O_2(Et\text{-}sao)_6(O_2CPh)_2(EtOH)_4(H_2O)_2]$) (Figure 11) was the first $[Mn^{III}_6]$ complex that had all three Mn–O–N–Mn torsion angles above 30°, and this complex was the first $[Mn^{III}_6]$ complex to display ferromagnetic exchange, with an $U_{eff} = 36.8$ cm^{-1} and exhibiting hysteresis up to 3 K.[21-22] As the ligand distorted the geometry, bulkier additions to the ligand would likely increase the hysteresis of this complex.

The triangle motif shown by the $[Mn^{III}_6]$ complexes is common in the literature when salicylaldoxime is used as the ligand system. This structural subunit arises when both the phenol and oxime groups are deprotonated, allowing 6-membered and 5-membered rings to form with three salicylaldoximes acting as bridges and

coordinating two metal ions each, as shown in Figure 11. These salicylaldoximes can also be 'strapped' together as shown in Figure 10, increasing the donor atoms per ligand and forming a ligand that has a potential to form structures other than the triangle motif (Figure 11), such as box and helicate structures (Figure 10).[17]

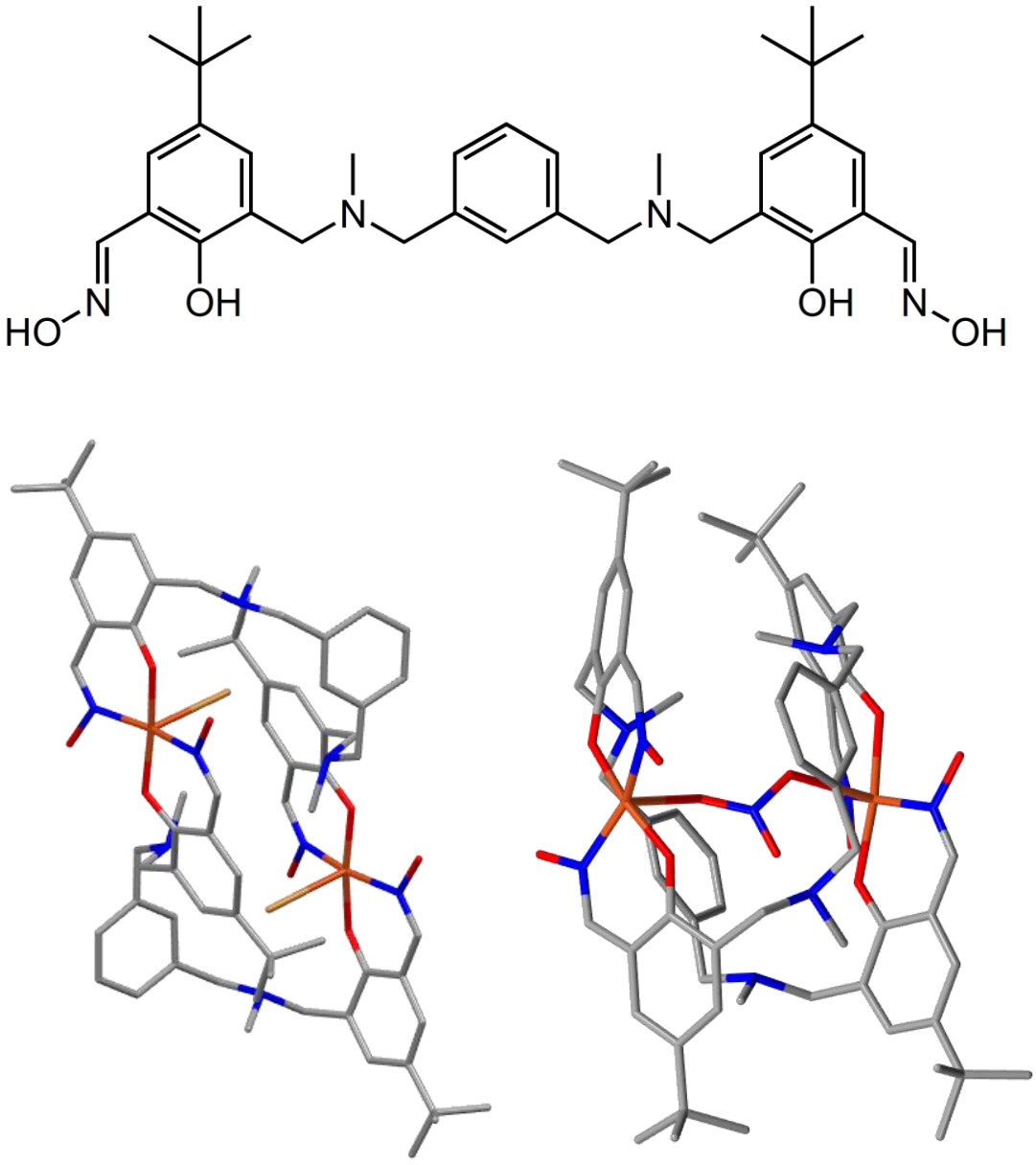

Figure 10. Top: Ligand used in the formation of both the box and helicate structures. Bottom left: $[2Br\subset(Cu_2L_2)](Br)_2$ Each copper is coordinated by two nitrogen moieties from the oxime, two oxygen from the phenol moiety and an axial coordinated bromine, forming a box structure. Bottom right: $[NO_3\subset(Cu_2L_2)](NO_3)_3$ similar bonding to the box structure, with each copper being bound by two nitrogen and two oxygen. However both coppers are bound to the same central NO_3, causing the ligands to form a helicate structure around the two metal ions. Cu = orange, N = blue, O = red, C = grey, Br = yellow. Hydrogens omitted for clarity.

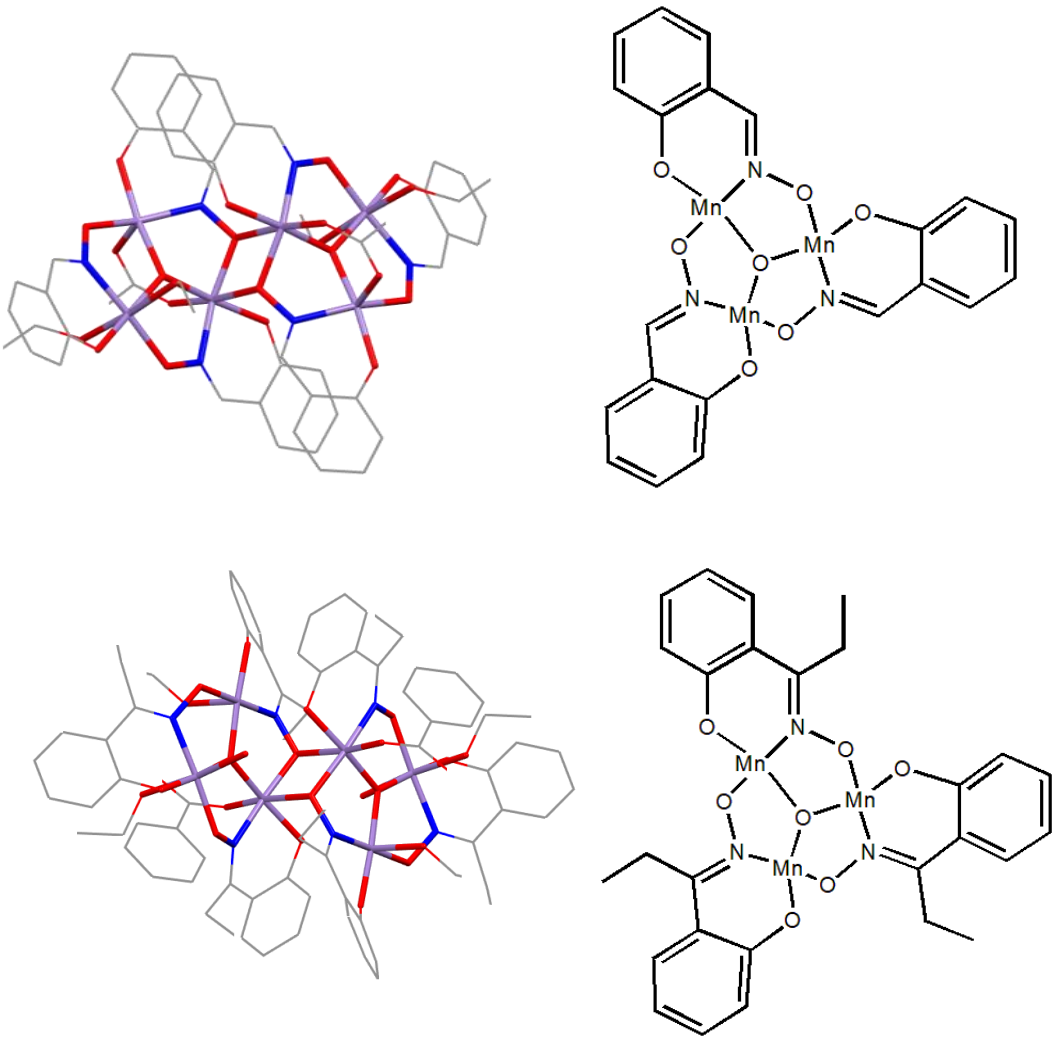

Figure 11. Top left: The first $Mn_6(sao)_6$ complex made. Note the two triangles consisting of three Mn^{III} each. Top right: Structure of one of the triangles. Bottom left: The first Mn_6 complex to display ferromagnetic exchange, where the salicylaldoxime has been derivitised to have ethyl chains on the oximate carbon. Bottom right: Structure of one of the triangles. Mn = purple, N = blue, O = red, C = grey. Hydrogens omitted and ligands made thinner for clarity.

The ability of salicylaldoxime ligands to bind to two different metal atoms and the ease at which it can be added to a bridging ligand to form a double headed ligand makes it a good candidate for SMM formation. It is also readily available with a *tert*-butyl group, which is an easy way to add bulk to a ligand system. Salicylaldoxime based ligands show potential for making SMMs, however, as with all potential routes for making SMMs, more work is required to find out the best way to make them.

1.3 [2.2]Paracyclophane

[2.2]Paracyclophane ([2.2]PC, Figure 12) provides an interesting scaffold for synthesizing new constructs due to its unique electronic structure caused by having two aromatic rings held within the van der Waals radii of carbon.[23] Its rigid backbone can also provide a source of chirality when a substituent is added.[23-25] These properties have made [2.2]PC useful in many diverse areas of research, from asymmetric synthesis and supramolecular chemistry through to biomedical research into bioisoteres.[23-26] [2.2]PC shows a twist angle of 12.83° between the two rings at 15 K that decreases as the temperature rises, disappearing completely above 55 K.[27]

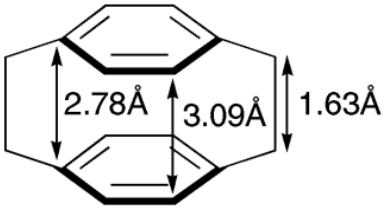

Figure 12. Structure and carbon atom distances of [2.2]PC.

[2.2]PC has been used as the basis for a ligand system for a magnetic complex,[28] however it is not a common ligand to use. While [2.2]PC does have lots of potential for use in the formation of SMMs, due to the electronic properties of [2.2]PC and the distorted geometry that it exhibits, especially at low temperatures, the problems with synthesising appropriate structures have precluded the use of [2.2]PC as a ligand system in the formation of SMMs. As I believed that adding a [2.2]PC structure into a larger ligand system for a SMM could be beneficial, I decided to see if I could synthesize a suitable ligand system. While [2.2]PC and its derivatives are regularly resistant to traditional chemical transformations commonly found in standard aromatic chemistry, due to the combination of steric effects, distorted structure and unique π-interactions caused by having the aromatic rings held within close proximity to each other, there are some standard reactions that have been developed that work on a variety on [2.2]PC derivatives.[23,29]

One magnetic system that used [2.2]PC was a diruthenium(II,II) trifluoroacetate complex ($[Ru_2(O_2CCF_3)_4]$, Figure 13).[28] The purpose of using [2.2]PC in this system was to bridge metal centres through interactions between the Ru(II) centres and the aromatic rings of [2.2]PC, and it was hoped that the unusual structure of [2.2]PC

would facilitate magnetic interactions between metal centres of individual diruthenium clusters. Reaction of the Ru complexes with [2.2]PC led to the formation of a crystalline solid with an interesting structure; it formed a 1-dimensional polymeric chain with alternating metal, [2.2]PC units (Figure 13). This is unusual, as there are very few examples where both aromatic rings of [2.2]PC are involved in the coordination of metal centres.[28,30] This is because the donation of electron density from one ring deactivates the second, due to electronic communication between the rings. Unfortunately the addition of the [2.2]PC bridge did not promote magnetic interactions along the polymeric chain, as the chain had the same magnetic measurements as the single diruthenium complexes. One benefit of making this polymeric chain however was that while $[Ru_2(O_2CCF_3)_4]$ is extremely hydroscopic, the polymeric chain was found to be only mildly moisture sensitive, allowing for much easier handling.

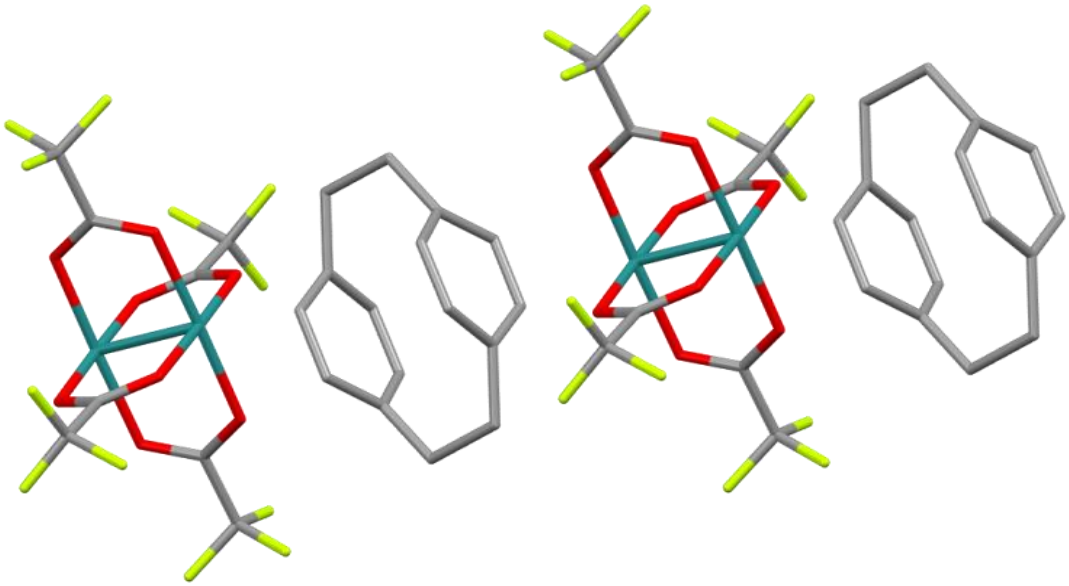

Figure 13. Polymeric unit of alternating $[Ru_2(O_2CCF_3)_4]$ and [2.2]PC. Ru = blue, F = yellow, O = red, C = grey. Hydrogens omitted for clarity.

[2.2]PC derivatives have also been used as bridging backbones for metal-chelating ligands. Examples of [2.2]PC being used as the backbone of metal-chelating ligands include [2.2]PHANEPHOS,[31] 4,16-bis(methyl-picolinaldimine)-[2.2]PC,[32] and 4,16-dicyano[2.2]PC (Figure 14).[33] These ligands have been used in a variety of different roles, such as enantioselective asymmetric catalysis, mediating electronic communication, and as a way to introduce a rigid backbone into a ligand.

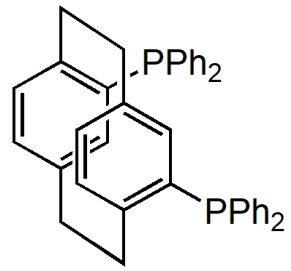

[2.2]PHANEPHOS

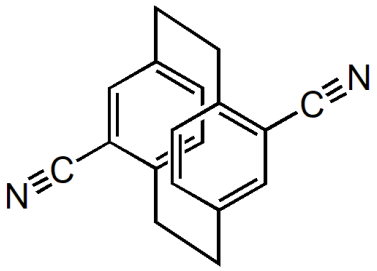

4,16-dicyano[2.2]PC

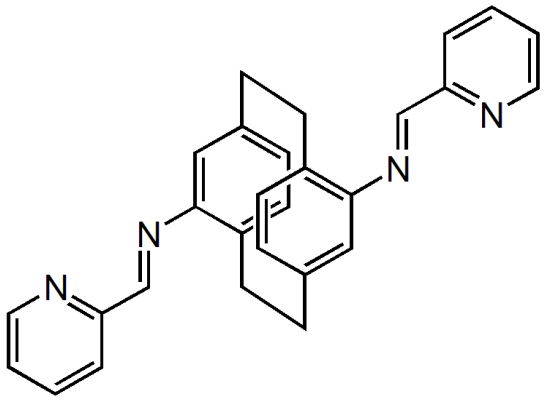

4,16-bis(methyl-picolinaldimine)[2.2]PC

Figure 14. Three examples of [2.2]PC based bridging ligands.

There are multiple reasons why [2.2]PC is of interest as the basis of a SMM ligand system. The bulkiness of [2.2]PC should provide good separation of molecules, keeping them from exhibiting bulk magnetism. The distortion of [2.2]PC's geometry at low temperatures is also of interest, especially for a bridging backbone, as this may promote stronger SMM behaviour. [2.2]PC also has a tendency to form ordered crystals, and so this may assist in preparing X-ray quality crystals. Another factor in favour of using [2.2]PC is that it is an unusual bridging moiety and has not been used for any SMMs to date. Any SMMs formed with [2.2]PC would be novel and help to increase knowledge around how to form usable SMMs.

1.4 Pyrazine

Pyrazine (1,4-diazine) is an electron deficient 6 member aromatic heterocycle that has two nitrogens located para to each other. This allows pyrazine to function as a bridge, as it can coordinate through both nitrogens, and the conjugation allows coordinated metals on both ends to communicate with each other. This was shown with the Creutz-Taube ion, $[Ru(NH_3)_5]_2(C_4H_4N_2)^{5+}$,[34] which consists of two pentaammine ruthenium units, each coordinated to one of the nitrogens on pyrazine (Figure 15). The metal communication in this complex is shown by both metal centres having an oxidation state of 2.5. This can only happen if the metals share electrons through the pyrazine moiety.

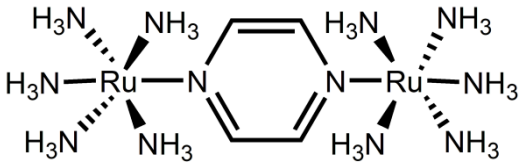

Figure 15. Structure of the Creutz-Teube ion.

The electron deficiency of pyrazine allows for nucleophilic attack on the carbon atoms, allowing for the ring to be functionalised. When functionalised in the 2 and 5 positions, as shown in Figure 16, it is possible to form ligands that, when complexed with metals, form either square (Figure 17) or triangular structures (Figure 18).[35-36] Due to the coordination that occurs with the pyrazine nitrogens, these ligands bind in a helicate-like fashion, with the ligand coordinating to the front of one metal and the back of the other. Grid structures are interesting as they offer multiple accessible metal centres that may be magnetically and/or redox active, such as the complex shown in Figure 17 which has 4 quasi-reversible oxidation processes.[35] Grid structures are usually the result of the self-assembly of linear ligands with octahedral metals, as is the case with the structure shown in Figure 16. Triangular structures are even more interesting, as they have higher stability while still having accessible metal centres for magnetic and/or redox applications.

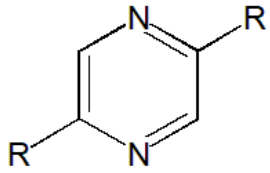

Figure 16. Basic structure of 2,5-derivatised pyrazine.

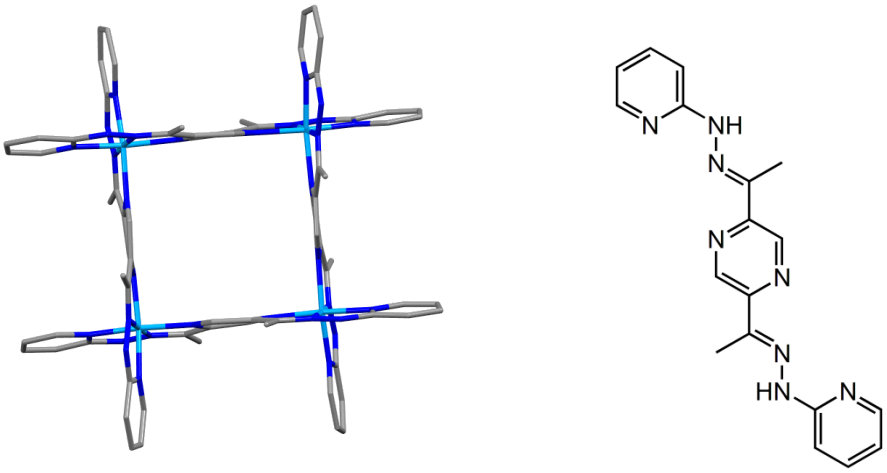

Figure 17. Left: Grid structure formed with Co. Right: Ligand used in formation of Co grid. Co = cyan, N = blue, C = grey. Hydrogens omitted for clarity.

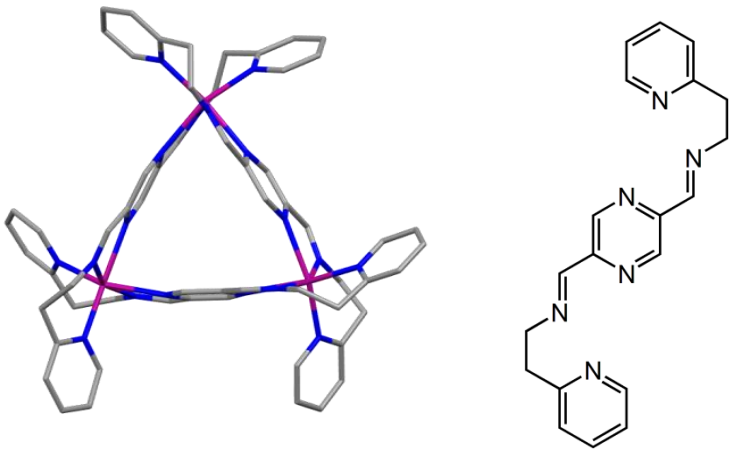

Figure 18. Left: Triangular structure formed with Zn. Right: Ligand used in formation of Zn triangle. Zn = purple, N = blue, C = grey. Hydrogens omitted for clarity.

Derivatives of pyrazine are another group of compounds that can be used as bridging ligands between two metal centres. Two examples of these ligands and the metal complex formed from them are shown in Figures 17 and 18, and another one is shown in Figure 19. This ligand system is a diamido pyrazine formed from dimethyl

pyrazine-2,5-dicarboxylate and 2-(2-aminoethyl)pyridine. It was complexed with Co(II)$(BF_4)_2$ in MeCN (with Et_3N) to form a cyclohelicate square complex where each of the four ligands act as a N_3-N_3 bis-terdentate chelate.[37] This gives each cobalt centre a distorted octahedral geometry, as can be seen in Figure 19. This complex showed very weak coupling in magnetic studies however, and did not show SMM behaviour.

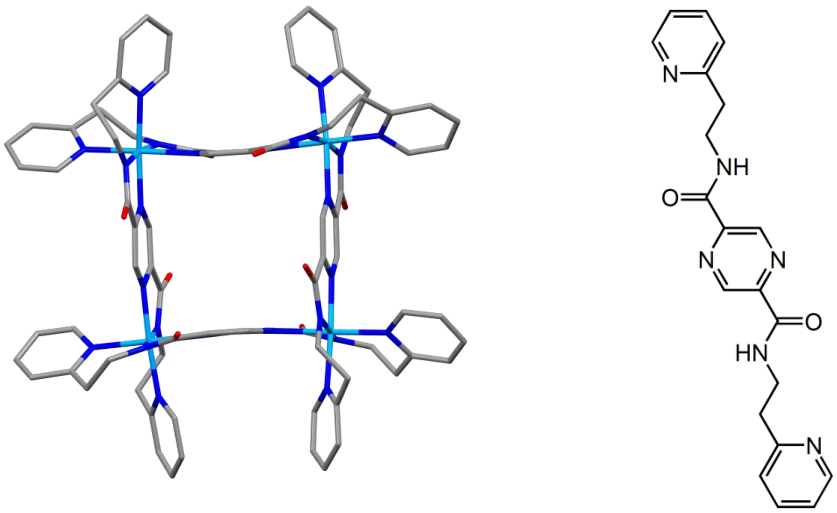

Figure 19. Left: Grid structure formed with Co. Right: Ligand used in formation of Co grid. Co = cyan, N = blue, O = red, C = grey. Hydrogens omitted for clarity.

1.5 Aims of this research

SMMs show promise for use in a wide range of applications, however a lot of research is still required before they can be used in practical situations. The largest area that needs to be addressed is ligand design. Currently it is known that having distorted metal-ligand geometry and bulky ligands are two areas that can greatly increase the U_{eff} of a complex, but there are fewer other guiding principles. In fact, a quick survey of the literature suggests more luck is involved than rational design. [2.2]PC shows promise in this area as a backbone for a ligand system, due to its bulk, as well as the unique π-interactions of the aromatic rings having the potential to affect the magnetics of any complexes formed. It is also expected to provide a basis for order between individual molecules due to interactions between [2.2]PC groups, allowing for ordered crystals to be grown.

The main aim of my project was to synthesize a ligand that combined [2.2]PC and salicylaldoxime and complex it with transition metals (Figure 20). I also wished to attempt to make double headed ligands with 4,16-diamino[2.2]PC (Figure 20).

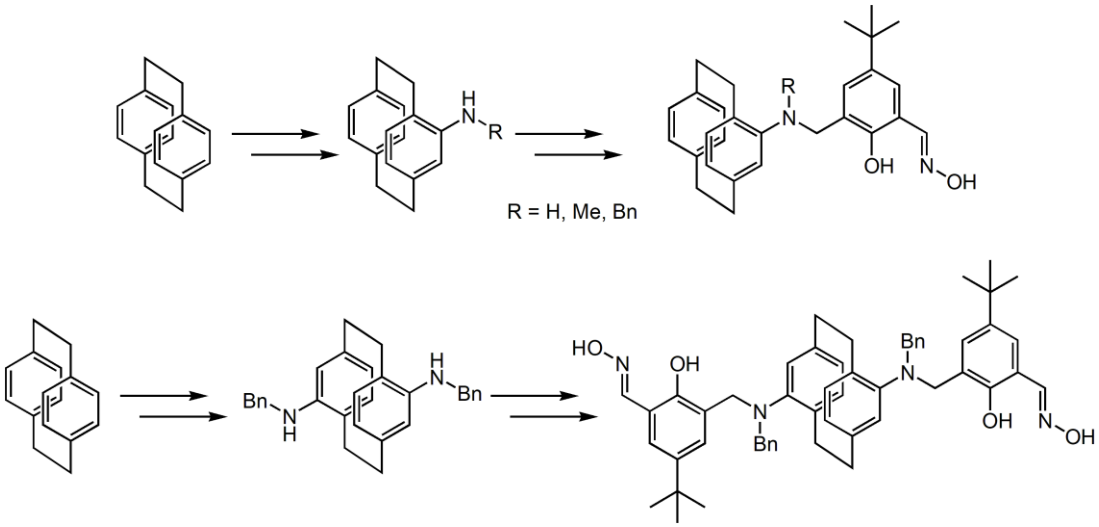

Figure 20. Top: Simplified scheme for the mono-[2.2]PC ligand. Bottom: Simplified plan for the double headed [2.2]PC ligand.

Pyrazine is an interesting molecule that has been shown to be able to be functionalized and complexed to produce many interesting structures, including triangle structures which are highly interesting for magnetic applications. Because of this, I wished to synthesize a double headed bridging ligand based on pyrazine, and chose 2,5-diaminopyrazine as our target molecule (Figure 21). This is an unreported

molecule, however I believed that it would be highly valuable as a linker due to the variety of functionality allowed by the amine groups.

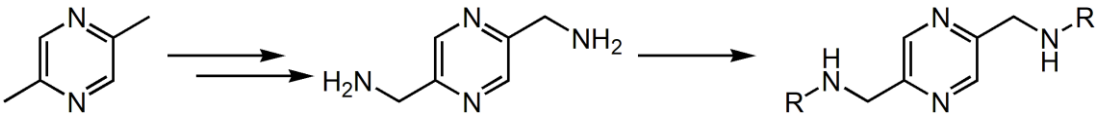

Figure 21. Simplified scheme for the formation of 2,5-diaminopyrazine and subsequent formation of double headed ligands.

2. Results and Discussion.

2.1 [2.2]Paracyclophane ligand synthesis

As the aim was to couple [2.2]PC to our salicylaldehyde compound, I required a suitable derivative of [2.2]PC. 4-Amino[2.2]PC was chosen as the desired derivative of [2.2]PC as literature couplings on salicylaldehyde are predominately achieved by amine alkylation, leaving the aldehyde free to be converted to the oxime for metal binding (Scheme 1).

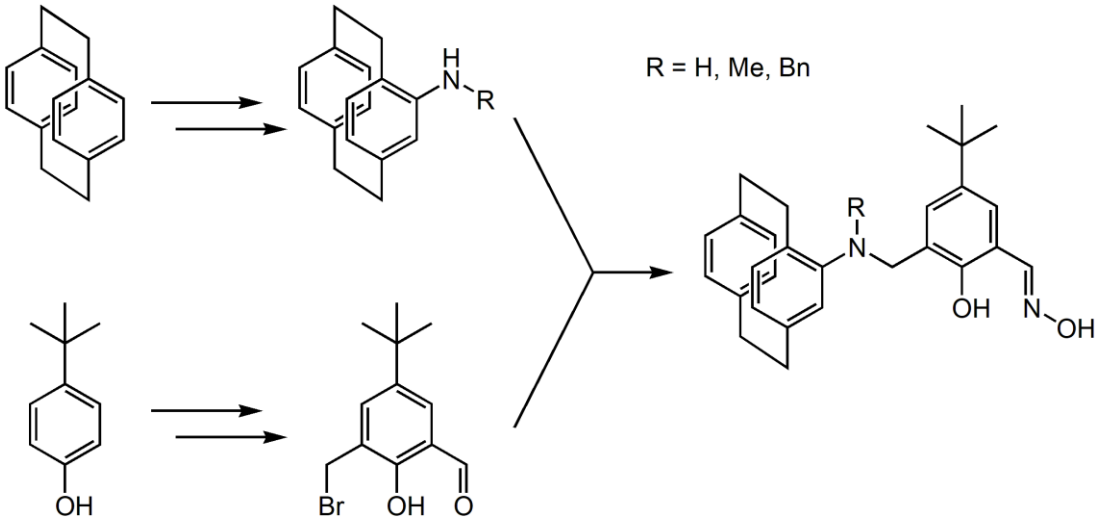

Scheme 1. Planned synthesis of mono-substituted [2.2]PC ligand and salicylaldehyde

There are a variety of ways to synthesize 4-amino[2.2]PC, with the most direct route being nitration followed by reduction.[38-40] Other common routes include the Curtius rearrangement of 4-carboxy[2.2]PC,[41-44] the electrophilic amination of 4-bromo[2.2]PC,[43,45-46] and the transition metal-catalysed amination of 4-bromo[2.2]PC.[29] None of these routes are particularly reliable, with the Curtius rearrangement involving multiple steps and the use of organic azides and the amination of 4-bromo[2.2]PC giving variable yields and requiring harsh reaction conditions. The nitration route was attempted for a period of time, however this reaction is capricious and results were far from satisfactory (Figure 22). The nitration step is problematic, with a mixture of unreacted starting material, over nitration and other oxidation products being formed along with the desired 4-nitro[2.2]PC.[38-40] There are many optimized conditions reported in the literature but these all disagree on every variable, including quantities of reagents, temperature, and time of reaction.

The reduction with HCl and Fe powder was even more temperamental, with some reductions simply failing and the yield of those that did work being extremely low.

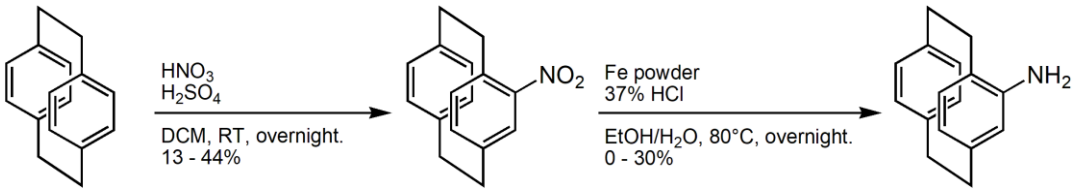

Figure 22. Synthetic route to produce 4-amino[2.2]PC through the nitration and subsequent reduction of [2.2]PC.

Because of the issues with the nitration route, I tried to use longer reaction sequences that employed more reliable transformations to improve the yield of 4-amino[2.2]PC. One such route developed by the Rowlands group provides 4-amino[2.2]PC in three simple steps with a maximum yield of 32% (Figure 23).[29] The first step was the formylation of [2.2]PC, which can be achieved by a Rieche formylation in good yield.[47] This involves the reaction of [2.2]PC with dichloromethyl methyl ether and $TiCl_4$, and presumably occurs through a Friedel-Crafts-like reaction. Initially the titanium aids the formation of the strongly electrophilic oxonium species. The electron rich [2.2]PC readily adds to this as shown (Figure 24). This gives the α-chloroether, which undergoes acid hydrolysis on the addition of water to give 4-formyl[2.2]PC (Figure 24). This reaction can reliably be achieved on a 10 gram scale and does not require purification before proceeding to the next step.

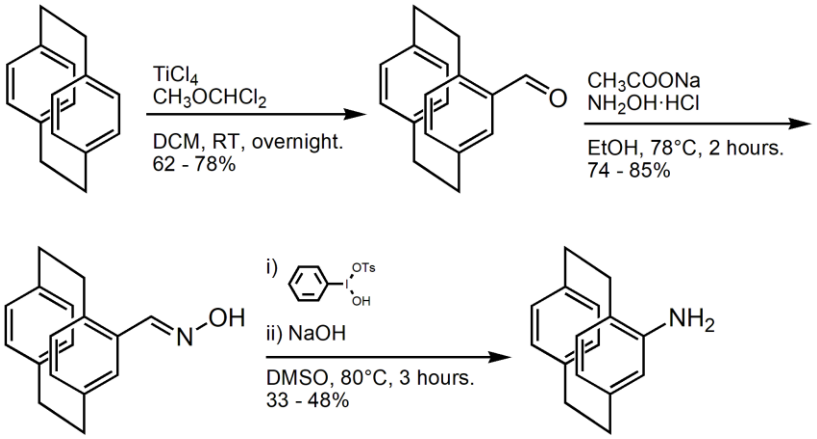

Figure 23. Synthetic route to produce 4-amino[2.2]PC developed by the Rowlands group.

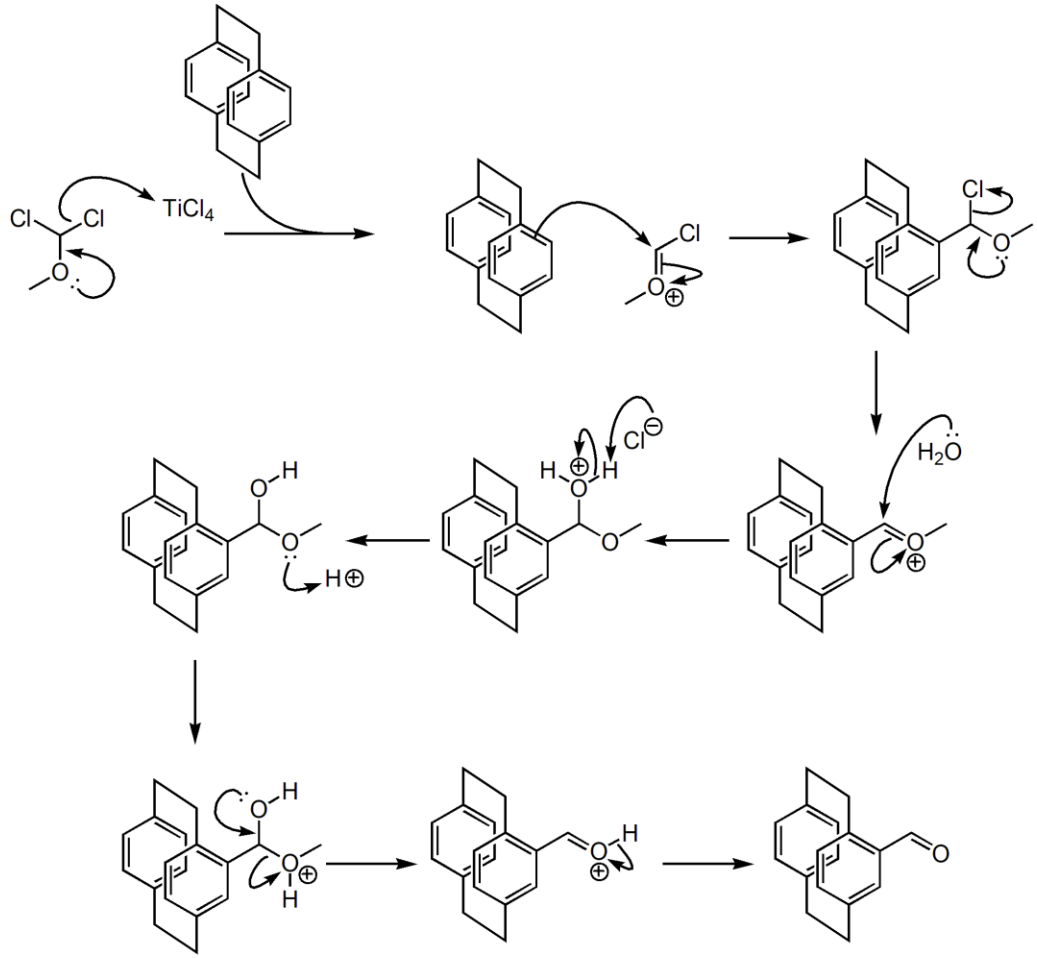

Figure 24. Mechanism of the Rieche formylation reaction.

With the aldehyde in hand, I then wanted to convert it into an amine. This was achieved by a modification of the Lossen rearrangement. First the aldehyde was condensed with hydroxylamine to give an oxime. This oxime was treated with Koser's reagent, oxidising it to a hydroxamic acid. This probably occurs via a nitrile oxide intermediate that undergoes base-mediated Lossen rearrangement to form an isocyanate. The isocyanate then reacts with remaining hydroxamic acid to give the final product (Figure 25). Silica gel column chromatography eluting with 4:1 hexane:EtOAc afforded 4-amino[2.2]PC in 33-48% yield.

Due to problems preparing Koser's reagent, a hypervalent iodine species, the rearrangement gave inconsistent results. I considered initiating the rearrangement in other ways, however I was cognizant that the Beckmann rearrangement of aldehyde derived oximes frequently gives nitriles, and that I needed to avoid this.[48-50]

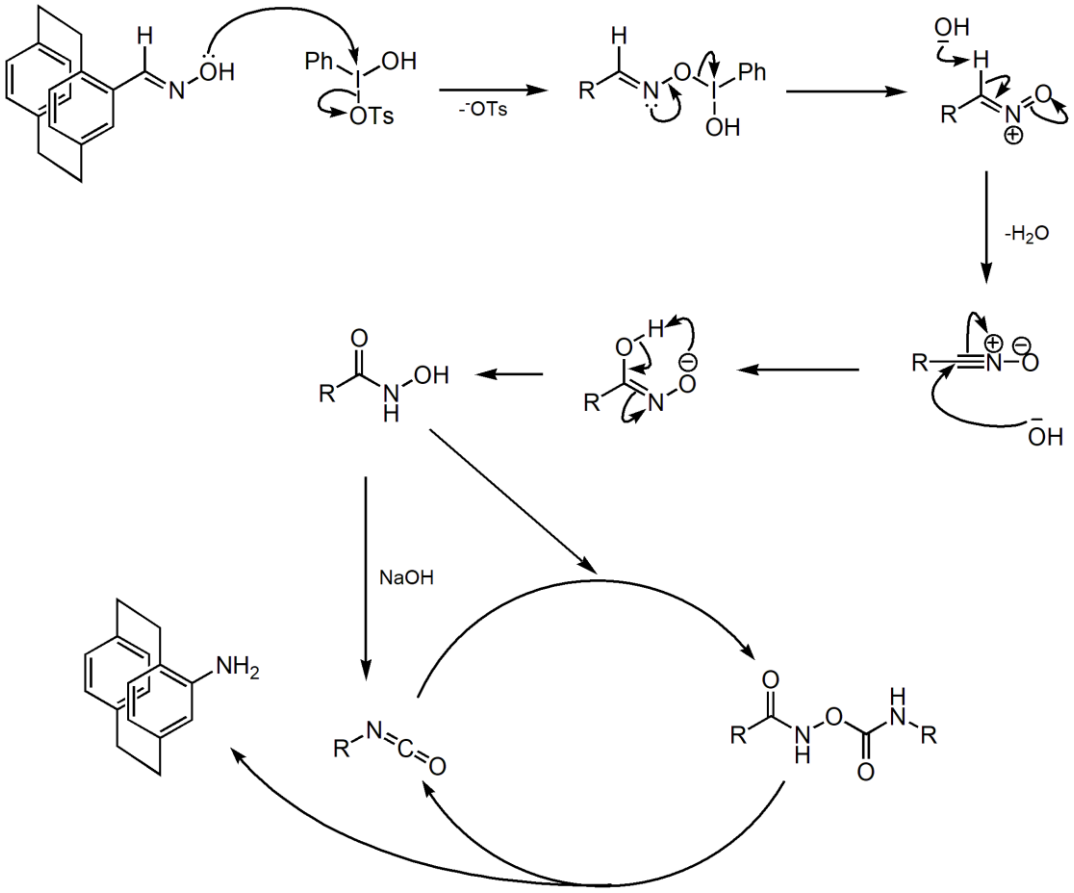

Figure 25. Mechanism for the rearrangement of the oxime to get 4-amino[2.2]PC.

The results were capricious but I found that they were more reliable if Koser's reagent was freshly prepared.

I wished to use a secondary amine as it was believed that it would make the ligand more stable, as well as preventing a double addition of the salicylaldehyde molecule further on in the synthesis. Initially I attempted to add a methyl group, as it is a small group and would not interfere sterically with the addition of the salicylaldehyde. The first method attempted was reductive amination, as this should only add a single methyl group to the nitrogen (Figure 26).[51] However no sign of addition was observed in the NMR spectrum of the reaction mixture. Because of the low reactivity in the previous reaction, an alkylation route was attempted. Amine alkylation can be troublesome as multiple alkylations occur but the previous reaction suggested that this aniline derivative was less reactive and so might escape this fate. Unfortunately, the half expected dimethylamine[2.2]PC was formed (Figure 26). This occurs because the secondary amine formed by a single addition of an alkyl

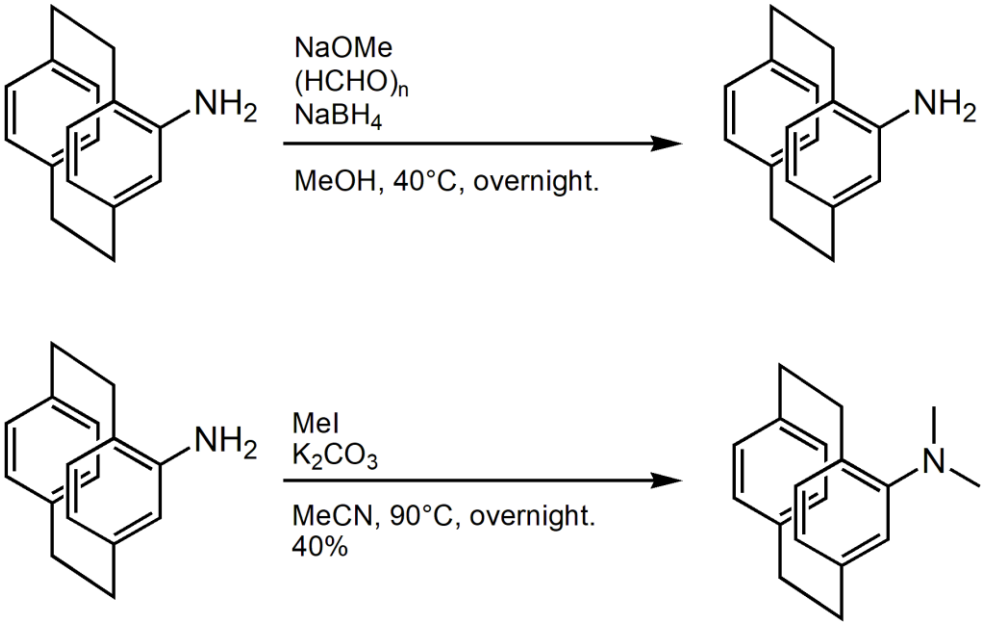

Figure 26. Two methods used to attempt to make *N*-methyl-4-amino[2.2]PC

group is more nucleophilic than the primary amine, and therefore reacts preferentially to form the tertiary amine.

As I was experiencing difficulties with both the amine formation and its subsequent alkylation I thought it might be possible to kill two birds with one stone and use the Buchwald-Hartwig reaction to install an alkyl amine directly. This reaction would start with readily available 4-bromo[2.2]PC and use methylammonium chloride as the amine source (Figure 27). This reaction has been reported by Bräse to proceed in high yield,[52] and so this reaction was expected to work. The Buchwald-Hartwig amination forms a carbon-nitrogen bond through the cross-coupling of an amine with an aryl halide catalysed by a palladium(0) complex (Figure 28). The use of a phosphine ligand, such as 2,2'-bis(diphenylphosphino)-1,1'-binapthyl (BINAP), in these reactions assists the catalysis and result in faster and higher yielding reactions. Two of these reactions were attempted, using sodium *tert*-butoxide as the base, tris(dibenzylideneacetone)dipalladium(0) ($[Pd_2(dba)_3]$) as the Pd catalyst and methylammonium chloride as the source of the methylamine group. The two reactions differed by the phosphine ligand used, the first used a bidentate ligand in the form of BINAP while the second used a monodentate phosphine, tri-*tert*-butylphosphonium tetrafluoroborate ($[^tBu_3PH][BF_4]$). The first reaction resulted in less than 10% conversion of the starting material into the desired product, while the second gave only the product of protodebromination but no addition of the

methylamine. Previous work in the Rowlands group has found the Buchwald-Hartwig reactions of [2.2]PC derivatives to be challenging, so I did not pursue these any further.

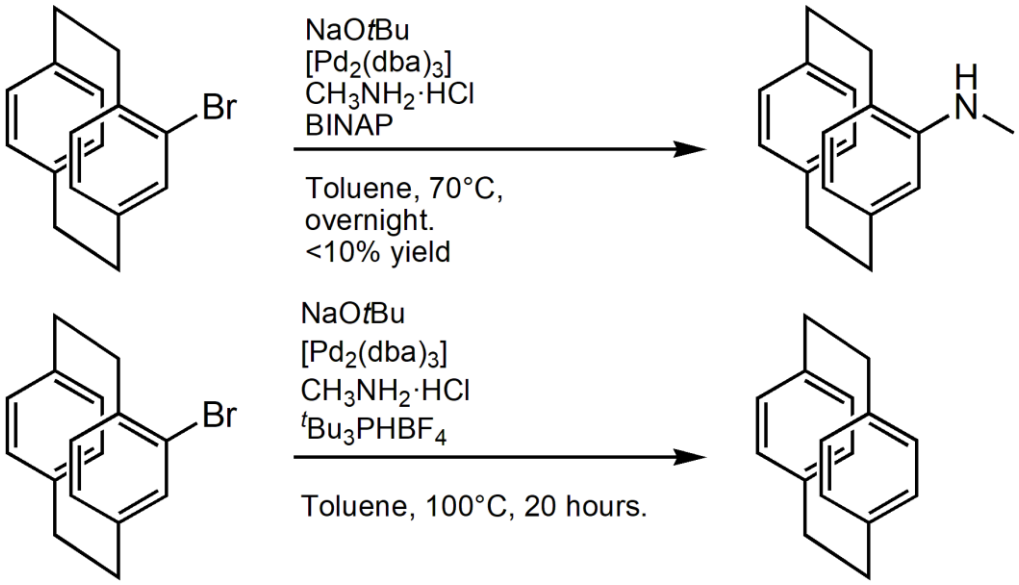

Figure 27. Attempts to make *N*-methyl-4-amino[2.2]PC by the Buchwald-Hartwig reaction.

Due to the issues in making 4-(methylamino)[2.2]PC, I decided to investigate the synthesis of 4-(benzylamino)[2.2]PC instead. I believed that the more user-friendly benzyl group would provide greater scope for successful alkylation. While literature methods exist for the formation of the compound, none of them started from 4-amino[2.2]PC. One used Buchwald-Hartwig chemistry to couple 4-bromo[2.2]PC and benzylamine, while the other was a 5 step route involving NaN_3.[38,52] These routes were considered, but the potential fickleness of the Pd catalysed coupling (see above) ruled this one out while the length of the azide sequence made this unattractive. Therefore I decided to attempt the synthesis of 4-(benzylamino)[2.2]PC from 4-amino[2.2]PC. Stirring 4-amino[2.2]PC and benzaldehyde together in EtOH resulted in the Schiff base product shown in Figure 29, which was purified by cooling the solution and filtering off the crystals formed. This purification was required prior to reduction as excess benzaldehyde was converted to benzyl alcohol, which could not be separated from the desired benzylamine. Reduction of the imine was required shortly after purification, as the compound was unstable. Initial attempts to reduce the imine were unsuccessful, with low or no conversion of the imine to the amine. It was found that the addition of boric acid protonated the imine and facilitated sodium borohydride reduction (Figure 29).This synthesis is a novel

method of making 4-(benzylamino)[2.2]PC, and has an average 75% yield over the two steps. A one pot procedure was attempted for this reaction, but a mixture of the desired product and benzylalcohol was always formed. As stated, this could not be removed and so the two step protocol was adopted instead.

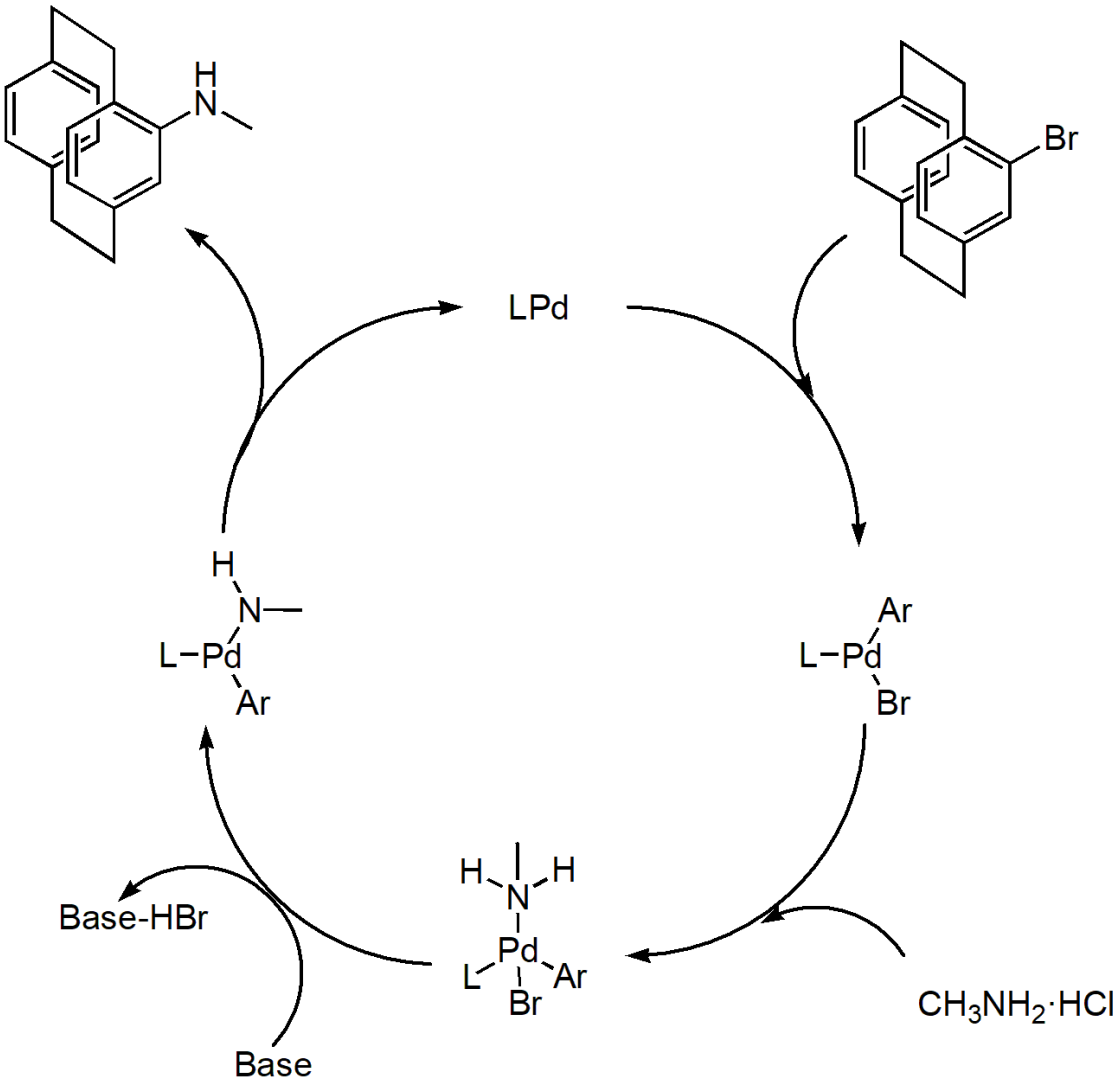

Figure 28. Mechanism of the Buchwald-Hartwig amination. L is the bidentate ligand used in the catalysis, as they readily displace the dba from the Pd.

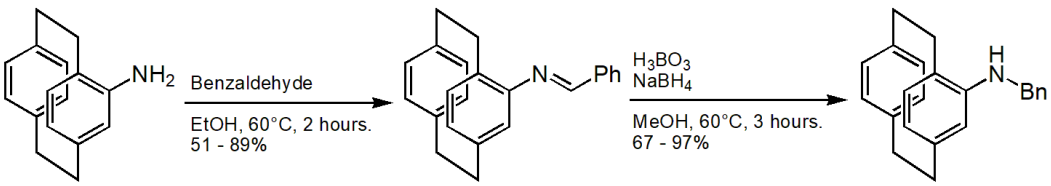

Figure 29. Benzylation of 4-amino[2.2]PC,

The requisite salicylaldehyde derivative, 3-(bromomethyl)-5-*tert*-butyl-2-hydroxybenzaldehyde, was synthesized from 4-*tert*-butylphenol in two steps (Figure 30). The first reaction was the formylation of the phenol by the Reimer-Tiemann reaction. In this transformation the $CHCl_3$ is both the solvent and the source of the aldehyde group (Figure 31). First, the chloroform is deprotonated by NaOH to form the stabilized chloroform carbanion. This rapidly undergoes α-elimination, with one chlorine atom being expelled to form dichlorocarbene. This is a highly electrophilic species, which is attacked by the phenoxide to give the *ortho* dichloromethylene compound. Under the highly basic reaction conditions, the dichloroacetal is hydrolysed to the aldehyde. This reaction was not high yielding, with an average yield of only 10%, however the reaction could be performed on a 10 gram scale, using cheap and readily available reagents, alleviating some of the problem of such a low yield.

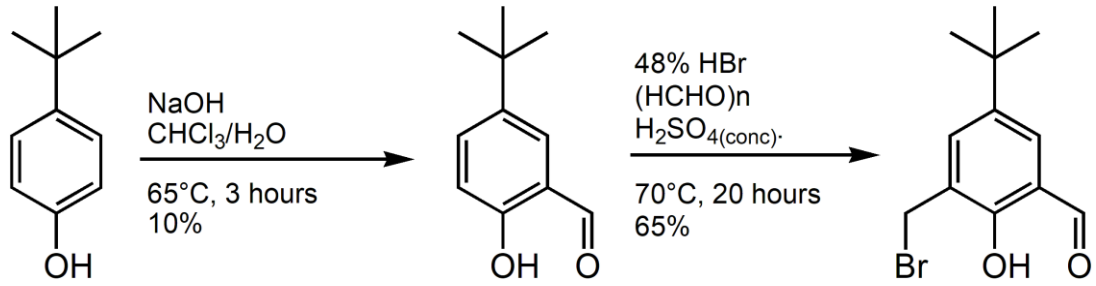

Figure 30. 2 step route to synthesizing 3-(bromomethyl)-5-*tert*-butyl-2-hydroxybenzaldehyde.

The second reaction was to add a bromomethyl group to 5-*tert*-butyl-2-hydroxybenzaldehyde. Reaction of the phenol with a 48% solution of HBr, paraformaldehyde and H_2SO_4 (Figure 32) gave an average yield of 65%, giving an overall yield for the two reactions of 6.5%. The mechanism for this reaction involves converting the paraformaldehyde to formaldehyde, which is then protonated by the acid. The phenol then attacks this highly electrophilic species to give an alcohol. The hydroxyl group is protonated by the acidic solution and a bromide ion displaces the oxonium ion to form 3-(bromomethyl)-5-*tert*-butyl-2-hydroxybenzaldehyde. While this is a low yielding sequence of reactions, it was possible to form approximately 1 gram of product for every 10 grams of cheap starting material, which was enough to carry on to the next stage. Only a few of these reactions were required, as I was able to obtain 3-(bromomethyl)-5-*tert*-butyl-2-hydroxybenzaldehyde from colleagues when they began large scale synthesis for their own use.

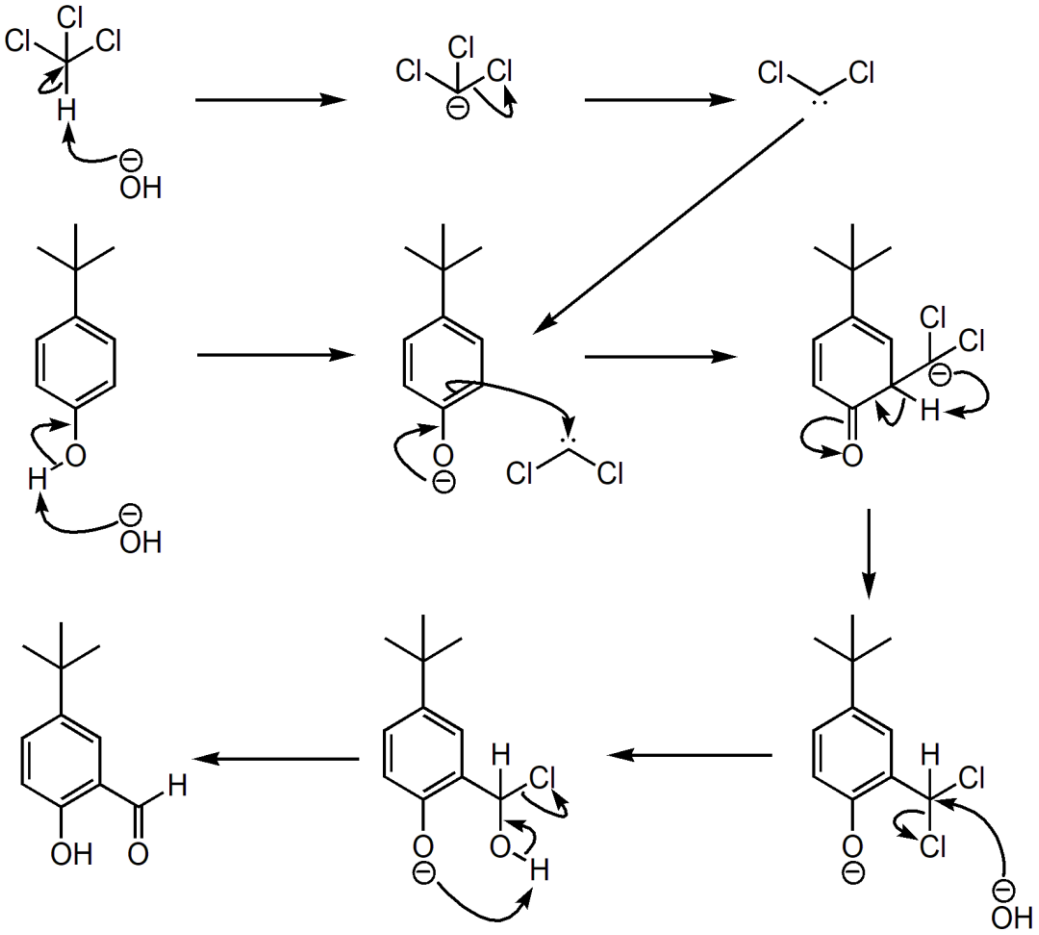

Figure 31. Mechanism for the formation of 5-*tert*-butyl-2-hydroxybenzaldehyde from 4-*tert*-butylphenol with $CHCl_3$ and NaOH.

Coupling the salicylaldehyde derivative with 4-amino[2.2]PC and 4-(benzylamino)[2.2]PC was achieved in the presence of base (Figure 33). Initially K_2CO_3 was used, however a cleaner reaction with simpler purification was possible when Et_3N was used. The reaction with 4-amino[2.2]PC gave the secondary amine in lower yield than the analogous tertiary amine. The secondary amine proved to be unstable, as it decomposed even when kept under Ar and refrigerated over 5 weeks. This instability could be the reason for the low yield. (*E*)-5-(*tert*-Butyl)-3-(benzyl[2.2]paracyclophan-4-yl methylamino)-2-hydroxy benzaldehyde (Pre-L_1) on the other hand was stable. It has been noted that many [2.2]PC amines are unstable.[29] Most rapidly colourize and I think that the already electron rich [2.2]PC rings are further activated by the amine functionality and this leads to a variety of decomposition pathways. It is possible that the stability of Pre-L_1 is due to the benzyl group changing the conformation of the C-N bond and preventing delocalisation of the nitrogen lone pair of electrons into [2.2]PC. Because of this I concentrated on

making the 4-(benzylamino)[2.2]PC based ligand. These reactions are a simple amine alkylation, where the bromine electronegativity makes the neighbouring carbon an electrophile. This results in the lone pair on the amine attacking the carbon in what is likely an S_N2 substitution. However, it is possible that this reaction proceeds by an S_N1 substitution, as the aromatic ring could stabilise the carbocation. The base then neutralises the protonated amine to give the desired product (Figure 34).

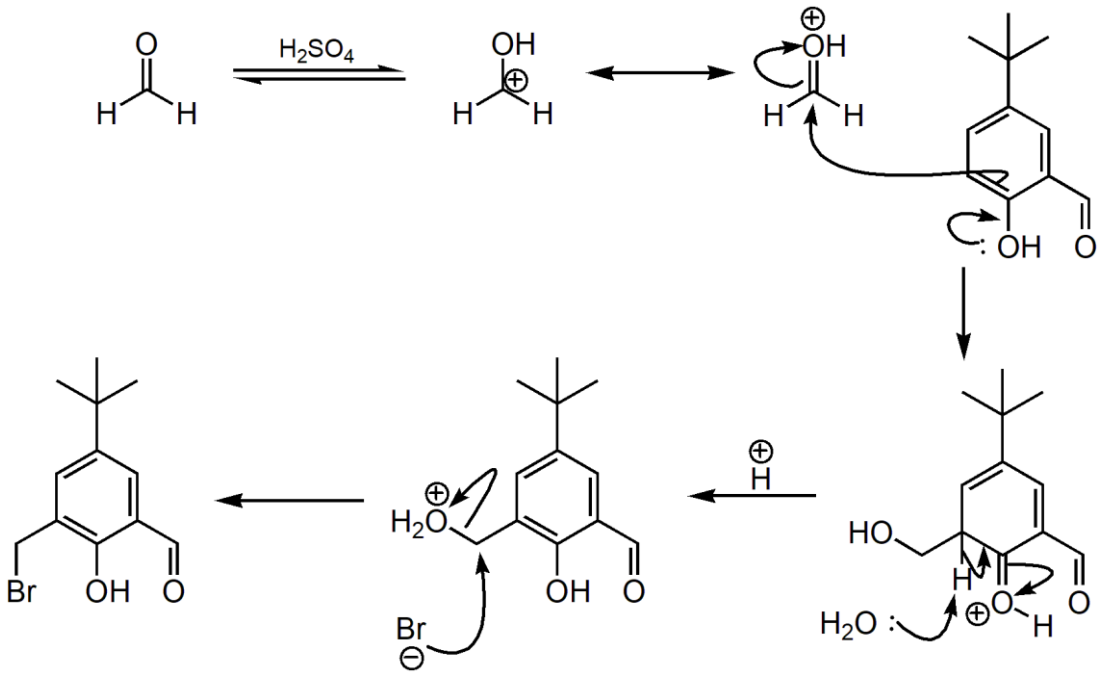

Figure 32. Methylbromination mechanism to form 3-(bromomethyl)-5-*tert*-butyl-2-hydroxybenzaldehyde.

I was originally unsure if Pre-L_1 had been successfully made, as the ^{1}H NMR did not have the right number of aromatic peaks and had one too many aliphatic peaks (Figure 35). I believed that I had formed Pre-L_1, and that it was giving an unusual NMR due to an altered conformation, as in the ^{1}H NMR the aromatic range is missing a peak, with only 13 out of 14 peaks being present, while the bridging CH_2 region has an additional peak at 3.7 ppm. I decided to test if Pre-L_1 had been successfully made by subjecting it to oximation. This was done using the same reaction conditions as before (Figure 36). Due to the lower yield and lack of stability in (*E*)-5-(*tert*-butyl)-3-([2.2]paracyclophan-4-yl methylamino)-2-hydroxy benzaldehyde, only Pre-L_1 was oximated to make the final ligand (L_1).

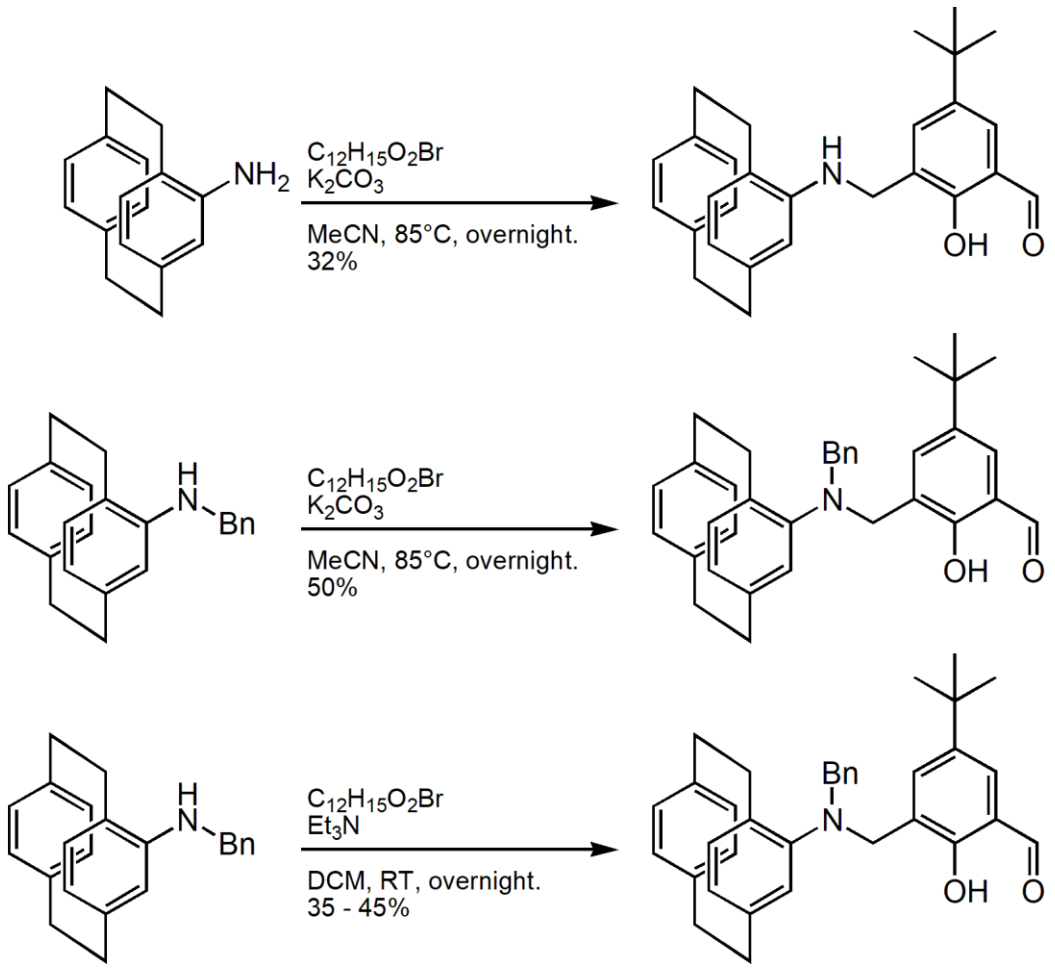

Figure 33. Coupling of the salicylaldehyde derivative to 4-amino[2.2]PC and 4-(benzylamino)[2.2]PC.

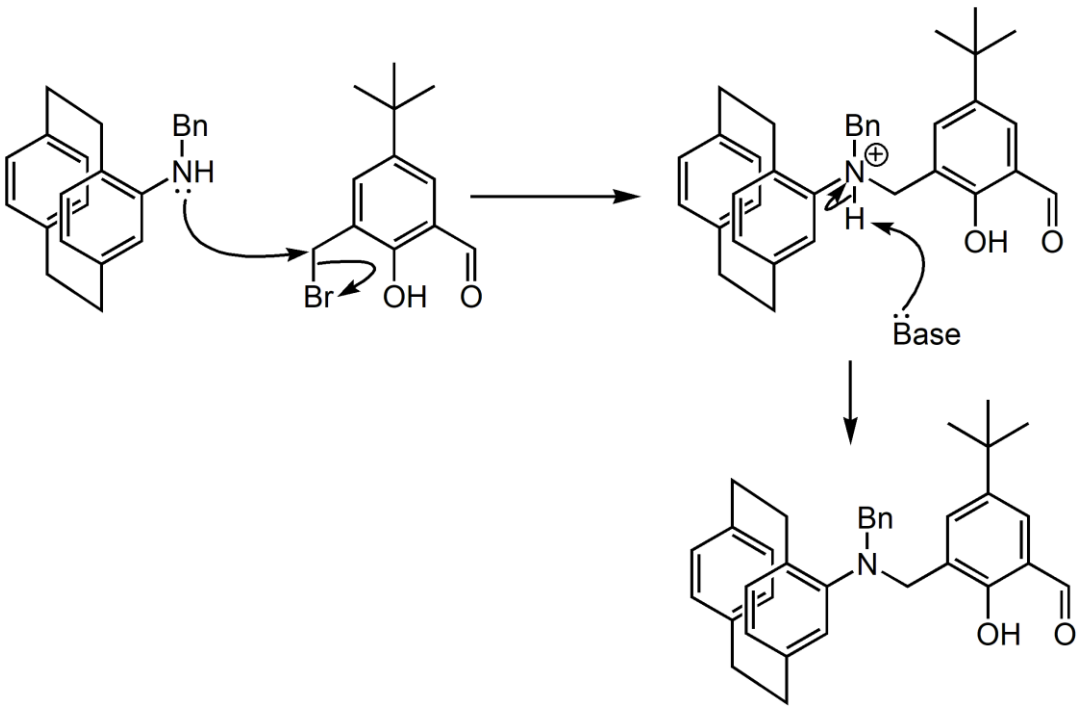

Figure 34. Mechanism for the coupling of 4-(benzylamino)[2.2]PC and the salicylaldehyde derivative.

The success of the oximation (Figure 37) suggested that Pre-L_1 had been made. The issues in the ^{1}H NMR for Pre-L_1 were resolved in the L_1 ^{1}H NMR. It is unclear why the Pre-L_1 NMR was different than expected but I think that the conformation of pre-L_1 is such that one of the aromatic hydrogens, likely from the salicylaldehyde, is perpendicular to an aromatic ring and is heavily shielded by the ring current of an aromatic ring. This would explain why it is much further upfield than would be expected. Figure 38 shows a potential conformation of Pre-L_1, which explains how the shielding may occur. As can be seen in the pre-L_1 ^{1}H NMR, the aldehyde and phenol hydrogen peaks are at 11.2 and 9.9 ppm, while in the L_1 ^{1}H NMR the aldehyde peak disappears and a peak appears at 8.2. This peak is characteristic of the oxime, and with the disappearance of the aldehyde peak, indicate oxime formation. 2D NMR were taken of pre-L_1, however these were unable to provide a definite solution to the conformation of this compound. Attempts to grow crystals of pre-L_1 were undertaken to determine the structure, however these were unsuccessful (Table 1).

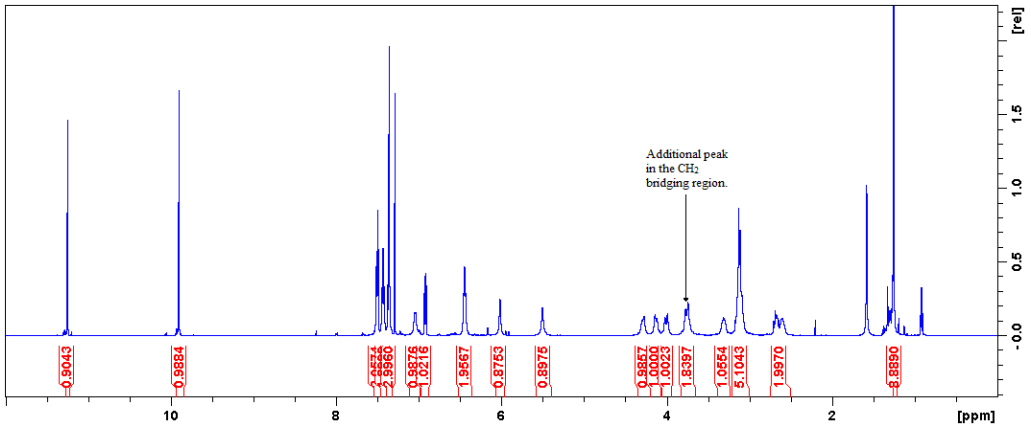

Figure 35. ^{1}H NMR of pre-L_1 ($CDCl_3$).

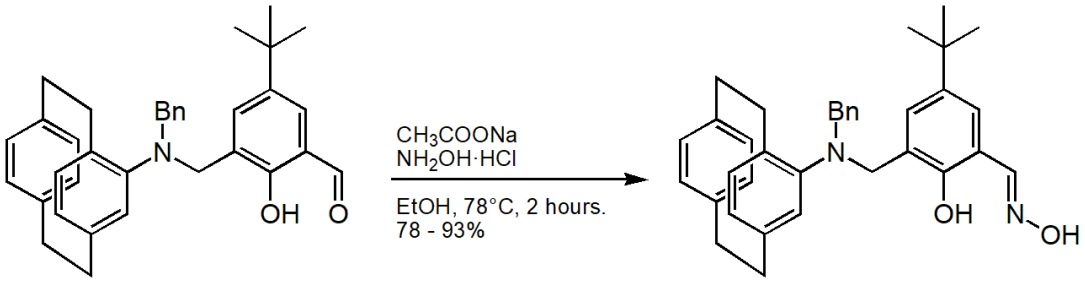

Figure 36. Oximation of (*E*)-5-(*tert*-butyl)-3-(benzyl[2.2]paracyclophan-4-yl methylamino)-2-hydroxy benzaldehyde

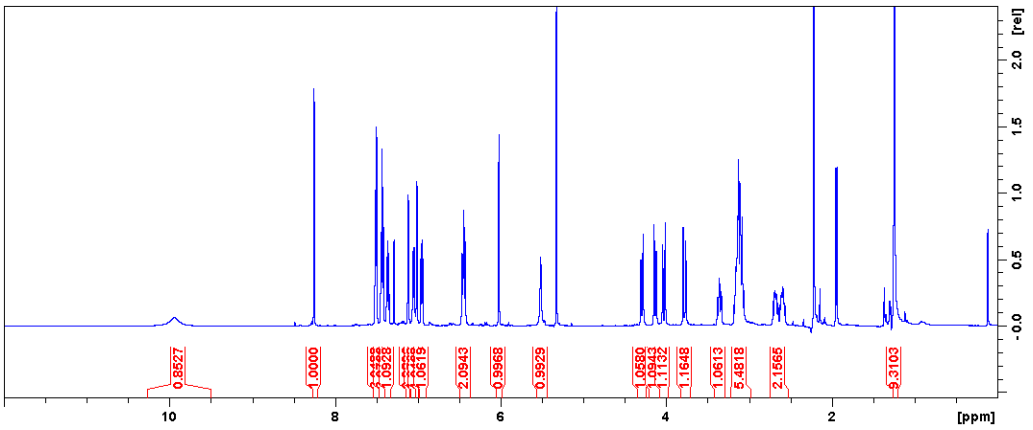

Figure 37. ^{1}H NMR of L_1 ($CDCl_3$). Peak at 5.3 is DCM.

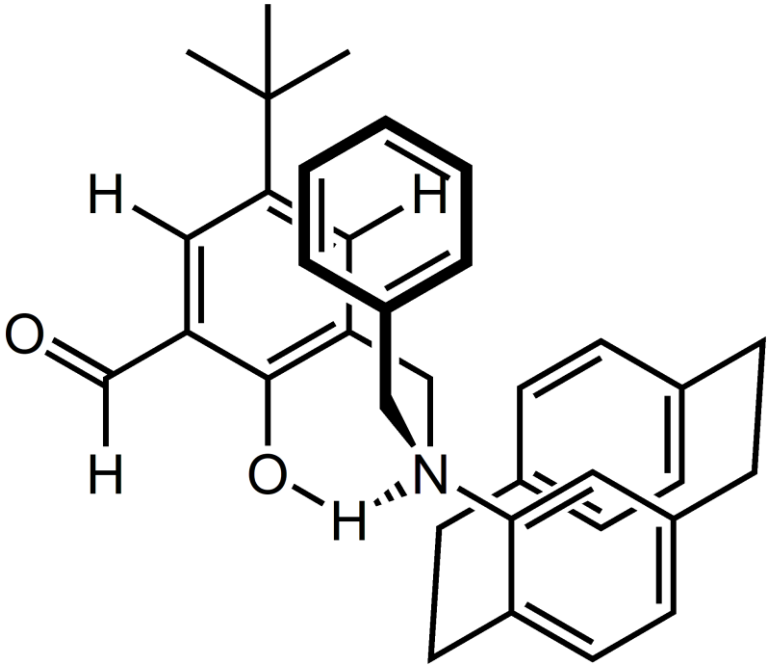

Figure 38. Potential conformation of Pre-L_1, showing the shielded H

Complexations with various transition metal salts were undertaken with L_1 and crystallizations attempted. All complexation attempts resulted in the colour of the solution changing rapidly, indicating the ligand binding to the metal. This is due to the interaction of the d-orbital electrons from the metal with the ligand results in an energy separation that can change the absorption band of the initial metal salt, giving a different colour. Comprehensive attempts were made to form complexes with L_1 and to grow crystals. Unfortunately, I was unable to obtain crystals suitable for X-ray crystallography. The vials were left for a longer period to see if crystallization would occur, but this was unsuccessful. Information of the

complexation and crystallization attempts are given in the experimental section. Mass spectrometry results did not show any peaks that could be attributed to formation of a complex, however this is not surprising as the probe is run at 300°C, and it is common for complexes to fall apart from the high temperature. The ligand was present in all samples, showing that the complexation had not altered the ligand itself.

Compound	Recrystallization attempts
Pre-L_1	Hot solvent evaporation: • Ethyl Acetate • n-Hexane • Methanol • Ethanol • Chloroform • Cyclohexane • 1,4-dioxane • Benzene • Acetonitrile • Diethyl Ether • 1:1 Acetonitrile:Ethanol • 1:1 Acetonitrile:Methanol • 1:1 Acetonitrile:n-Hexane • 1:1 Acetonitrile:Ethyl Acetate • 1:1 Acetonitrile:Chloroform

Table 1. Hot solvent evaporation attempts of pre-L_1.

I was also interested in using [2.2]PC to bridge two salicyaldoximes together, as this would produce a unique bridging system for magnetic studies. Bridging ligands derived from [2.2]PC have been used to study electronic communication through space but have not been used in the study of magnetism.[32] Our initial target was 4,16-diamino[2.2]PC, as this would be a symmetric bridge. For the synthesis I hoped that this molecule would behave as two isolated anilines and that I could use the chemistry developed above (Scheme 2). The synthesis of this molecule is not trivial, as the regioselectivity needed to be controlled. Nitration does not offer a feasible

route as dinitration is reported to occur non-selectively. The literature showed that 4,16-dibromo[2.2]PC could be readily formed so I investigated converting this to the desired amine. One literature route was to use Buchwald-Hartwig amination to add benzophenone imine to 4,16-dibromo[2.2]PC, which was then hydrolysed to give 4,16-diamino[2.2]PC.[32] Yet again I was unable to get the Buchwald-Hartwig reaction to work, and so a different method had to be utilized.

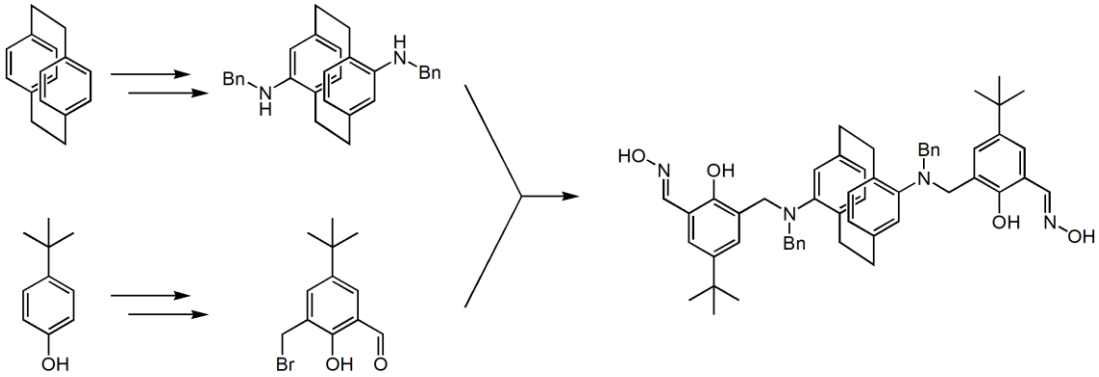

Scheme 2. Planned synthesis of di-substituted [2.2]PC ligand and salicylaldehyde

I was interested in developing a direct amination instead of using a protected amine such as that used in the above Buchwald-Hartwig amination. I decided to attempt a copper-mediated route, as this route was successful in forming 4-amino[2.2]PC from 4-bromo[2.2]PC.[29] This conversion is believed to occur by forming the aryl azide, which is then reduced *in situ*. Adding proline into the reaction as a ligand to bind to the copper has been shown to result in cleaner reactions.[53] The optimum conditions for the conversion of 4,16-dibromo[2.2]PC into 4,16-diamino[2.2]PC used Cu_2O as the copper source with 6.5 eq of NaN_3 in the presence of proline in DMSO. Interestingly, these reactions had to be performed under microwave heating. When the reaction was conducted under conventional heating 4-amino-16-bromo[2.2]PC was formed (Figure 39), along with 4-amino[2.2]PC and [2.2]PC. With microwave heating the diamine was added to this mixture. It is unclear why the two modes of heating differ. I wonder if formation of the first 'aniline' results in an electron rich system that is communicated to the lower ring. This in turn makes insertion of the copper into the C-Br bond harder, thus requiring additional energy to push the reaction forward. New results suggest that pressure is the key to making the diamino. The length of time required for this reaction is an issue, as both methods require an extended period of heating. Any change in time results in significantly reduced

yields. The diamine was found to be unstable in solution, and decomposition was observed if the diamine was left in the reaction mixture after the reaction was complete. The crude solution must be stirred with EDTA for 30 minutes, failure to do this resulted in little to no recovery of the diamine, suggesting that the diamine coordinates with the copper. Crude NMR of the microwave reactions showed that the other product formed was 4-amino-16-bromo[2.2]PC, along with the starting material and [2.2]PC.

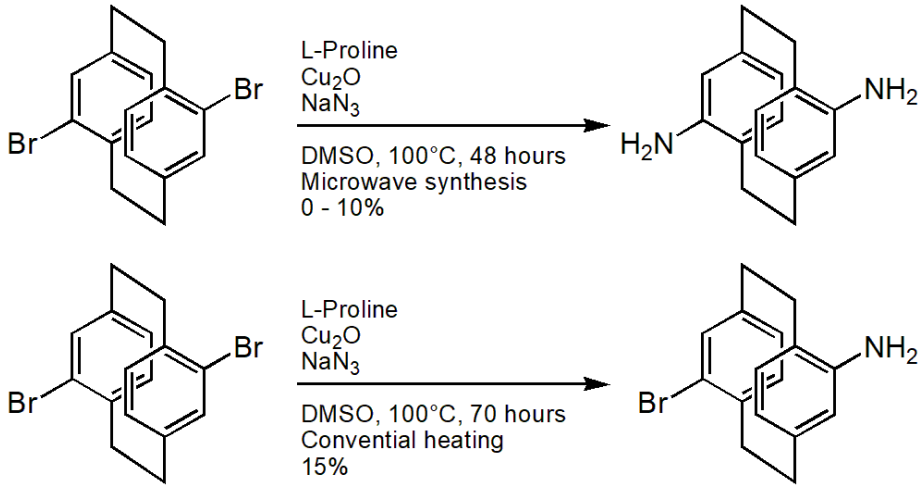

Figure 39. Synthesis of 4,16-diamino[2.2]paracyclophane and 4-amino-16-bromo[2.2]paracyclophane.

The mechanism of the reaction is unknown, however it is likely that the first part of the reaction is oxidative insertion of copper into the C-Br bond. The azide would then swap Cu-Br to Cu-N_3 and reductive elimination would occur to form the C-N bond and regenerate the copper catalyst (Figure 40). The proline is a bidentate ligand that binds to the copper(I) and provides stability in this reaction. This is supported by the fact that an identified side product in the diamination reactions is 4-amino[2.2]PC, which would be produced when hydrogen is coupled to the [2.2]PC rather than an azide.

Azide reduction could occur in a number of possible ways. The copper(I) could act as a reductant, transferring a single electron to the azide resulting in the expulsion of nitrogen gas. Alternatively copper nitrene could be formed through coordination of the copper to the azide, followed by insertion with displacement of nitrogen gas. The

resulting N=Cu bond would then be hydrolysed, returning copper oxide and the desired 4,16-diamino[2.2]PC (Figure 41).

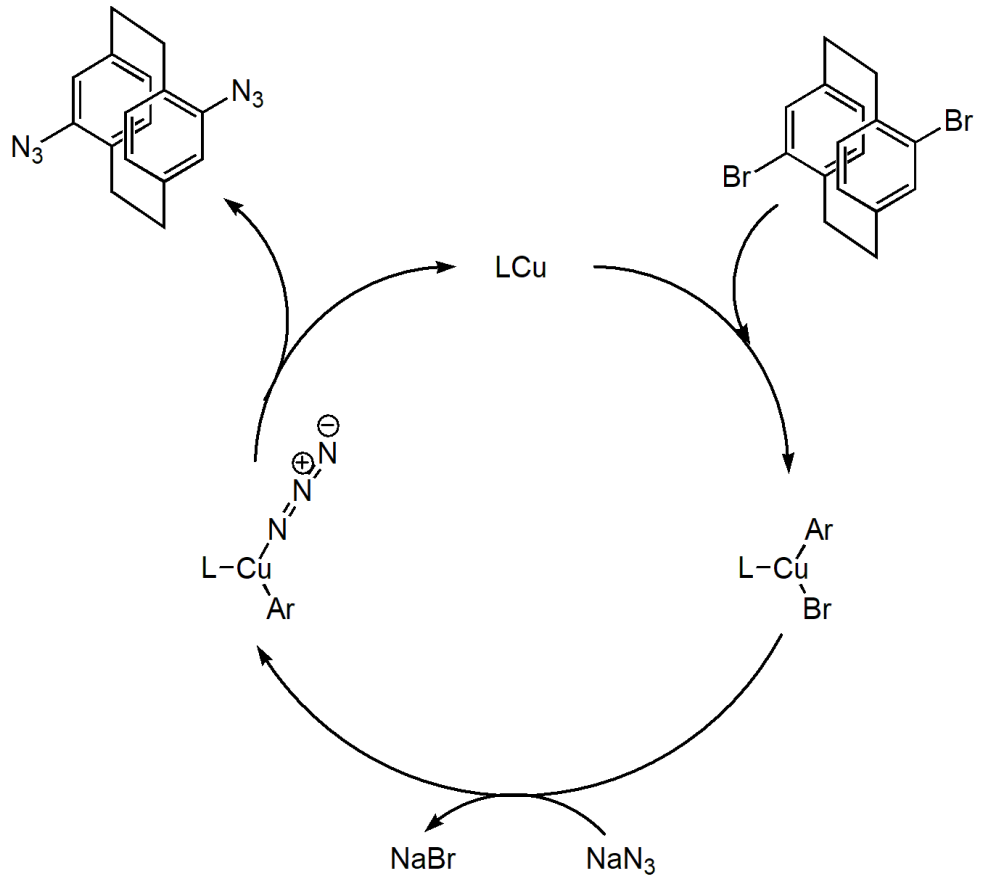

Figure 40. Potential mechanism for the formation of a diazide intermediate for the formation of 4,16-diamino[2.2]PC.

This reaction proved to be problematic in a variety of ways. The yield was extremely low, with an average yield of 10%, or around 15 milligrams. This coupled with the time of the reaction meant that I had a very low throughput of material. The reaction also used a large excess of sodium azide, which is highly toxic and explosive. Only a small mass of sodium azide was used in each reaction however, as I was unable to scale the reaction up due to size limitations with our microwave vessels. Another problem was that the reaction is not clean, and purification proved to be extremely problematic. After a variety of different methods and conditions were attempted, it was found that dissolving the crude product in hot 1,4-dioxane, cooling and washing with n-hexane resulted in 4,16-diamino[2.2]PC crashing out of solution.

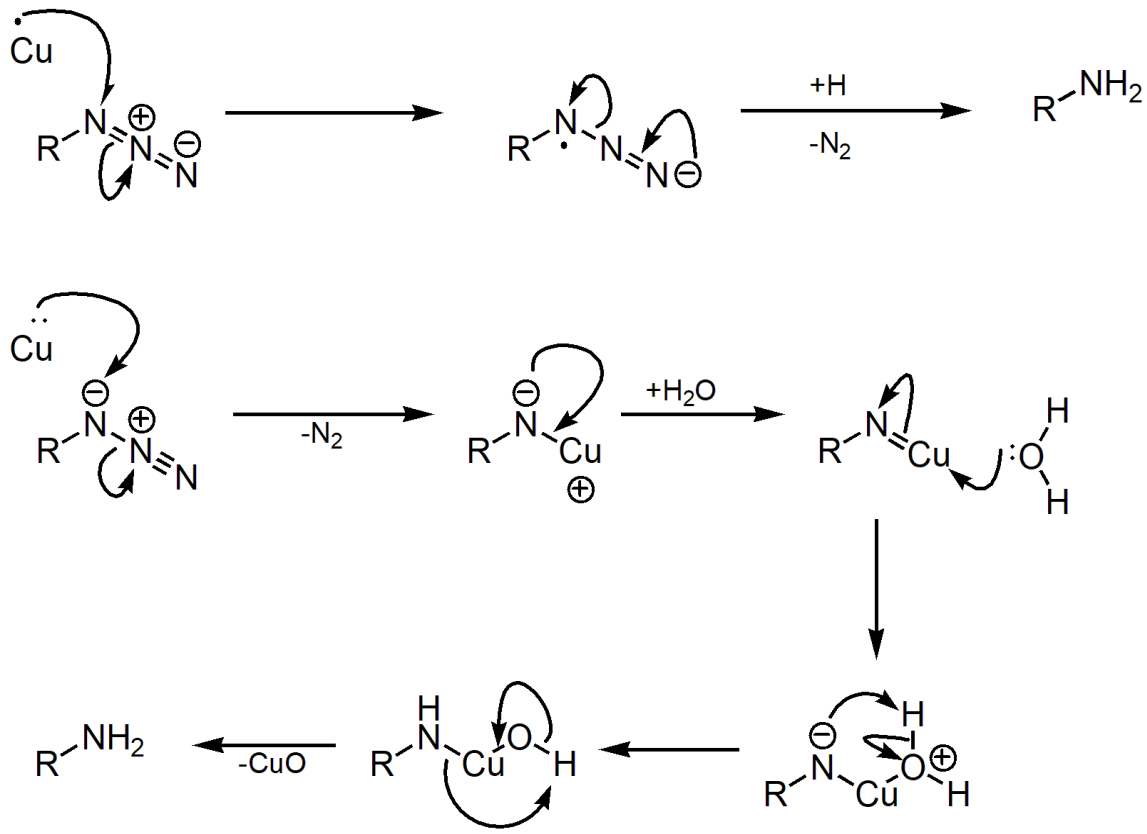

Figure 41. Two potential reduction mechanisms from the azide to amine. Top: reduction via radical addition from Cu(I) oxidising to Cu(II). Bottom: Formation of copper nitrene with subsequent hydrolysis to copper oxide.

An attempt at making the 4,16-di(benzylamino)[2.2]PC was made, however this was unsuccessful and only returned starting materials (Figure 42). This was unexpected, as I had observed no issues with the imine formation on 4-amino[2.2]PC. Due to the issues in the synthesis of the diamino product, predominately the length of time required and the low yield, attempts to make a [2.2]PC based linker were halted and I decided to attempt to synthesize a novel 2,5-dimethylpyrazine linker instead.

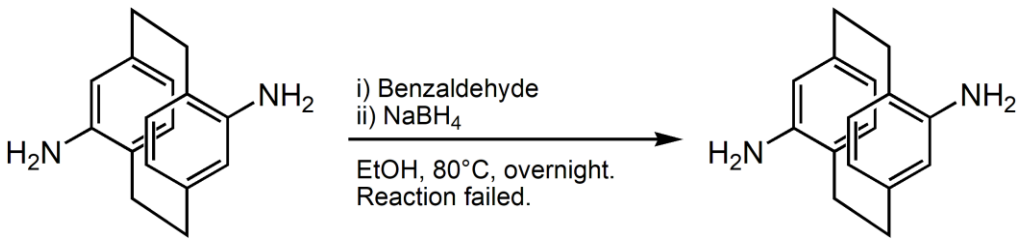

Figure 42. Attempted dibenzylation of 4,16-diamino[2.2]paracyclophane. Starting material returned.

2.2 2,5-Dimethylpyrazine ligand synthesis

The initial goal for the 2,5-dimethylpyrazine synthesis was to develop a route to making 2,5-di(methylamino)pyrazine (Scheme 3). This is because I wanted a diamine linker with which I would be able form a variety of different ligands. 2,5-di(carbaldehyde)pyrazine is commonly used as a bridging linker, however I wished to use the amine as it would allow me to add aldehydes or undertake alkylations, giving more freedom.

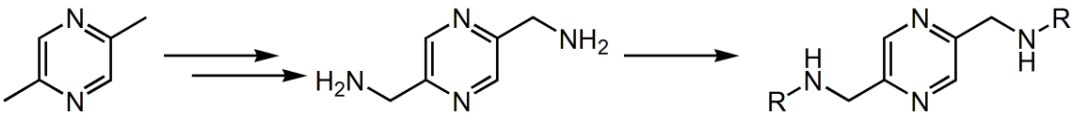

Scheme 3. Basic scheme for the pyrazine bridging linker. R is a metal-binding group.

2,5-Dimethylpyrazine is a readily available starting material, so I based our chemistry on converting this to the desired amine. Our first route was based on the known bromination of the methyl groups,[54] followed by substitution with an azide and reduction to give the desired diamine linker. While the bromination did furnish 2,5-di(bromomethyl)pyrazine (Figure 43), it was always contaminated with 2,5-di(dibromomethyl)pyrazine. All attempts to separate the two compounds were unsuccessful. I considered carrying the crude mixture forward and separating at a later stage, but as the next step was substitution with azide groups, this idea was abandoned. I was concerned that the amount of nitrogen in the molecule was too high. It is generally accepted that the ratio of carbon atoms to nitrogen atoms should be 3:1 or greater to reduce the chance of forming an explosive. While the desired product would have a 3:4 ratio of carbon:nitrogen, below the safe ratio, the tetraazo product that would be produced by the substitution of the tetrabromo would result in a carbon:nitrogen ratio of 3:7, which is, frankly, frightening. Attempts to avoid over bromination by altering the stoichiometry of the reaction were unsuccessful.

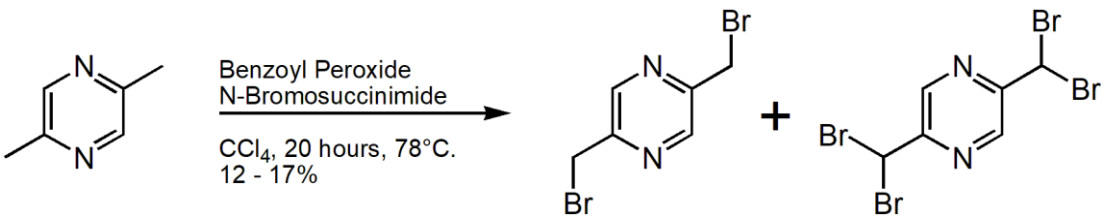

Figure 43. Bromination of 2,5-dimethylpyrazine forming 2,5-di(bromomethyl)pyrazine and 2,5-di(dibromomethyl)pyrazine.

Our alternative route was based on the oxidation of the methyl groups and conversion of the resulting alcohols into leaving groups. While the route is longer, I felt it would be more selective and give me more flexibility. Once I had the desired leaving groups I could form the diazide and reduce it to the diamine. The target diol, 2,5-di(hydroxymethyl)pyrazine, is a known compound and was synthesized according to literature methods (Figure 44).[55] While low yielding, with an overall yield range from 2.2 – 5.7%, the sequence could be conducted on a 20 gram scale, resulting in around 1 gram of 2,5-di(hydroxymethyl)pyrazine. The first reaction to form the nitrogen-oxide is a simple oxidation of the nitrogen, however it gave a much lower yield than reported in the literature. It is possible that the *m*-CPBA used was of a lower purity than indicated due to decomposition.

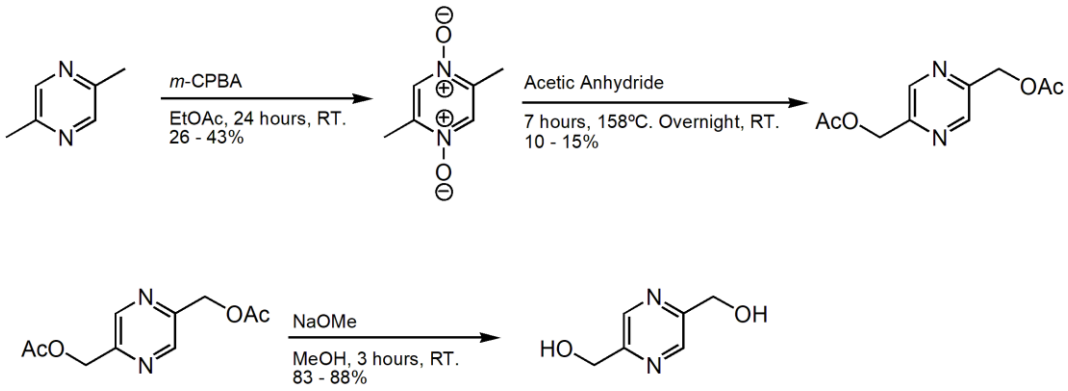

Figure 44. Formation of 2,5-di(hydroxymethyl)pyrazine from 2,5-dimethylpyrazine in 3 steps.

The second step also gave a poor yield. The analogous rearrangement of similar pyridine *N*-oxides is low yielding, indicating that this reaction is generally fickle. The likely mechanism for the rearrangement involves acetylation of the *N*-oxide. This activates the methyl groups, allowing the carboxylate anion to deprotonate the methyl to give an enamine-like species. There are two ways that the acetoxymethyl is formed, either by a nucleophilic attack on the methylene by an acetoxy group, or a [3,3]-sigmatropic rearrangement (Figure 45). For purification the acetic anhydride needed to be removed, with the residue then being stirred with diethyl ether for 2 hours and filtered. The filtrate was then columned (40% EtOAc in hexane) and recrystallized from EtOAc/hexane to give the pure product.

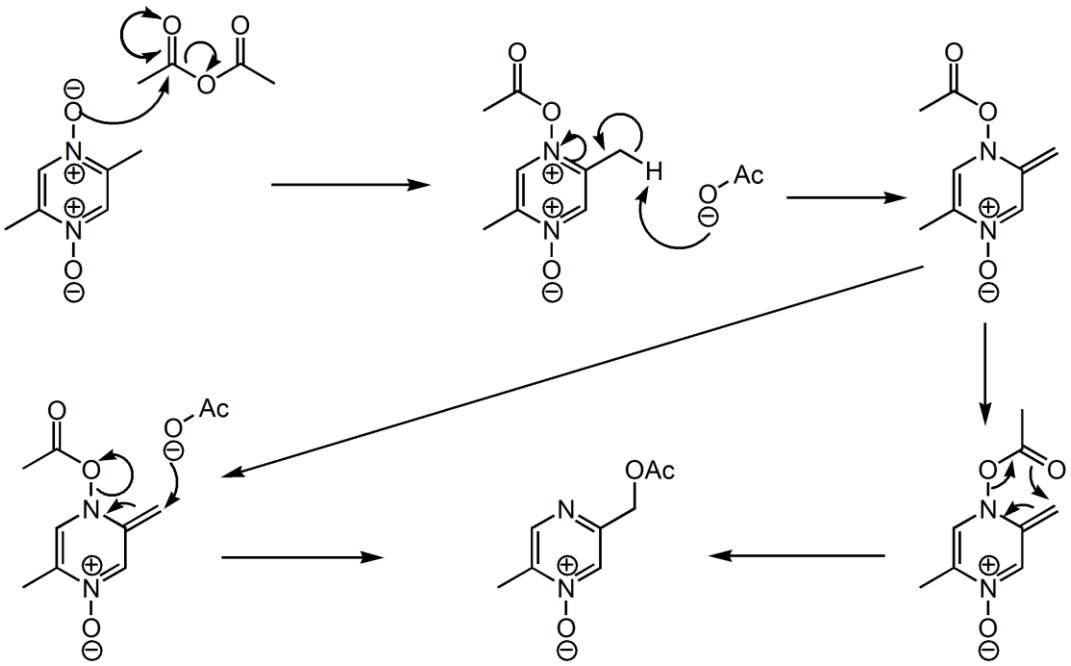

Figure 45. Mechanism for the rearrangement of 2,5-dimethylpyrazine-1,4-dioxide to 2,5-di(acetoxymethyl)pyrazine.

To produce 2,5-di(hydroxymethyl)pyrazine, 2,5-di(acetoxymethyl)pyrazine is hydrolysed with sodium methoxide in methanol (Figure 44). This is a simple deprotection and is quenched by the addition of ammonium chloride. It is high yielding, as would be expected from such a straight forward reaction.

As hydroxy groups are poor leaving groups, they were converted to tosylate groups by treatment with sodium hydroxide and 4-toluenesulfonyl chloride (Figure 46). This proceeded without incident. Substitution of the tosylate group with sodium azide was then attempted. It was found that just heating the tosylate with sodium azide in DMF overnight resulted in a moderate yield of 2,5-di(azidomethyl)pyrazine as an oil (54% average yield, Figure 47). Dissolving the oil in EtOAc and washing with H_2O removed the impurities from this product, which was fortuitous as distillation of azide oils is highly dangerous, therefore I was originally planning on proceeding with impure diazide and undertaking purification on the subsequent diamine.

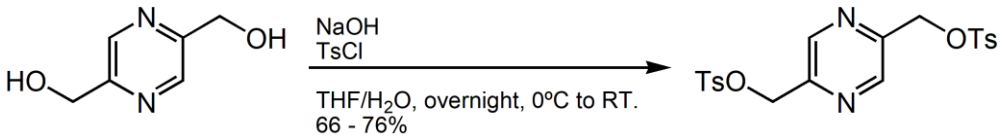

Figure 46. Tosylation of 2,5-di(hydroxymethyl)pyrazine

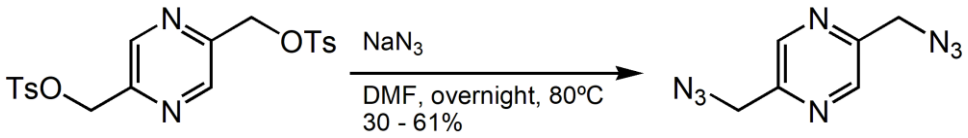

Figure 47. Substitution of tosylate for azido groups.

Conscious that the diazide had a high nitrogen to carbon ratio I was concerned that this molecule may be highly energetic/explosive. To test this, a small sample of the pure compound (~5 milligrams) was placed in an open flame. This resulted in a pop and a large flame. This fun experiment supports the idea that 2,5-di(azidomethyl)pyrazine was indeed a potential explosive, and care around this compound is required.

With the diazide in hand I looked at the reduction to give the requisite diamine. Testing different reduction conditions was undertaken on a small scale (70 – 100 mg) of the diazide, as I wanted to avoid storing large quantities of the azide due to the risk. A variety of reduction attempts were tried. For the first attempt I used $NaBH_4$ and *n*-Bu_4NI with a solvent mixture of THF and H_2O in a 3:2 ratio (Figure 48).[56] The *tetra*-butyl ammonium iodide was required for the phase transfer of the borohydride anion into the organic phase. These conditions have been successfully employed in the reduction of an azide to 4-amino[2.2]PC. The reaction was monitored by TLC, and additional $NaBH_4$ was added after 2 days, as it decomposes in H_2O. After 4 days the diazide spot on TLC was gone, and the solution was extracted with DCM and washed with H_2O. NMR of the organic layer confirmed that the diazide had been consumed, however no trace of the diamine was observed. A portion of the aqueous layer was freeze dried and a D_2O NMR run of the solid, revealing that the 2,5-di(aminomethyl)pyrazine had gone into the aqueous layer. Unfortunately the salts present in the aqueous layer prevented an accurate yield of the product.

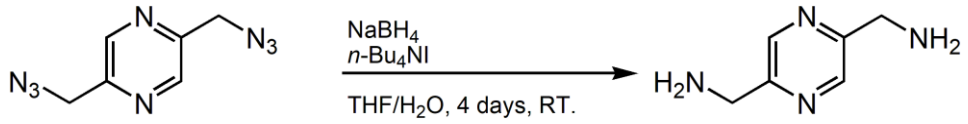

Figure 48. Reduction of 2,5-di(azidomethyl)pyrazine with $NaBH_4$. Product is water soluble.

The mechanism for this reduction begins with the azido group being attacked by a hydride from $NaBH_4$ (Figure 49). This anion is able to cross the phase barrier from

the aqueous to organic due to the *tetra*-butyl ammonium iodide acting as a phase transfer catalyst.[57] Nitrogen gas is then expelled simultaneously with the resulting NH- species being protonated by water to give 2,5-di(aminomethyl)pyrazine. The water solubility of the diamine should not have come as a surprise; the nitrogen atoms and amine functionality make this molecule both a good hydrogen bond donor and acceptor. The diamine was unable to be purified, and so different reduction attempts were undertaken.

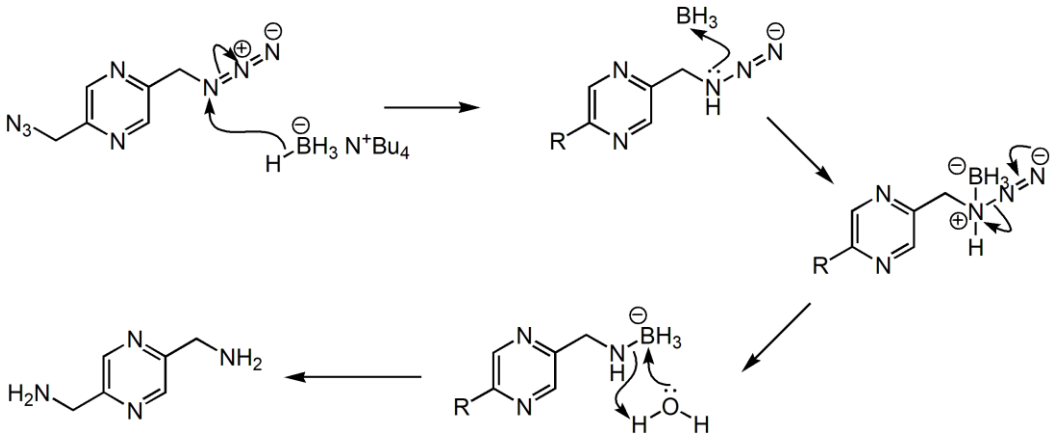

Figure 49. Reduction of 2,5-di(azidomethyl)pyrazine with $NaBH_4$.

Next I attempted hydrogenation of the diazide with hydrogen gas over Pd/C, however this was unsuccessful and returned only diazide (Figure 50). I then attempted a reduction with triphenylphosphine (Figure 51) otherwise known as the Staudinger reduction, as this reaction only requires a small quantity of H_2O to form the amine from an iminophosphorane (Figure 52). This reduction occurs by a phosphazide being formed by the triphenylphosphine attacking the azide. Nitrogen gas is then expelled to form an iminophosphorane which can be hydrolysed by the addition of H_2O to form the amine and phosphine oxide.[58] Unfortunately, while the reduction was successful, there was enough H_2O present for the diamine to remain in the aqueous phase.

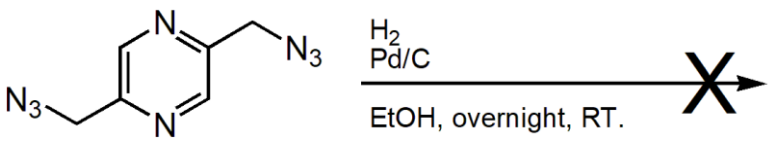

Figure 50. Attempted reduction of 2,5-di(azidomethyl)pyrazine with hydrogen gas over Pd/C.

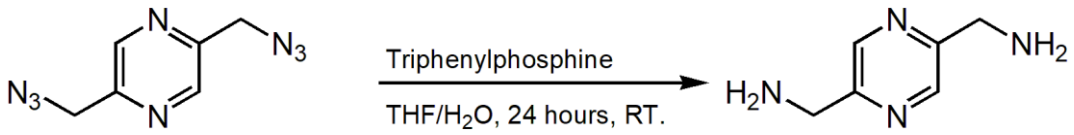

Figure 51. Reduction of 2,5-di(azidomethyl)pyrazine with triphenylphosphine.

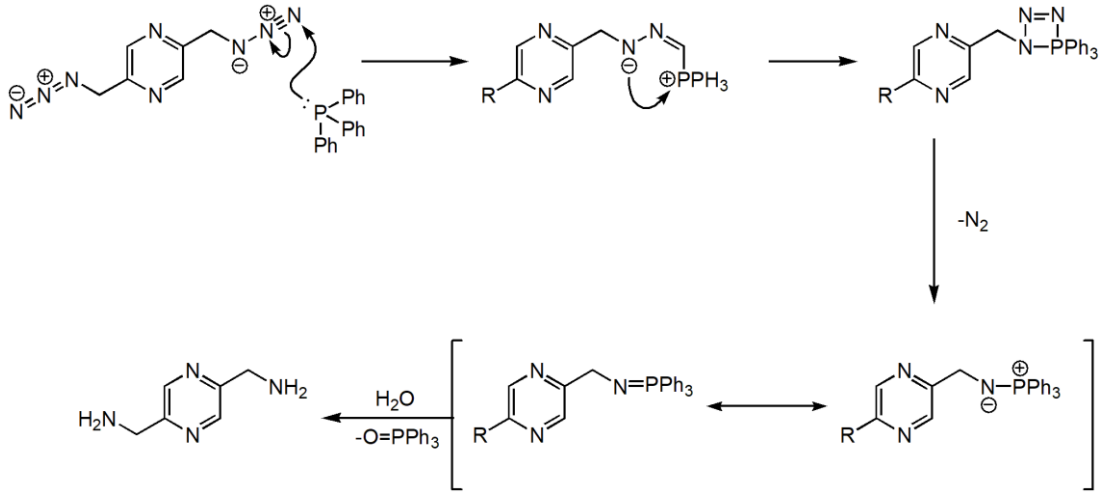

Figure 52. Mechanism for the reduction of 2,5-di(azidomethyl)pyrazine with triphenylphosphine.

Due to the issues in obtaining and purifying 2,5-di(aminomethyl)pyrazine, I decided to attempt to couple the 2,5-di(azidomethyl)pyrazine to our previously made salicylaldehyde molecule (Figure 30, middle) through the aza-Wittig reaction.[59] I did not use the brominated derivative of the salicylaldehyde molecule because I wanted to be certain that the coupling would occur between the aldehyde and the pyrazine. The aza-Wittig reaction works by forming an iminophosphorane, as shown above in Figure 52. However, instead of adding H_2O to form the amine, an aldehyde or ketone is added and an imine bond between the carbonyl carbon and the nitrogen of the iminophosphorane is formed (Figure 53).

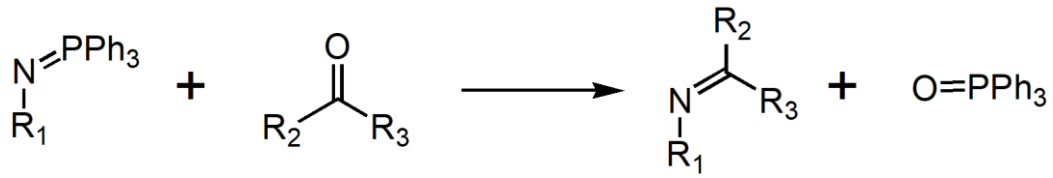

Figure 53. aza-Wittig reaction motif.

The diazide was stirred with triphenylphosphine in dry THF overnight to form the iminophosphorane. Next 5-*tert*-butyl-2-hydroxybenzaldehyde in THF was added and stirred for an additional 6 hours. This formed ((*E*)-2,5-bis((5-*tert*-

butyl-2-hydroxybenzylideneamino)methyl)) pyrazine (L_2, Figure 54). Purification was achieved by silica gel column chromatography, requiring 2 drops of triethylamine per litre of solvent to prevent hydrolysis of the imine.

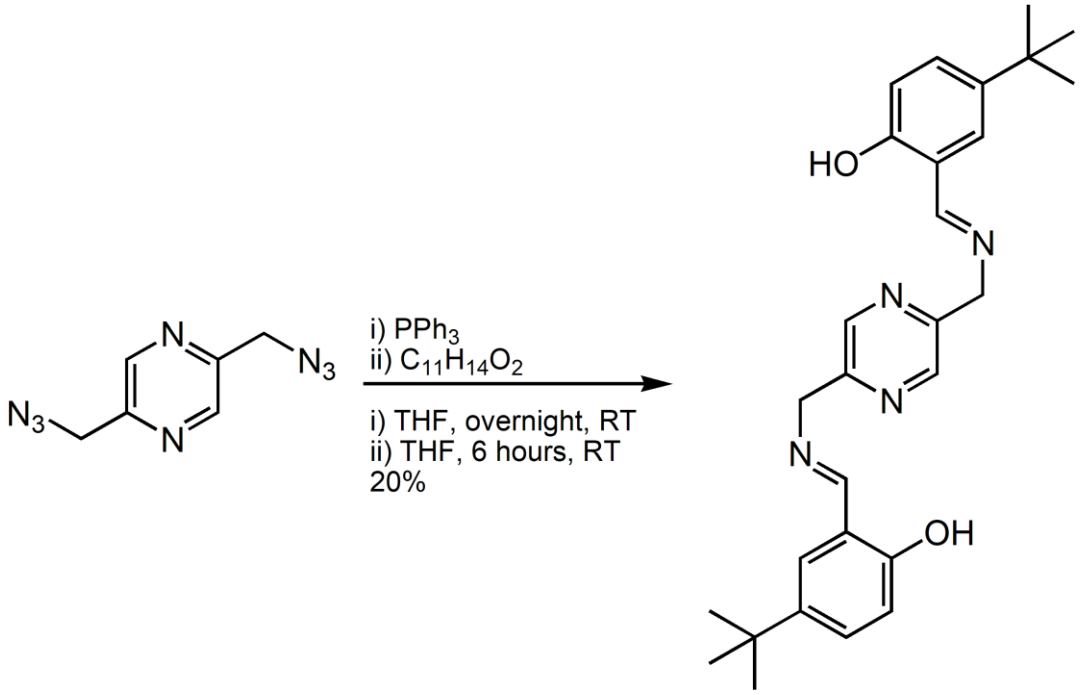

Figure 54. Formation of L_2

An attempt to make (*E*)-2,5-bis((pyridin-2-ylmethyleneamino)methyl)pyrazine was undertaken using the same method with 2-pyridinecarboxaldehyde, however I was unable to obtain the desired product (Figure 55). The crude NMR from this reaction showed that some diazide remained, while 2-pyridinecarboxaldehyde was not present. Due to the large triphenylphosphine oxide peaks present in the crude NMR, purification was attempted by silica gel column chromatography. Unfortunately the only product obtained from this column was the triphenylphosphine oxide. Even with the addition of triethylamine in the solvent, any product that may have been present may still have been hydrolysed, as unlike L_2 it would not have the hydrogen bonding between the phenol and imine to stabilise the imine bond. It would be good to repeat this reaction with an alternative alkylphosphine. While these are malodorous and some are pyrophoric, they are more reactive and would allow for the inspection of the aromatic region of the ^{1}H NMR spectrum.

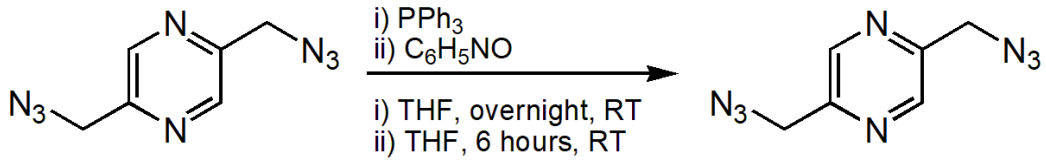

Figure 55. Attempted reaction to make (*E*)-2,5-bis((pyridin-2-ylmethyleneamino)methyl) pyrazine.

Complexations and subsequent crystallizations of L_2 were undertaken (see experimental for details). No base was required in the complexations as only the phenol required deprotonating, and the metal salt was strong enough to do this. While colour changes were observed upon stirring, mass spectrometry results only returned peaks matching L_2, indicating that either the complexations did not work, or more likely, that the complex falls apart on the probe due to the high temperature required. Crystallization attempts were unsuccessful.

I was still interested in introducing pyridine onto a pyrazine linker, in part due to previous work which incorporates these two groups in various ways.[35-37] Using a variation of the aza-Wittig reaction, I stirred 2,5-di(azidomethyl)pyrazine, triphenylphosphine and picolinic acid together at 110°C for 48 hours (Figure 56).[60-61] This reaction was inspired by the Staudinger ligation, and I had hoped that this would result in 2,5-di(picolinamidomethyl)pyrazine (L_3), however this was not the case. Due to the failure of this method, I decided to go through the full Staudinger reduction to form 2,5-di(aminomethyl)pyrazine, to which I would add the acyl chloride of picolinc acid in a one pot reaction to form L_3 (Figure 57).[62] This was successful, and so I attempted a complexation with cobalt due to previously reported complexes with similar ligands showing an affinity for forming cobalt complexes. I wished to use $Co(BF_4)_2$ as the metal salt, however that was unavailable so I used $CoCl_2$ with $NaBF_4$ added to provide the BF_4 anions. A colour change from purple to brown was observed, and platelet crystals were grown by diffusing Et_2O into a solution of the complex in MeOH. Unfortunately no single crystals were able to be isolated, and as such X-ray data was unable to be collected.

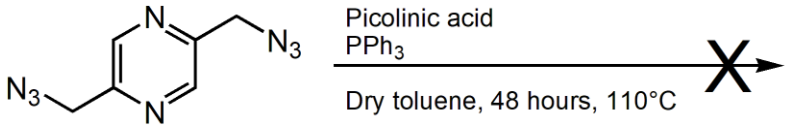

Figure 56. Attempted reaction between 2,5-di(azidomethyl)pyrazine and picolinic acid.

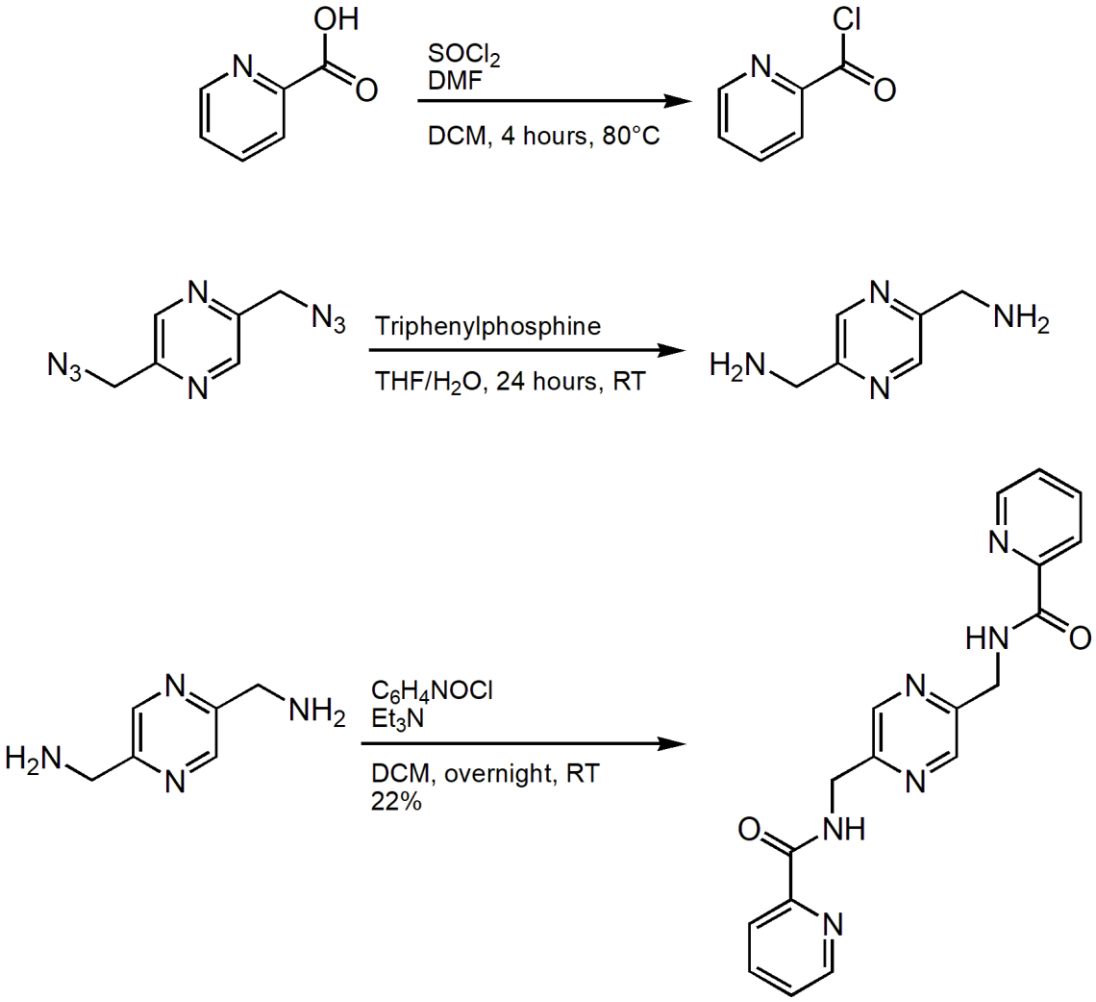

Figure 57. Formation of L_3.

3. Conclusion

This project had a number of successes; a novel synthesis of 4-(benzylamino)[2.2]PC was developed and this provided a route to [2.2]PC-based ligands for the potential formation of SMMs. Three new [2.2]PC compounds, two of which are able to be used as ligands, were synthesized during this research (Figure 58).

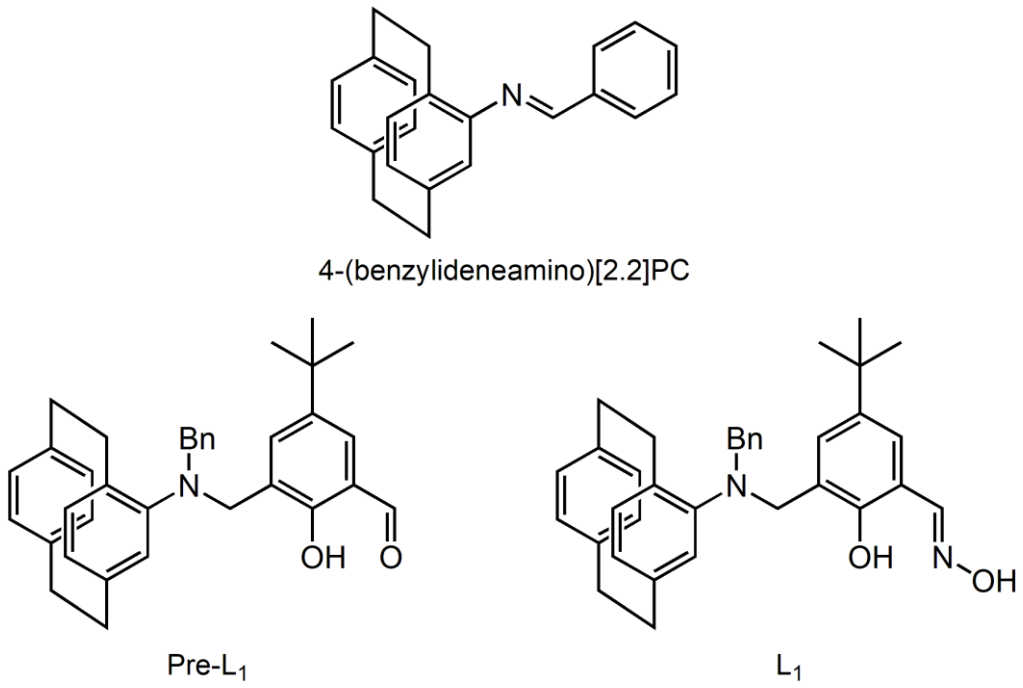

Figure 58. The three new [2.2]PC compounds synthesized during this research.

A new route to make 4,16-diamino[2.2]PC was developed (Figure 59), along with the first reported purification method for this compound.[29] Unfortunately poor yields of this compound coupled with an inability to scale the reaction resulted in work on this being stopped for more productive research avenues.

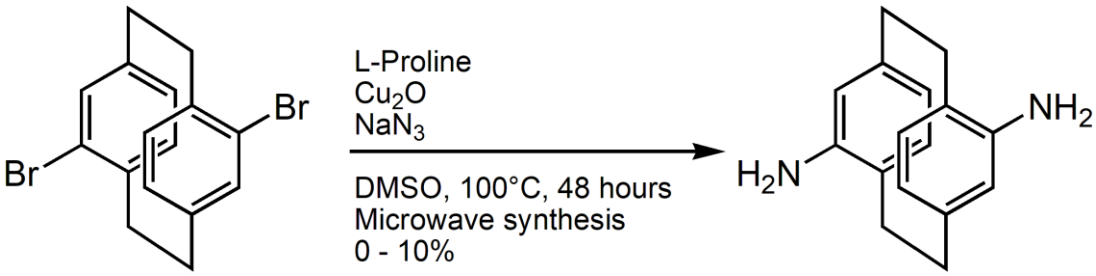

Figure 59. Synthesis of 4,16-diamino[2.2]PC.

Success was also had developing a route to make ligands with a pyrazine bridging moiety, with 2,5-di(azidomethyl)pyrazine and 2,5-di(aminomethyl)pyrazine being successfully synthesized and used in the formation of new pyrazine ligands. 2,5-Di(azidomethyl)pyrazine in particular shows great potential for the synthesis of new ligands. Five new pyrazine compounds were synthesized during this research, two of which are ligands (Figure 60).

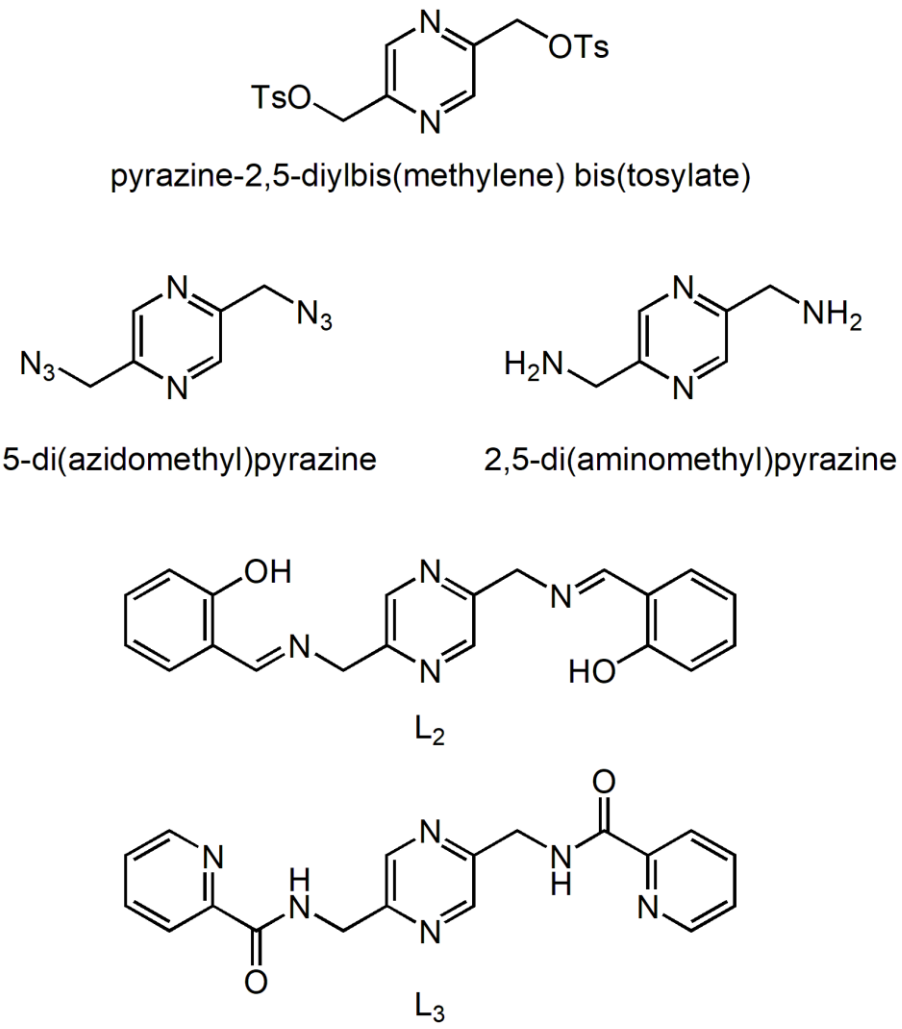

Figure 60. The five new pyrazine compounds synthesized during this research.

Complexation attempts with all three ligands were undertaken, however crystals of sufficient quality to obtain X-ray crystallography data from were unable to be obtained. With more time I am confident that this hurdle could have been overcome.

4. Future Work

Multiple avenues for future work exist from the work done in this research. One project of considerable interest would be making more Pre-L_1 and obtaining a crystal structure so that the solid state conformation of the compound could be determined. A key goal would be either the synthesis of enantiomerically enriched 4-(benzylamino)[2.2]PC or the resolution of one of the intermediates. With a pure enantiomer, I believe growth of suitable crystals would be easier as there would not be the formation of diastereomeric mixtures. Synthesis of enantiomerically pure 4-amino[2.2]PC would also facilitate the study of linked/bridged ligands, such as bridging two units of Pre-L_1 together with various bridge lengths and functionalities and complexing them with various metals (Figure 61). Another avenue of future work with mono[2.2]PC is successfully growing X-ray quality crystals of L_1 complexes and testing them for SMM behaviour.

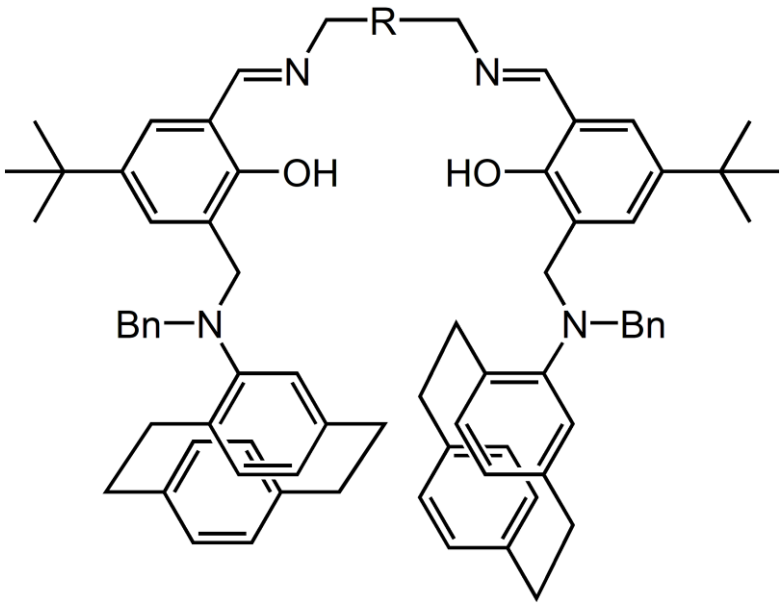

Figure 61. Basic structure of a bridged [2.2]PC based structure.

Improving the synthesis of 4,16-diamino[2.2]PC is another area that requires more work, as this compound would have a variety of potential uses if it could be produced on a large scale. Potential changes that could improve this synthesis include putting the reaction under increased pressure, trying different ligands in the reaction or trying a different amination route.

2,5-Di(azidomethyl)pyrazine and its derivatives show huge potential for the synthesis of new ligands. I have already shown that it can be used to form a bridging linker through aza-Wittig and Staudinger reactions, allowing for a variety of novel ligands to be synthesized with relative ease (Figure 62). This molecule also has the potential to be used in the alkyne-azide cycloaddition or ‘click’ reaction, providing another route to produce novel polycyclic bridged ligands. (Figure 62).

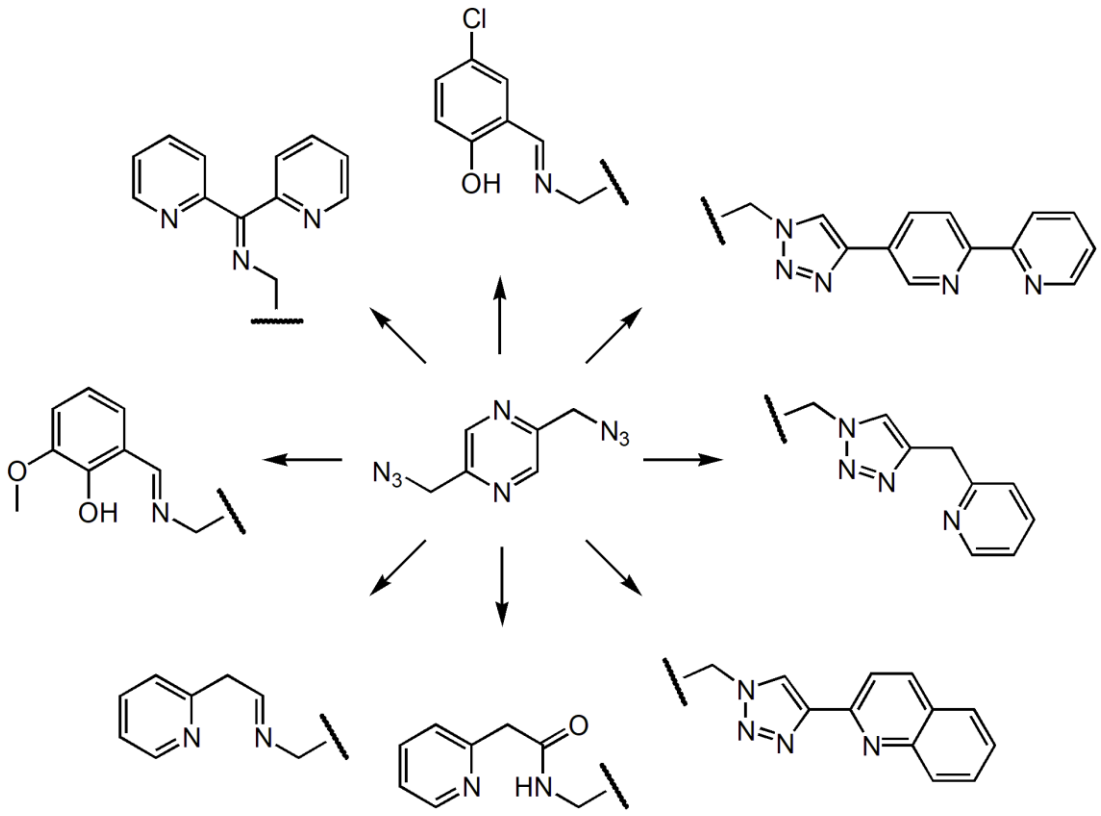

Figure 62. Future work for 2,5-di(azidomethyl)pyrazine.

5. Experimental Methods

All starting compounds and solvents were used as received from commercial sources without further purification unless otherwise noted. All reactions were performed in oven-dried glassware under an atmosphere of argon or nitrogen unless otherwise stated. Column chromatography was carried out on silica gel (grade 60, mesh size 230–400, Scharlau). Visualisation techniques employed included using ultraviolet light (254 nm), potassium permanganate, or ninhydrin when applicable. NMR spectra were recorded at room temperature on Bruker-400 or Bruker-500 Avance instruments, with the use of the solvent proton as an internal standard. Melting points were recorded on a Gallenkamp melting point apparatus and are uncorrected. Mass spectra and high-resolution mass spectrometry were performed at Massey University, using a ThermoScientific Q Exactive Focus Hybrid Quadrupole-Orbitrap Mass Spectrometer.

Numbering method of [2.2]paracyclophane

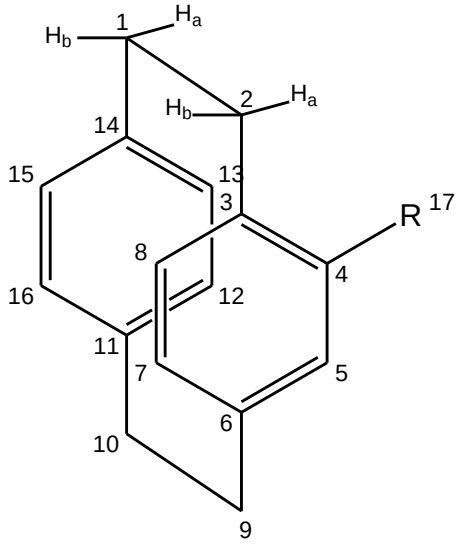

Synthesis of 4-formyl[2.2]paracyclophane

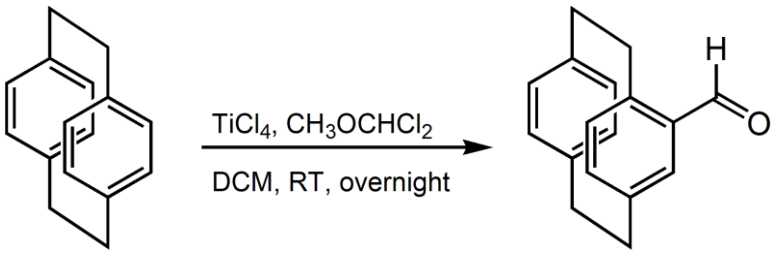

To a solution of [2.2]paracyclophane (2.00 g, 9.62 mmol, 1 eq.) in DCM (48 ml, 0.2 M) at -10°C under argon was added $TiCl_4$ (3.65 g, 2.10 ml, 19.23 mmol, 2 eq.) and CH_3OCHCl_2 (1.22 g, 0.96 ml, 10.59 mmol, 1.1 eq.). The solution was warmed to room temperature and stirred overnight. Ice was added to quench the reaction and the product was extracted into DCM (3 x 20 ml). The combined organics were washed with saturated $NaHCO_3$ (10 ml), H_2O (10 ml), and brine (10 ml), dried ($MgSO_4$) and filtered. The solvent was removed under reduced pressure to give a white powder. The product was purified by silica gel column chromatography eluting with 5:1 hexane:EtOAc, resulting in a white powder (1.41 g, 5.96 mmol, 62%).

^{1}H NMR ($CDCl_3$, 500 MHz): δ = 9.98 (1H, s, H-17), 7.04 (1H, d, J = 1.9 Hz, H-5), 6.76 (1H, dd, J = 7.5, 1.9 Hz, C<u>H</u>), 6.62 (1H, d, J = 7.7 Hz, C<u>H</u>), 6.59 (1H, dd, J = 7.7, 1.8 Hz, C<u>H</u>), 6.53 (1H, dd, J = 7.7, 1.8 Hz, C<u>H</u>), 6.46 (1H, dd, J = 7.7, 1.8 Hz, C<u>H</u>), 6.40 (1H, dd, J = 7.7, 1.8 Hz, C<u>H</u>), 4.13 (1H, t, J = 11.6 Hz, H-2a), 3.34 – 2.95 (7H, m, H-1, H-2b, H-9, H-10). Data comparable to that reported in the literature.[63]

Synthesis of [2.2]paracyclophane-4-carbaldehyde oxime

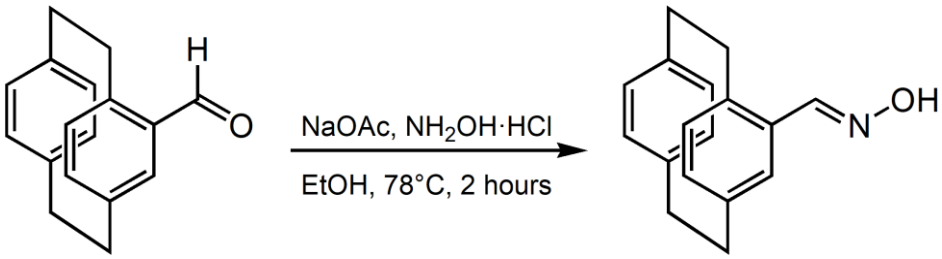

A solution of 4-formyl[2.2]paracyclophane (9.29 g, 39.22 mmol, 1 eq.) and sodium acetate (16.09 g, 196.20 mmol, 5 eq.) in EtOH (240 ml) was heated to reflux. $NH_2OH{\cdot}HCl$ (10.92 g, 157.06 mmol, 4 eq.) was added in portions over 5 minutes and the solution was refluxed for 2 hours. The solvent was then removed under reduced pressure and the solid was washed with H_2O (40 ml) and extracted with DCM (2 x 40 ml). Combined organics were dried ($MgSO_4$) and filtered. The solvent was removed under reduced pressure to give the desired product as a white powder that was pure by NMR (8.37 g, 33.4 mmol, 85%).

^{1}H NMR (500 MHz, $CDCl_3$): δ = 8.16 (1H, s, H-17), 6.77 (1H, d, J = 1.1 Hz, H-5), 6.66 (1H, d, J = 7.8 Hz, C<u>H</u>), 6.56 (1H, dd, J = 7.8, 1.9 Hz, C<u>H</u>), 6.53 – 6.43 (4H, m, C<u>H</u>), 3.62 – 3.56 (1H, m, H-2a), 3.20 – 2.84 (7H, m, H-1, H-2b, H-9, H-10). Data comparable to that reported in the literature.[64]

Synthesis of hydroxy(tosyloxy)iodobenzene (Koser's reagent)

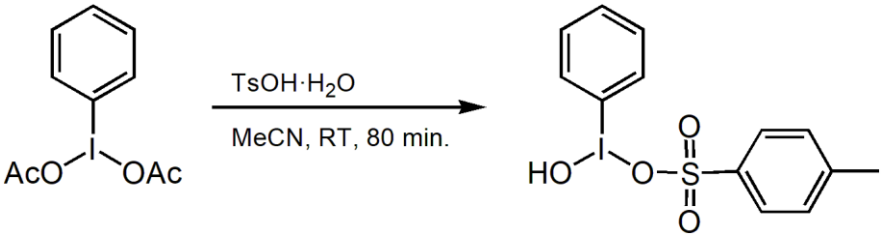

Iodobenzene diacetate (6.03 g, 18.72 mmol, 1 eq.) was suspended in MeCN (44 ml), and toluene-4-sulfonic acid-monohydrate (7.09 g, 37.29 mmol, 2 eq.) was dissolved in the minimum of MeCN (~45 ml). The toluene-4-sulfonic acid solution was then added dropwise to the suspended iodobenzene diacetate while stirring. The suspension dissolved and a white precipitate formed shortly afterwards. The combined solutions were then left to stand at room temperature for 80 minutes, after which the precipitate was filtered off and washed with acetone (30 ml). Product is a white solid, pure by NMR (5.24 g, 13.36 mmol, 71%).

^{1}H NMR (500 MHz, DMSO): δ = 9.78 (1H, brs, O<u>H</u>), 8.30 (2H, dd, J = 8.3, 0.9 Hz), 7.73 (1H, t, J = 7.4 Hz), 7.63 (2H, t, J = 7.7 Hz), 7.49 (2H, d, J = 8.1 Hz), 7.12 (2H, d, J = 8.1 Hz), 2.30 (3H, s, C<u>H</u>$_3$). Data is comparable to that found in the literature.[65]

Synthesis of 4-amino[2.2]paracyclophane

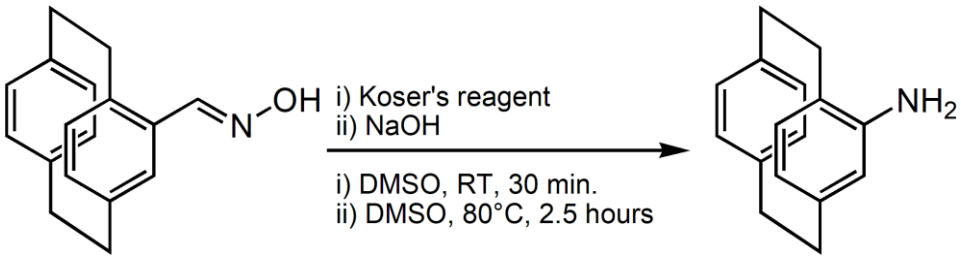

A solution of [2.2]paracyclophane-4-carbaldehyde oxime (1.03 g, 4.08 mmol, 1 eq.) and Koser's reagent (1.74 g, 4.41 mmol, 1.1 eq.) in DMSO (13 ml) was stirred at room temperature for 30 minutes. The solution was then heated to 80°C and stirred for one hour. Crushed NaOH (0.33 g, 8.15 mmol, 2 eq.) was added to the solution and it was refluxed for another 90 minutes. H_2O (20 ml) was added to quench the reaction, with a precipitate being formed. The product was extracted with EtOAc (3 x 30 ml) and the combined organics were washed with H_2O (30 ml). Solution was dried ($MgSO_4$), filtered and the solvent was removed under reduced pressure. Product was purified by silica gel column chromatography eluting with 4:1 hexane:EtOAc, resulting in a yellow powder (0.40 g, 1.92 mmol, 44%).

^{1}H NMR (500 MHz, $CDCl_3$): δ = 7.20 (1H, dd, J = 7.8, 1.7 Hz, Ar-H), 6.61 (1H, dd, J = 7.8, 1.7 Hz, Ar-H), 6.42 (2H, m, Ar-H), 6.30 (1H, d, J = 7.8 Hz, H-8), 6.17 (1H, dd, J = 7.8, 1.7 Hz, H-7), 5.38 (1H, d, J = 1.6 Hz, H-5), 4.09 – 3.42 (2H, brs, NH_2), 3.20 – 2.94 (6H, m, H-1b, H-2b, H-9, H-10), 2.91 – 2.82 (1H, m, H-1a), 2.75 – 2.65 (1H, m, H-2a). Data is comparable to that found in the literature.[45,56]

Synthesis of 4-nitro[2.2]paracyclophane

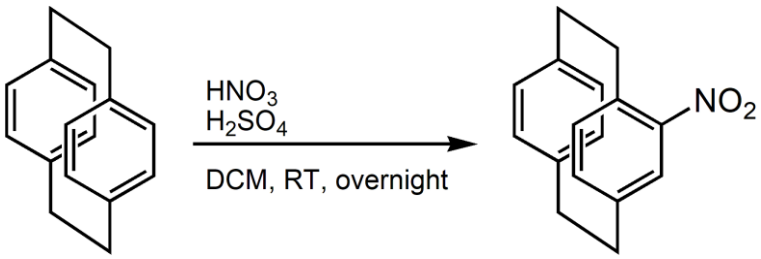

Crushed [2.2]paracyclophane (5.94 g, 28.56 mmol, 1 eq.) was dissolved in DCM (150 ml) and added slowly to a solution of H_2SO_4 (6.42 ml, 117.10 mmol, 4.1 eq.) and HNO_3 (3.42 ml, 74.26 mmol, 2.6 eq.) in DCM (300 ml) at 0°C. The solution was stirred for 15 minutes, allowed to return to room temperature and stirred overnight. The solution was carefully poured over ice, taking care to keep the black oil in the reaction vessel. The solution that was poured over the ice was extracted with DCM (3 x 50 ml), combined organics were washed with H_2O (3 x 50 ml), dried with anhydrous $MgSO_4$ and filtered. Solvent removed under vacuum, product given as an orange powder (2.36 g, 9.43 mmol, 33%).

^{1}H NMR (500 MHz, CDCl3): δ = 7.22 (1H, d, J = 1.8 Hz, Ar-H), 6.79 (1H, dd, J = 7.9, 1.8 Hz, Ar-H), 6.63 (2H, dd, J = 7.8, 2.4 Hz, Ar-H), 6.57 (2H, ddd, J = 14.0, 7.8, 1.7 Hz, Ar-H), 6.48 (1H, dd, J = 7.8, 1.8, Ar-H), 4.03 (1H, ddd, J = 13.2, 9.5, 1.9 Hz, CH_2), 3.24–3.04 (6H, m , CH_2), 2.90 (1H, ddd, J= 13.2, 9.9, 7.2 Hz , CH_2). Data comparable to that reported in the literature.[66]

Synthesis of 4-amino[2.2]paracyclophane

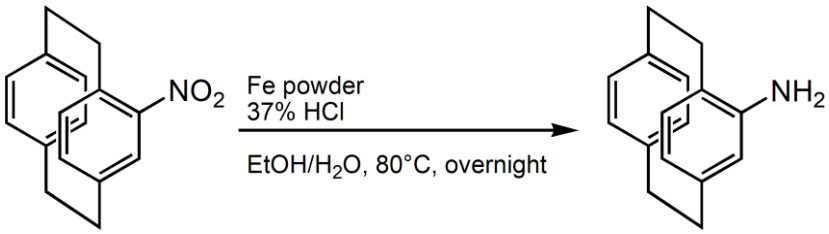

Iron powder (2.94 g, 52.60 mmol, 11.8 eq.) was added to a solution of 4-nitro[2.2]paracyclophane (1.12 g, 4.43 mmol, 1 eq.) in EtOH/H_2O (1:1 ratio, 50 ml). Solution brought to 80°C and 37% HCl (16.1 ml, 530 mmol, 116 eq.) was added dropwise. Solution refluxed overnight, cooled to room temperature and poured slowly into cold $NaHCO_{3(aq., sat.)}$ (50 ml). Product extracted with EtOAc (3 x 50 ml), and the combined organics were washed with H_2O (3 x 50 ml). Dried with anhydrous $MgSO_4$, filtered and dried under vacuum. Product yielded as yellow/orange powder (0.30 g, 1.33 mmol, 30%). Data as before (See above).

Synthesis of 4-(benzylideneamino)[2.2]paracyclophane

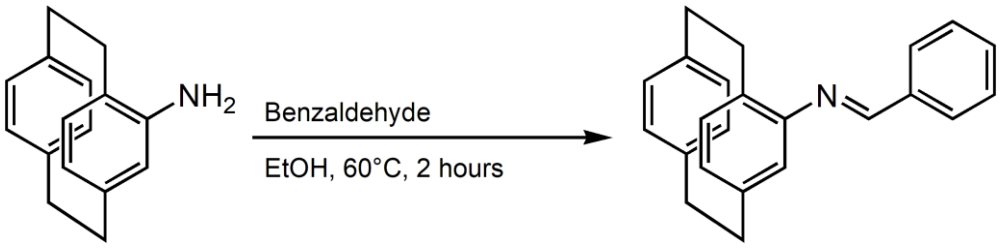

A solution of 4-amino[2.2]paracyclophane (0.50 g, 2.24 mmol, 1 eq.) in EtOH (25 ml) was heated to 60°C and C_7H_6O (0.46 ml, 4.48 mmol, 2 eq.) was added dropwise. The solution was stirred for 2 hours, cooled to room temperature and placed in the fridge overnight. The crystals that formed were filtered off and washed with cold EtOH (5 ml). The solvent was removed under vacuum, washed with cold EtOH (5 ml) and filtered again. The crystals formed were pure (0.57 g, 1.84 mmol, 82%).

^{1}H NMR (500 MHz, $CDCl_3$): δ = 8.19 (1H, s, N=C<u>H</u>), 8.00 (2 H, m, Ar-<u>H</u>), 7.54 (3H, m, Ar-<u>H</u>), 6.92 (1H, d, J = 7.8 Hz, Ar-<u>H</u>), 6.58 (2H, dd, J = 26.8, 11.1 Hz, Ar-<u>H</u>), 6.52 (2H, s, Ar-<u>H</u>), 6.39 (2H, d, J = 7.8 Hz, Ar-<u>H</u>), 5.92 (1H, s, Ar-<u>H</u>), 3.78 (1H, t, J = 6.2 Hz, C<u>H</u>$_2$), 3.36 (1H, m, C<u>H</u>$_2$), 3.20 – 2.97 (5H, m, C<u>H</u>$_2$), 2.74 (1H, m, C<u>H</u>$_2$).

^{13}C NMR (125 MHz, $CDCl_3$): δ = 157.3, 149.7, 141.3, 140.4, 138.8, 137.0, 135.3, 134.5, 133.3, 132.7, 131.9, 131.0, 130.7, 130.0, 128.8, 125.0, 35.3, 35.0, 34.6, 32.7.

Mp: 131.6-134.2 °C

HRMS-EI: *m/z* found: $[M]^+$, 312.1726. $C_{23}H_{21}N$ requires $[M]^+$, 312.1747.

IR: 2952, 2920, 2881, 2850, 1892, 1625, 1577, 1556, 1500, 1448, 1429, 1411, 1362, 1311, 1206, 1172, 1150, 1108, 1090, 1073, 1023 cm^{-1}

Synthesis of 4-(benzylamino)[2.2]paracyclophane

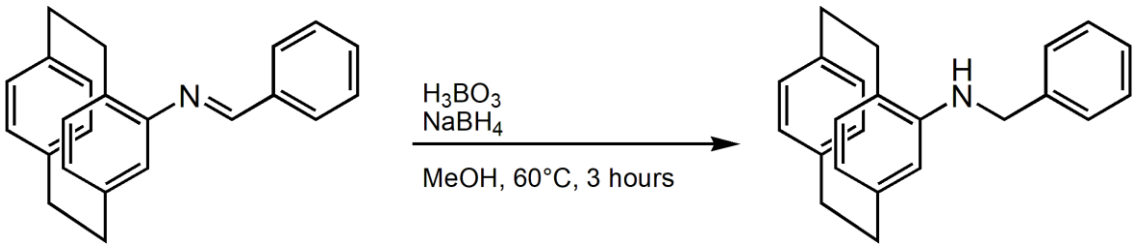

A solution of 4-(benzylideneamino)[2.2]paracyclophane (0.57 g, 1.82 mmol, 1 eq.) in dry MeOH (50 ml) was heated to 60°C. H_3BO_3 (0.1300 g, 2.10 mmol, 1.1 eq.) was added and small amounts of $NaBH_4$ were added every 5 minutes until the reaction stopped bubbling upon addition. H_2O (40 ml) was added and the solution cooled to room temperature. The product was extracted with DCM (3 x 30 ml) and the combined organics were washed with H_2O (30 ml). Dried with anhydrous $MgSO_4$, filtered and solvent removed under vacuum. Pure product yielded (0.43 g, 1.37 mmol, 75%).

^{1}H NMR (500 MHz, $CDCl_3$): δ = 7.49 (2H, d, J = 7.4 Hz, H-19, H-23), 7.43 (2H, t, J = 7.4 Hz, H-20, H-22), 7.36 (1 H, t, J = 7.3 Hz, H-21), 7.03 (1H, d, J = 7.20 Hz, Ar-H), 6.60 (1H, dd, J = 7.78, 1.53 Hz, Ar-H), 6.45 – 6.38 (2H, m, Ar-H), 6.33 (1H, d, J = 7.55 Hz, Ar-H), 6.16 (1H, d, J = 6.70 Hz, Ar-H), 5.46 (1H, br, H-5), 4.28 (1H, d, J = 12.90 Hz, H-17), 4.12 (1H, d, J = 13.00 Hz, H-17), 3.81 (1H, brs, NH), 3.20 – 2.90 (7H, m, H-1, H-2b, H-9, H-10), 2.85 – 2.78 (1H, m, H-2a). Data comparable to that reported in the literature.[52]

Synthesis of 5-*tert*-butyl-2-hydroxybenzaldehyde

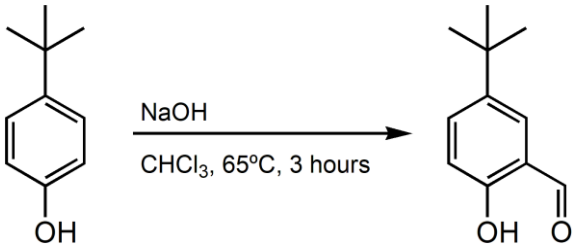

4-*tert*-Butylphenol (10.02 g, 66.70 mmol, 1 eq.) and crushed NaOH (22.23 g, 555.80 mmol, 8.3 eq.) were added to a mixture of $CHCl_3$ (150 ml) and H_2O (2.4 ml) and refluxed at 65°C for 1 hour. Additional NaOH (10.80 g, 270.00 mmol, 4 eq.) and H_2O (1.2 ml) was added, and the mixture was refluxed for another hour, repeated once. The solution was cooled to room temperature and the pH brought to 5 with addition of concentrated HCl. H_2O (100 ml) was added, and the product was extracted with DCM (3 x 50 ml). The combined organics were washed with H_2O (3 x 25 ml), dried with anhydrous $MgSO_4$ and filtered. The solvent was removed under vacuum and the product was purified with silica gel chromatography using a gradient from pure hexane to a 1:3 DCM:hexane solution (1.30 g, 7.34 mmol, 11%). TLCs were run with a 9:1 hexane:EtOAc solution.

^{1}H NMR (500 MHz, $CDCl_3$): δ = 10.80 (1H, s, Ar-O<u>H</u>), 9.82 (1H, s, Ar-C<u>H</u>O), 7.52 (1H, dd, J = 2.4 Hz, Ar-<u>H</u>), 7.44 (1H, d, J = 2.4 Hz, Ar-<u>H</u>), 6.86 (1H, s, Ar-<u>H</u>), 1.25 (9H, s, C-(C<u>H</u>$_3$)$_3$. Data comparable to that reported in the literature.[67]

Synthesis of 3-(bromomethyl)-5-*tert*-butyl-2-hydroxybenzaldehyde

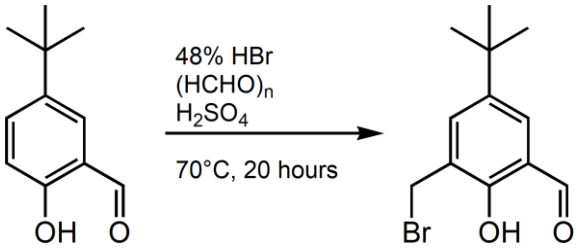

To a mixture of 5-*tert*-butyl-2-hydroxybenzaldehyde (1.31 g, 7.36 mmol, 1 eq.) and paraformaldehyde (0.35 g, 11.66 mmol, 1.6 mmol) was added 48% HBr in acetic acid (3 ml, 54.14 mmol, 7.5 eq.) and concentrated H_2SO_4 (10 drops). Solution stirred at 70°C for 20 hours, cooled to room temperature and H_2O (20 ml) was added. Product extracted with DCM (3 x 20 ml), dried with anhydrous $MgSO_4$ and filtered. Solvent removed under vacuum, product yielded as brown solid (0.97 g, 3.61 mmol, 49%).

^{1}H NMR (500 MHz, $CDCl_3$): δ = 11.35 (1H, s, C<u>H</u>O), 9.92 (1H, s, O<u>H</u>), 7.66 (1H, d, J = 2.5 Hz, Ar-<u>H</u>), 7.53 (1H, d, J = 2.5 Hz, Ar-<u>H</u>), 4.61 (2H, s, C<u>H</u>$_2$Br), 1.36 (9H, s, C-(C<u>H</u>$_3$)$_3$. Data comparable to that reported in the literature.[68]

Synthesis of (E)-5-(*tert*-butyl)-3-(benzyl[2.2]paracyclophan-4-yl methylamino)-2-hydroxy benzaldehyde (Pre-L_1)

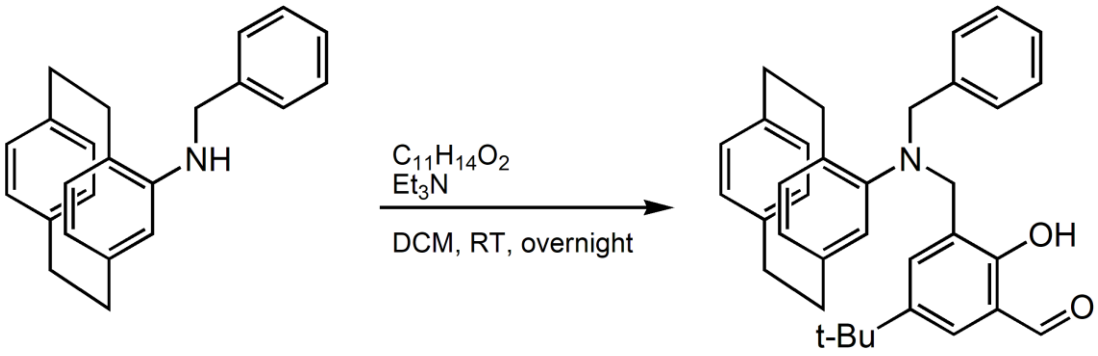

A solution of 4-(benzylamino)[2.2]paracyclophane (0.20 g, 0.64 mmol, 1 eq.) in DCM/MeOH (10 ml, 19:1) and a solution of 3-(bromomethyl)-5-*tert*-butyl-2-hydroxybenzaldehyde (0.18 g, 0.65 mmol, 1 eq.) in DCM (10 ml) were added slowly and simultaneously to a stirred solution of Et_3N (0.09 ml, 0.64 mmol, 1 eq.) in DCM (15 ml). The solution was then stirred at room temperature overnight. The solvent was then removed, solid dissolved in $CHCl_3$ and filtered. Filtrate washed with H_2O (3 x 20 ml), organic layer dried with anhydrous $MgSO_4$, filtered and solvent removed under vacuum. Product was purified by silica gel column chromatography eluting with 4:1 hexane:EtOAc, resulting in a yellow powder (0.11 g, 0.22 mmol, 35%).

^{1}H NMR (500 MHz, $CDCl_3$): δ = 11.24 (1H, s, C<u>H</u>O), 9.90 (1H, s, O<u>H</u>), 7.50 – 7.49 (2H, m, Ar-<u>H</u>), 7.43 (2H, t, J = 7.15 Hz, Ar-<u>H</u>), 7.37 – 7.35 (3H, m, Ar-<u>H</u>), 7.04 (1H, d, J = 7.25 Hz, Ar-<u>H</u>), 6.92 (1H, dd, J = 7.57, 1.58 Hz, Ar-<u>H</u>), 6.47 – 6.42 (2H, m, Ar-<u>H</u>), 6.01 (1H, s, Ar-<u>H</u>), 5.50 (1H, s, Ar-<u>H</u>), 4.29 (1H, d, J = 12.30 Hz, C<u>H</u>$_2$), 4.13 (1H, d, J = 12.61 Hz, C<u>H</u>$_2$), 4.00 (1H, d, J = 15.76 Hz, C<u>H</u>$_2$), 3.80 – 3.69 (2H, m , Ar-<u>H</u>, C<u>H</u>$_2$), 3.35 – 3.26 (1H, m, C<u>H</u>$_2$), 3.18 – 3.05 (5H, m, C<u>H</u>$_2$), 2.72 – 2.63 (1H, m, C<u>H</u>$_2$), 2.63 – 2.55 (1H, m, C<u>H</u>$_2$), 1.26 (9H, s, CH_3).

^{13}C NMR (125 MHz, $CDCl_3$): δ = 197.0, 158.2, 157.4, 142.2, 139.8, 139.0, 138.7, 135.3, 135.0, 133.9, 132.2, 131.7, 129.9, 129.8, 129.4, 129.0, 128.0, 127.6, 127.1, 125.0, 120.3, 119.5, 60.4, 34.5, 34.1, 34.0, 33.9, 33.3, 32.5, 31.6, 31.3, 31.2, 31.1, 22.7, 14.2.

Mp: 162-166 ºC

HRMS-EI: *m/z* found: $[M]^{+}$, 504.2895. $C_{35}H_{37}NO_2$ requires $[M]^{+}$, 504.2897.

IR: 3416, 3030, 3008, 2953, 2853, 1655, 1599, 1566, 1506, 1455, 1411, 1363, 1314, 1294, 1267, 1216, 1100, 1028 cm^{-1}.

Synthesis of (E)-5-(*tert*-butyl)-3-(benzyl[2.2]paracyclophan-4-yl methylamino)-2-hydroxy benzaldehyde oxime (L_1)

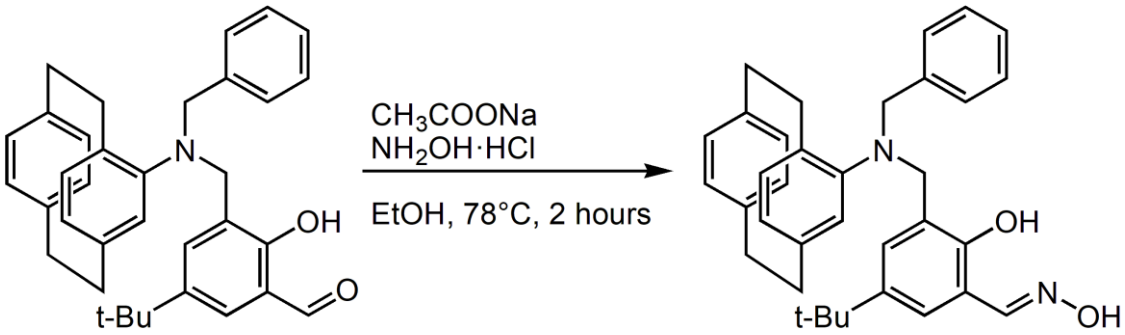

Pre-L_1 (0.29 g, 0.58 mmol, 1 eq.) and sodium acetate (0.23 g, 2.85 mmol, 5 eq.) were dissolved in EtOH (50 ml) and the solution heated to reflux. $NH_2OH{\cdot}HCl$ (0.16 g, 2.30 mmol, 4 eq.) was added in portions and the solution refluxed for 2 hours. The solution was cooled to room temperature and the solvent removed under reduced pressure. The solid was washed with H_2O (30 ml) and extracted with DCM (3 x 20 ml). Combined organics were dried ($MgSO_4$), filtered and solvent removed under vacuum to give the pure product as a yellow powder (0.25 g, 0.49 mmol, 84%).

^{1}H NMR (500 MHz, $CDCl_3$): δ = 9.99 (1H, brs, O<u>H</u>), 8.26 (1H, s, C<u>H</u>=N), 7.51 (2H, d, J = 7.30 Hz, C<u>H</u>), 7.44 (2H, t, J = 7.48 Hz, C<u>H</u>), 7.37 (1H, t, J = 7.33 Hz, C<u>H</u>), 7.13 (1H , d, J = 2.2 Hz, C<u>H</u>), 7.07 (1H, d, J = 1.45 Hz, C<u>H</u>), 7.05 (1H, d, J = 1.40 Hz, C<u>H</u>), 7.02 (1H, d, J = 2.30 Hz, C<u>H</u>), 6.96 (1H, dd, J = 7.85, 1.65 Hz, C<u>H</u>), 6.45 (2H, t, J = 5.78 Hz, C<u>H</u>), 6.03 (1H, s, C<u>H</u>), 5.52 (1H, s, C<u>H</u>), 4.30 (1H, d, J = 12.95 Hz, C<u>H</u>$_2$), 4.14 (1H, d, J = 12.95 Hz, C<u>H</u>$_2$), 4.04 (1H, d, J = 15.65 Hz, C<u>H</u>$_2$), 3.79 (1H, d, J = 15.70 Hz, C<u>H</u>$_2$), 3.37 (1H, qd, J = 6.15, 2.40, 2.05 Hz, C<u>H</u>$_2$), 3.20 – 3.05 (5H, m, C<u>H</u>$_2$), 2.73 – 2.64 (1H, m, C<u>H</u>$_2$), 2.64 – 2.56 (1H, m, C<u>H</u>$_2$), 1.25 (9H, s, C-(C<u>H</u>$_3$)$_3$)

^{13}C NMR (125 MHz, $CDCl_3$): δ = 171.3, 153.7, 152.9, 145.1, 141.9, 139.8, 139.3, 139.0, 136.8, 133.0, 131.1, 130.0, 129.7, 129.0, 128.6, 128.3, 128.2, 127.4, 125.2, 123.9, 118.6, 115.1, 60.5, 48.6, 34.0, 33.9, 33.4, 33.0, 32.6, 32.4, 31.4, 21.1, 14.2

Mp: 179-189.5 ºC

HRMS-EI: *m/z* found: $[M]^+$, 519.2999. $C_{35}H_{38}N_2O_2$ requires $[M]^+$, 519.2933.

IR: 3421, 3031, 2959, 2861, 1599, 1566, 1504, 1454, 1409, 1392, 1362, 1262, 1218, 1100, 1077, 1028 cm^{-1}.

Synthesis of 4,16-dibromo[2.2]paracyclophane

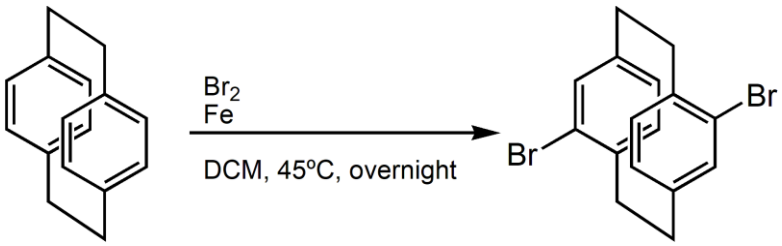

A solution of Br_2 (10.9 ml, 212 mmol, 2.2 eq.) in DCM (55 ml) was made, and 7 ml of this solution was added to iron powder (0.26 g, 4.71 mmol, 0.05 eq.) and stirred at room temperature for 1 hour. This solution was then added to a solution of [2.2]paracyclophane (20.00 g, 96.15 mmol, 1 eq.) in DCM (900 ml). Solution heated to 45°C, and the remaining Br_2/DCM solution was slowly added. Solution refluxed overnight, cooled to room temperature and filtered. Filtrate dried under vacuum (H_2O aspirated rotary evaporator), solid suspended in DMF (100 ml), filtered and the precipitate washed with DMF (2 x 20 ml). Precipitate recrystallized with $CHCl_3$ to give the product as an off-white powder (8.78 g, 24.04 mmol, 25%).

^{1}H NMR (500 MHz, $CDCl_3$): δ = 7.16 (2H, dd, J = 6.3, 1.6 Hz, Ar-H), 6.53 (2H, d, J = 1.6 Hz, Ar-H), 6.46 (2H, d, J = 6.3 Hz, Ar-H), 3.43 – 3.52 (2H, m, CH_2), 3.09 – 3.20 (2H, m, CH_2), 2.77 – 2.98 (4H, m, CH_2). Data comparable to that reported in the literature.[69]

Synthesis of 4-amino-16-bromo[2.2]paracyclophane

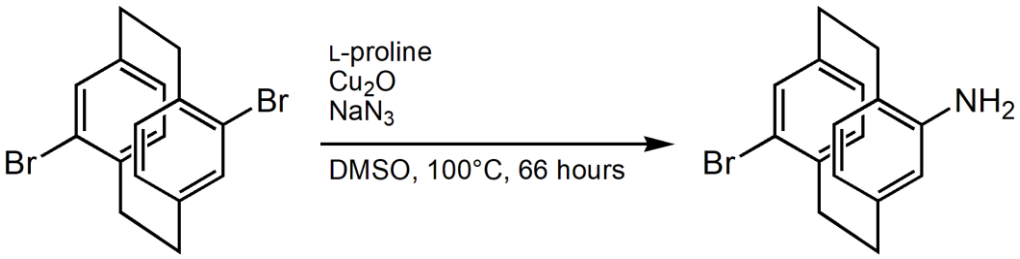

A solution of 4,16-dibromo[2.2]paracyclophane (1.02 g, 2.78 mmol, 1 eq.), L-proline (2.54 g, 22.11 mmol, 8 eq.), copper oxide (0.78 g, 5.48 mmol, 2 eq.) and sodium azide (1.44 g, 22.08 mmol, 8 eq.) in DMSO (27.3 ml, 0.1 M) was heated to 100°C and stirred for 66 hours. The solution was cooled to RT and a mixture of EDTA (1.3 M in H_2O, 4 eq. per 1 eq. Cu) and EtOAc (EDTA:EtOAc = 2:1) was added and stirred for 30 minutes. The mixture was filtered through celite and the layers were separated. Aqueous layer was extracted with EtOAc (3 x 20 ml), combined organics were washed with H_2O (20 ml) and brine (20 ml). Solution was dried ($MgSO_4$), filtered and the solvent was removed under vacuum. The product was purified by column chromatography eluted with 3:1 hexane:EtOAc (0.12 g, 0.41 mmol, 15%).

^{1}H NMR (500 MHz, $CDCl_3$): δ = 7.19 (1H, dd, J = 7.39, 1.7 Hz, Ar-H), 6.70 (1H, dd, J = 7.7, 1.7 Hz, Ar-H), 6.51 (1H, d, J = 1.2 Hz, Ar-H), 6.40 (1H, d, J = 7.7 Hz, Ar-H), 6.29 (1H, d, J = 7.7 Hz, Ar-H), 5.48 (1H, d, J = 1.2 Hz, Ar-H), 4.06 – 3.58 (1H, brs, NH_2), 3.50 (1H, t, J = 11.6 Hz, NH_2), 3.22 – 2.67 (8H, m, H-1, H-2, H-9, H-10). Data comparable to that reported in the literature.[29]

Synthesis of 4,16-diamino[2.2]paracyclophane

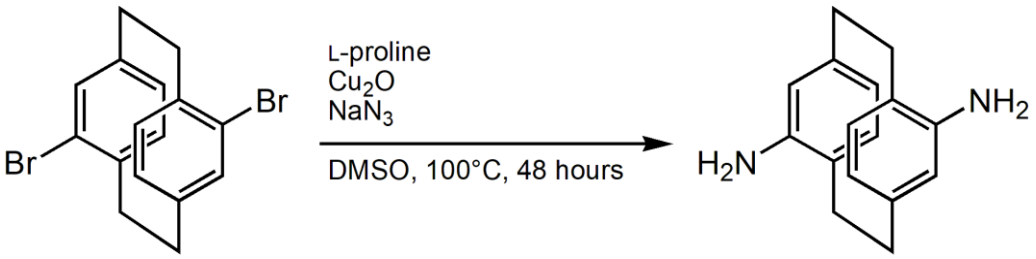

A solution of 4,16-dibromo[2.2]paracyclophane (0.26 g, 0.70 mmol, 1 eq.), L-proline (0.45 g, 3.93 mmol, 5.6 eq.), copper oxide (0.22 g, 1.51 mmol, 2.2 eq.) and sodium azide (0.36 g, 5.58 mmol, 8 eq.) in DMSO (13 ml, 0.05 M) was added to a 35 ml microwave flask and sealed. The solution was heated in a microwave for 48 hours at 100°C. The solution was immediately added to a mixture of EDTA (0.65 M in H_2O, 2 eq. per 1 eq. Cu) and EtOAc (EDTA:EtOAc = 2:1) and stirred for 30 minutes. The mixture was filtered through celite and the layers were separated. Aqueous layer was extracted with EtOAc (3 x 20 ml), combined organics were then washed with $NaHCO_3$ (20 ml), H_2O (20 ml) and brine (20 ml). Solution dried ($MgSO_4$), filtered and solvent removed under vacuum. Recrystallize from 1,4-dioxan by adding hexane, pure product yielded as solid (0.02 g, 0.24 mmol, 10%).

^{1}H NMR (500 MHz, $CDCl_3$): δ = 6.64 (2H, d, J = 7.7 Hz, Ar-H), 6.23 (2H, d, J = 7.7 Hz, Ar-H), 5.51 (2H, s, Ar-H), 3.19 (2H, ddd, J = 12.4, 9.7, 1.6 Hz, CH_2), 3.05 (2H, ddd, J = 15.6, 9.9, 5.9 Hz, CH_2), 2.91 (2H, ddd, J = 12.7, 10.8, 1.9 Hz, CH_2), 2.69 (2H, ddd, J = 16.4, 10.7, 5.7 Hz, CH_2). Data comparable to that reported in the literature.[29]

L_1 complexation attempts

$Mn(OAc)_2 \cdot 4H_2O$ with L_1

To a solution of L_1 (0.13 g, 0.25 mmol, 1 eq.) in MeOH (37 ml) was added a solution of $Mn(OAc)_2 \cdot 4H_2O$ (0.13 g, 0.51 mmol, 2 eq.) in MeOH (13 ml) and stirred for 20 minutes. The solution turned a dark green colour. Pyridine (2 ml) was added and the solution was stirred for an additional 3 hours. The solution was filtered, and the filtrate was left to evaporate for 72 hours. No crystal growth was shown, and vapour diffusion was set up as shown below. Conditions are shown in Table 2.

$Mn(ClO_4)_2 \cdot 6H_2O$ with L_1

Same conditions as above, using L_1 (0.10 g, 0.19 mmol, 1 eq.) and $Mn(ClO_4)_2 \cdot 6H_2O$ (0.07 g, 0.19 mmol, 1 eq.). Recrystallization conditions shown in Table 2.

$Fe(ClO_4)_2 \cdot 6H_2O$ with L_1

Same conditions as above, using L_1 (0.10 g, 0.20 mmol, 1 eq.) and $Fe(ClO_4)_2 \cdot 6H_2O$ (0.07 g, 0.20 mmol, 1 eq.). Recrystallization conditions shown in Table 2.

$CoCl_2 \cdot 6H_2O$ with L_1

Same conditions as above, using L_1 (0.07 g, 0.13 mmol, 1 eq.) and $CoCl_2 \cdot 6H_2O$ (0.06 g, 0.26 mmol, 2 eq.) with $NaBF_4$ (0.06 g, 0.53 mmol, 4 eq.) added. Recrystallization conditions shown in Table 2.

$Zn(OAc)_2 \cdot 2H_2O$ with L_1

Same conditions as above, using L_1 (0.13 g, 0.26 mmol, 1 eq.) and $Zn(OAc)_2 \cdot 6H_2O$ (0.13 g, 0.61 mmol, 2.34 eq.) with $NaBF_4$ (0.24 g, 2.2 mmol, 8.5 eq.) added. Recrystallization conditions shown in Table 2.

Vapour Diffusion setup

Vapour diffusion attempts were set up by dissolving the complex in methanol and putting 1 ml of this solution into a small vial which was sealed with a lid that had 5 needle holes in it. This small vial was then placed into a larger vial that had 5 ml of various solvents inside, the large vial was then sealed, wrapped with parafilm and left undisturbed for 2 weeks.

Metal salt	**Base**	**Recrystallization conditions**
$Mn(OAc)_2 \cdot 4H_2O$	Pyridine	Evaporation: • MeOH Vapour diffusion: • n-Hexane • Diethyl Ether • n-Pentane
$Mn(ClO_4)_2 \cdot 6H_2O$	Pyridine	Evaporation: • MeOH Vapour diffusion: • n-Hexane • Diethyl Ether • n-Pentane • Ethyl Acetate • Acetonitrile
$Fe(ClO_4)_2 \cdot 6H_2O$	Pyridine	Evaporation: • MeOH Vapour diffusion: • Chloroform • Ethanol • Ethyl Acetate • Acetonitrile • 3:2 Methanol:Acetonitrile
$CoCl_2 \cdot 6H_2O$ $NaBH_4$ added		Evaporation: • MeOH Vapour diffusion: • n-Hexane • Diethyl Ether • n-Pentane • 1:1 n-Hexane:n-Pentane

$Zn(OAc)_2 \cdot 2H_2O$ $NaBH_4$ added		Evaporation: • MeOH Vapour diffusion: • n-Hexane • Diethyl Ether • n-Pentane

Table 2. Metal salts and bases used in complexations with L_1. All run in MeOH at RT.

Synthesis of 2,5-di(bromomethyl)pyrazine + 2,5-di(dibromomethyl)pyrazine

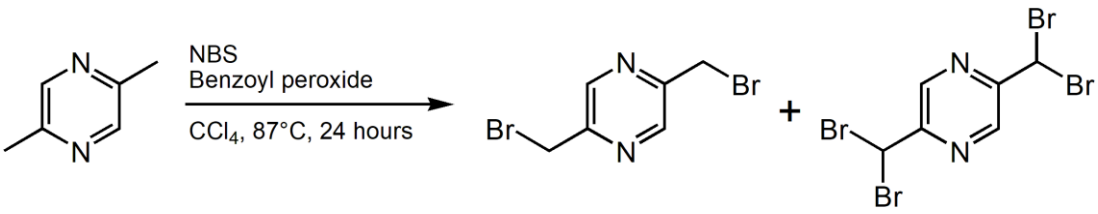

N-Bromosuccinimide (3.59 g, 20.2 mmol, 2 eq.) was added to a solution of 2,5-dimethylpyrazine (1.10 g, 10.1 mmol, 1 eq.) in CCl_4 (100 ml). The mixture was refluxed at 87°C under Ar for 45 minutes. Benzoyl peroxide (0.05 g, 0.21 mmol, 0.02 eq.) was added and the reaction was stirred for 8 hours, with additional benzoyl peroxide (0.04 and 0.03 g) being added after 4 and 8 hours. Mixture kept at reflux overnight and then cooled to RT. Solution filtered and washed with CCl_4, solvent removed from filtrate. Products yielded as a 1:1 mixture after silica gel chromatography (2:1 hexane:EtOAc) as a white solid (0.31 g, 1.21 mmol, 12%).

2,5-di(bromomethyl)pyrazine ^{1}H NMR (500 MHz, $CDCl_3$): δ = 8.67 (2H, s), 4.56 (4H, s). Data comparable to that reported in the literature.[54]

2,5-di(dibromomethyl)pyrazine ^{1}H NMR (500 MHz, $CDCl_3$): δ = 8.99 (2H, s), 6.69 (2H, s). Data comparable to that reported in the literature.[54]

Synthesis of 2,5-di(methylpyrazine-1,4-dioxide

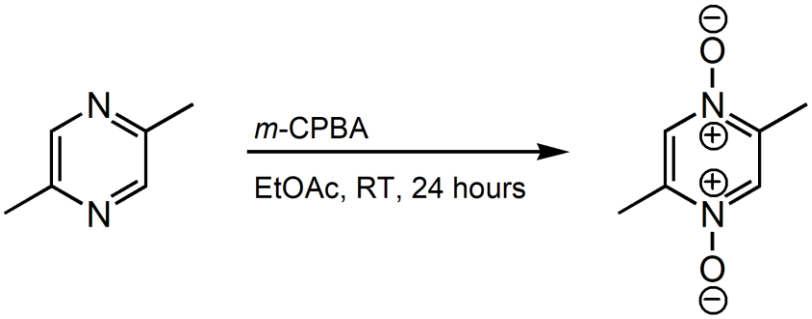

A solution of *m*-CPBA (70% purity, 100.0 g, 405.6 mmol, 2.2 eq.) in EtOAc (150 ml) was washed with brine (150 ml). The organic layer was separated, dried ($MgSO_4$) and filtered. The filtrate was added to a solution of 2,5-dimethylpyrazine (20.20 ml, 184.9 mmol, 1 eq.) in EtOAc (50 ml) and stirred for 24 hours at RT. The white precipitate was filtered, washed with EtOAc (3 x 100 ml) and dried to give the product as a white crystalline solid (4.50g, 31.4 mmol, 17%).

^{1}H NMR (500 MHz, D_2O): δ = 8.48 (2H, s), 2.42 (6H, s). Data comparable to that reported in the literature.[55]

Synthesis of 2,5-di(acetoxymethyl)pyrazine

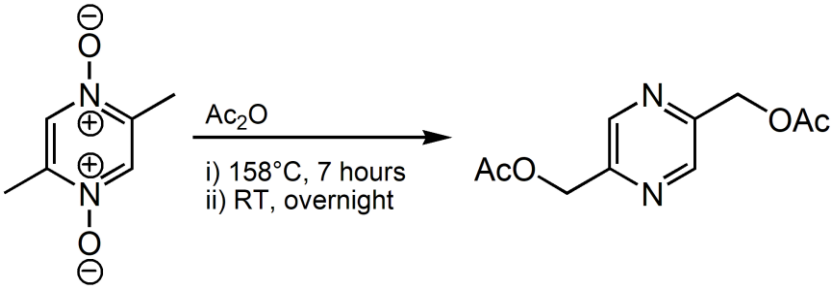

A stirred suspension of 2,5-dimethylpyrazine-1,4-dioxide (15.52 g, 110.9 mmol, 1 eq.) in acetic anhydride (75 ml) was heated at 158°C for 7 hours. The resulting mixture was then stirred at RT overnight. The acetic anhydride was removed under reduced pressure to give a black residue. Et_2O (250 ml) was added and stirred vigorously for 2 hours. The solution was then filtered and the residue washed with Et_2O (100 ml). The combined filtrate was concentrated under reduced pressure to give a yellow-brown liquid. Silica gel chromatography (2:3 EtOAc:*n*-hexane) of this liquid gave a yellow liquid which was recrystallized from 1:1 EtOAc:*n*-hexane overnight to give the product as a white crystalline solid (2.95 g, 13.3 mmol, 12%).

^{1}H NMR (500 MHz, $CDCl_3$): δ = 8.59 (2H, s), 5.23 (4H, s), 2.13 (6H, s). Data comparable to that reported in the literature.[55]

Synthesis of 2,5-di(hydroxymethyl)pyrazine

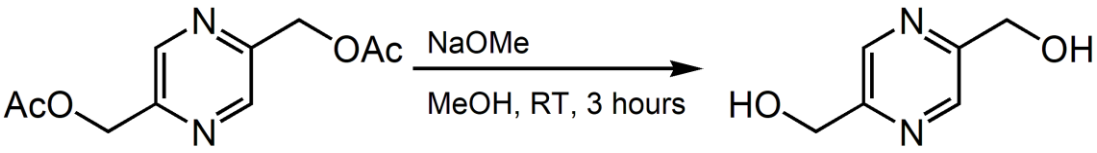

To a solution of 2,5-di(acetoxymethyl)pyrazine (3.43 g, 15.3 mmol, 1 eq.) in dry MeOH (100 ml) was added NaOMe (0.84 g, 15.63 mmol, 1.02 eq.) under argon and the resulting solution was stirred for 3 hours at RT. The reaction was quenched by adding solid NH_4Cl (1.5 g) and the solvent removed under reduced pressure. Silica gel chromatography (1:9 MeOH:$CHCl_3$) of the resulting solid gave the product as a white crystalline solid (1.82 g, 12.70 mmol, 83%).

^{1}H NMR (500 MHz, acetone-d_6): δ = 8.63 (2H, s), 4.89 (2H, br), 4.75 (4H, s). Data comparable to that reported in the literature.[55]

Synthesis of pyrazine-2,5-diylbis(methylene) bis(tosylate)

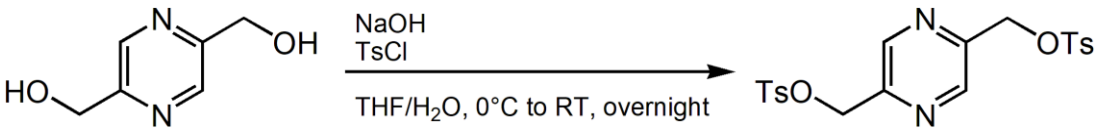

2,5-Di(hydroxymethyl)pyrazine (0.32 g, 2.3 mmol, 1 eq.) in a 1:1 mixture of THF:H_2O (6 ml) was brought to 0°C. Crushed NaOH (0.18 g, 4.8 mmol, 2.1 eq.) was added and a solution of TsCl (0.87 g, 4.6 mmol, 2 eq.) in THF (9 ml) was added dropwise. Solution was allowed to return to room temperature and was stirred overnight. The product was extracted with DCM (3 x 10 ml), combined organics washed with brine (2 x 10 ml) and dried ($MgSO_4$). Solvent removed under reduced pressure, pure product yielded as a pink solid that turned black rapidly (0.63 g, 1.52 mmol, 66%).

^{1}H NMR (500 MHz, $CDCl_3$): δ = 8.58 (2H, s), 7.83 (4H, d, J = 8.25 Hz), 7.37 (4H, d, J = 8.05 Hz), 5.19 (4H, s), 2.47 (6H, s)

^{13}C NMR (125 MHz, $CDCl_3$): δ = 149.2, 145.5, 142.7, 132.4, 130.1, 128.1, 69.3, 21.7

Mp: 83 – 88 °C

HRMS-EI: *m/z* found: $[M]^+$, 471.15. $C_{20}H_{20}N_2O_6S_2$ + Na requires $[M]^+$, 471.08.

IR: 2924, 1595, 1489, 1438, 1362, 1342, 1307, 1294, 1189, 1181, 1170, 1123, 1094, 1032, 1009 cm^{-1}.

Synthesis of 2,5-di(azidomethyl)pyrazine

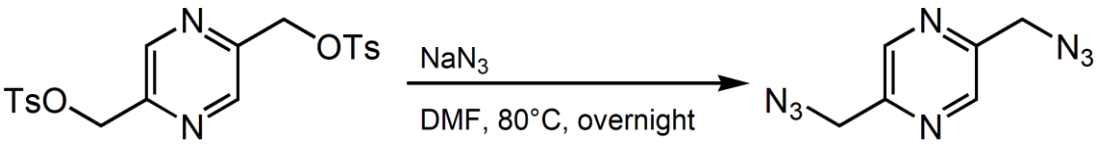

To a solution of pyrazine-2,5-diylbis(methylene) bis(tosylate) (0.31 g, 0.68 mmol, 1 eq.) in DMF (15 ml) was added NaN_3 (0.18 g, 2.7 mmol, 4 eq.). The solution was brought to 80°C and stirred overnight. The solvent was removed under reduced pressure, and the residue dissolved in EtOAc (25 ml). This solution was filtered through celite, washed with H_2O (20 ml) and dried ($MgSO_4$). Solvent removed under reduced pressure to yield the product as a yellow oil (0.09 g, 0.45 mmol, 66%)

^{1}H NMR (500 MHz, $CDCl_3$): δ = 8.64 (2H, s), 4.58 (4H, s)

^{13}C NMR (125 MHz, $CDCl_3$): δ = 150.8, 142.9, 53.1

HRMS-EI: *m/z* found: $[M]^{+}$, 191.0787. $C_6H_6N_8$ requires $[M]^{+}$, 191.0788.

IR: 3357, 2930, 2422, 2084, 1660, 1487, 1439, 1387, 1273, 1153, 1095, 1034 cm^{-1}.

Synthesis of 2,5-di(aminomethyl)pyrazine

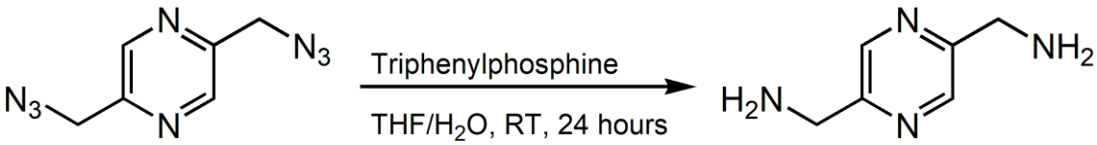

To a solution of 2,5-di(azidomethyl)pyrazine (0.07 g, 0.37 mmol, 1 eq.) in THF (4.5 ml) and H_2O (0.25 ml) was added triphenylphosphine (0.26 g, 0.99 mmol, 2.7 eq.). The solution was stirred at RT for 24 hours. DCM (5 ml) was added and the solution washed with 1M HCl (5 ml). Layers separated, aqueous layer had 1M NaOH added to bring the pH to 12, then extracted with DCM (5 x 10 ml). Combined organics dried ($MgSO_4$), filtered and solvent removed with reduced pressure. Product remained in aqueous phase, liquid removed on freeze drier to give a white powder.

^{1}H NMR (500 MHz, D_2O): δ = 8.52 (2H, s), 3.91 (4H, s)

Material used crude in the next reaction so no yield was determined.

Synthesis of ((E)-2,5-bis((5-*tert*-butyl-2-hydroxybenzylideneamino)methyl)) pyrazine (L_2)

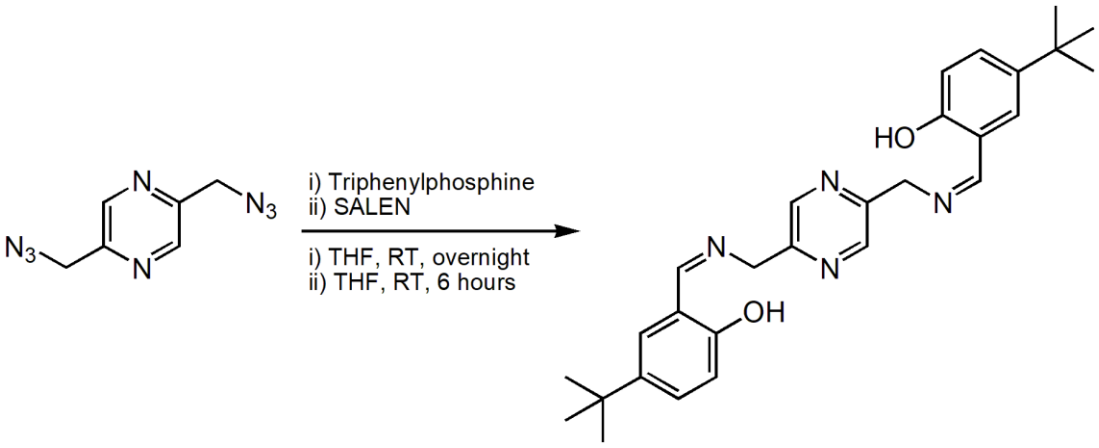

To a solution of 2,5-di(azidomethyl)pyrazine (0.11 g, 0.60 mmol, 1 eq.) in dry THF (5 ml) was added triphenylphosphine (0.40 g, 1.5 mmol, 2.5 eq.). The solution was stirred overnight at RT. A solution of 3-(bromomethyl)-5-*tert*-butyl-2-hydroxybenzaldehyde (0.22 g, 1.2 mmol, 2 eq.) in dry THF (1 ml) was added and the solution stirred at RT for 6 hours. Solvent was removed under reduced pressure. The product was purified by column chromatography eluted with gradient from 4:1 hexane:EtOAc to 2:1 hexane:EtOAc with 1 drop of Et_3N per 500 ml, giving a yellow solid (0.18 g, 0.40 mmol, 67%).

^{1}H NMR (500 MHz, $CDCl_3$): δ = 12.71 (2H, br), 8.64 (2H, s), 8.60 (2H, s), 7.41 (2H, dd, J = 8.65, 2.10 Hz), 7.32 (2H, d, J = 2.15), 6.94 (2H, d, J = 8.65 Hz), 4.99 (4H, s), 1.33 (18H, s)

^{13}C NMR (125 MHz, $CDCl_3$): δ = 168.0, 158.6, 152.2, 143.0, 141.6, 130.2, 128.2, 117.9, 116.6, 62.7, 34.0, 31.4

HRMS-EI: *m/z* found: $[M]^+$, 459.2748. $C_{28}H_{34}N_4O_2$ requires $[M]^+$, 459.2755.

IR: 3370, 2959, 1630, 1586, 1490, 1365, 1261, 1214, 1185, 1158, 1036 cm^{-1}.

Synthesis of (E)-2,5-bis((pyridine-2-ylmethyleneamino)methyl)pyrazine (L_3)

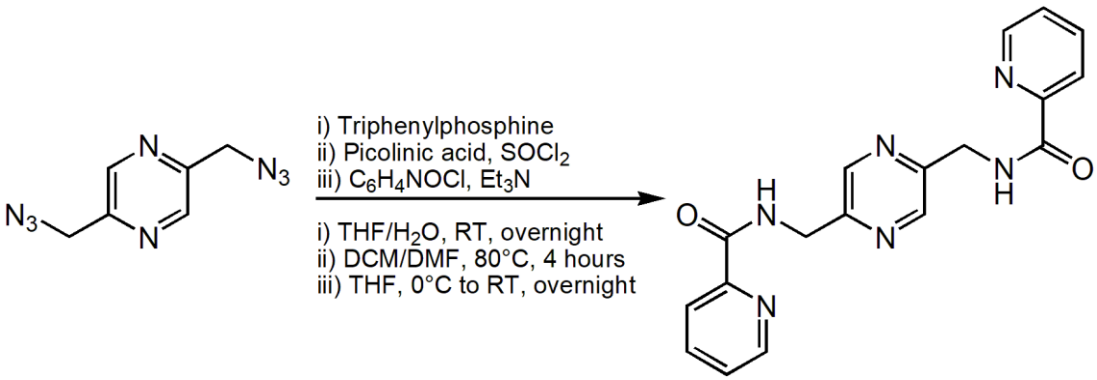

To a solution of 2,5-di(azidomethyl)pyrazine (0.08 g, 0.43 mmol, 1 eq.) in THF (5 ml) and H_2O (0.016 ml, 0.87 mmol, 2 eq.) was added triphenylphosphine (0.28 g, 1.1 mmol, 2.5 eq.). The solution was stirred overnight at RT.

To a solution of picolinic acid (0.11 g, 0.91 mmol, 2.1 eq.) in DCM (5 ml) was added $SOCl_2$ (0.75 ml) and dry DMF (1 drop). This was refluxed at 80°C for 4 hours. Solvent was removed under reduced pressure, and the residue dissolved in dry THF (10 ml). Solution cooled to 0°C, Et_3N (0.3 ml) and the above diazido reaction mixture was added dropwise to the solution. Solution returned to room temperature and stirred overnight. The solution was then extracted with DCM (3 x 10 ml), combined organics washed with H_2O (2 x 10 ml) and dried ($MgSO_4$). Silica gel chromatography with 4:1 hexane:EtOAc gave a mixture of the product and triphenylphosphine oxide. This mixture was recrystallized with Et_2O, the solid from this was then recrystallized with EtOAc and the filtrate from this was recrystallized from Et_2O to give the product as a white powder (0.04 g, 0.09 mmol, 21%).

^{1}H NMR (500 MHz, $CDCl_3$): δ = 8.85 (2H, br), 8.68 (2H, s), 8.60 (2H, d, J = 4.45 Hz), 8.23 (2H, d, J = 7.80 Hz), 7.89 (2H, dt, J = 7.73, 1.4 Hz), 7.47 (2H, dd, J = 12.25, 1.80 Hz), 4.86 (4H, d, J = 5.80 Hz)

^{13}C NMR (125 MHz, $CDCl_3$): δ = 164.6, 151.4, 149.5, 148.3, 143.0, 137.4, 126.4, 122.3, 42.4

HRMS-EI: *m/z* found: $[M]^+$, 349.1402. $C_{18}H_{16}N_6O_2$ requires $[M]^+$, 349.1408.

IR: 3321, 1663, 1590, 1569, 1531, 1484, 1469, 1434, 1421, 1369, 1319, 1289, 1256, 1236, 1159, 1089, 1034, 1000 cm^{-1}.

L_2 complexation attempts

$Mn(OAc)_2 \cdot 2H_2O$ with L_2

To a solution of L_2 (0.05 g, 0.11 mmol, 1 eq.) in MeOH (10 ml) was added a solution of $Mn(Oac)_2 \cdot 2H_2O$ (0.07 g, 0.26 mmol, 2.4 eq.) in MeOH (2.5 ml) and stirred for 30 minutes. The solution turned a dark green colour and was left to sit overnight. The solution was filtered, and 2 ml of filtrate was left to evaporate. Vapour diffusion was set up on the remaining filtrate as shown below. Conditions are shown in Table 3.

$Ni(BF_4)_2 \cdot 6H_2O$ with L_2

Same conditions as above, using L_2 (0.05 g, 0.11 mmol, 1 eq.) and $Ni(BF_4)_2 \cdot 6H_2O$ (0.09 g, 0.25 mmol, 2.4 eq.). Recrystallization conditions shown in Table 3.

$Cu(BF_4)_2 \cdot 6H_2O$ with L_2

Same conditions as above, using L_2 (0.05 g, 0.11 mmol, 1 eq.) and $Cu(BF_4)_2 \cdot 6H_2O$ (0.09 g, 0.26 mmol, 2.4 eq.). Recrystallization conditions shown in Table 3.

Vapour Diffusion setup

Same as done for L_1 (see above)

Metal salt	**Colour change**	**Recrystallization conditions**
$Mn(OAc)_2 \cdot 2H_2O$	Pink to brown	Evaporation: • MeOH Vapour diffusion: • Diethyl ether
$Ni(BF_4)_2 \cdot 6H_2O$	Yellow to dark yellow	Evaporation: • MeOH Vapour diffusion: • Diethyl ether
$Cu(BF_4)_2 \cdot 6H_2O$	Blue to green	Evaporation: • MeOH Vapour diffusion: • Diethyl ether

Table 3. Metal salts used in complexations with L2. All run in MeOH at RT.

L_3 complexation attempts

$CoCl_2 \cdot 6H_2O$ with L_2

To a solution of L_3 (0.03 g, 0.08 mmol, 1 eq.) in MeCN (5 ml) was added $CoCl_2 \cdot 6H_2O$ (0.02 g, 0.09 mmol, 1.1 eq.) in MeCN (5 ml). $NaBF_4$ (0.02 g, 0.21 mmol, 2.5 eq.) and Et_3N (0.023 ml) were added and the solution stirred at RT for 60 minutes. Solution filtered, 2 ml of filtrate set aside to evaporate. Vapour diffusion was set up on the remaining filtrate as shown below. Conditions are shown in Table 4.

Vapour Diffusion setup

Vapour diffusion attempts were set up by dissolving the complex in methanol or MeCN and putting 1 ml of this solution into a small vial which was sealed with a lid that had 5 needle holes in it. This small vial was then placed into a larger vial that had 5 ml of Et_2O inside, the large vial was then sealed, wrapped with parafilm and left undisturbed for 2 weeks.

Metal salt	**Base**	**Colour change**	**Recrystallization conditions**
$CoCl_2 \cdot 6H_2O$ $NaBH_4$ added	Et_3N	Blue to brown	Evaporation: • MeOH • MeCN Vapour diffusion: • Diethyl ether

Table 4. Recrystallization of L_3 with $CoCl_2$.

5. References

1. Feltham, H. L. C.; Brooker, S., Review of purely 4*f* and mixed-metal n*d*-4*f* single-molecule magnets containing only one lanthanide ion. *Coordin. Chem. Rev.* **2014**, *276*, 1-33.

2. Goodwin, C. A. P.; Ortu, F.; Reta, D.; Chilton, N. F.; Mills, D. P., Molecular magnetic hysteresis at 60 kelvin in dysprosocenium. *Nature.* **2017**, *548*, 439-442.

3. Rinehart, J. D.; Fang, M.; Evans, W. J.; Long, J. R., A N_2^{3-} radical-bridged terbium complex exhibiting magnetic hysteresis at 14 K. *J. Am. Chem. Soc.* **2011**, *133*, 14236-14239.

4. Ding, Y. S.; Chilton, N. F.; Winpenny, R. E.; Zheng, Y. Z., On Approaching the Limit of Molecular Magnetic Anisotropy: A Near-Perfect Pentagonal Bipyramidal Dysprosium(III) Single-Molecule Magnet. *Angew. Chem. Int. Ed.* **2016**, *55*, 16071-16074.

5. Karotsis, G.; Teat, S. J.; Wernsdorfer, W.; Piligkos, S.; Dalgarno, S. J.; Brechin, E. K., Calix[4]arene-based single-molecule magnets. *Angew. Chem. Int. Ed.* **2009**, *48*, 8435-8438.

6. Ruiz-Molina, D.; Christou, G.; Hendrickson, D. N., Single-molecule magnets. *Mol. Cryst. Liq. Cryst.* **2000**, *343*, 335-345.

7. Sessoli, R.; Gatteschi, D.; Caneschi, A.; Novak, M. A., Magnetic Bistability in a Metal-Ion Cluster. *Nature.* **1993**, *365*, 141-143.

8. Blagg, R. J.; Ungur, L.; Tuna, F.; Speak, J.; Comar, P.; Collison, D.; Wernsdorfer, W.; McInnes, E. J.; Chibotaru, L. F.; Winpenny, R. E., Magnetic relaxation pathways in lanthanide single-molecule magnets. *Nat. Chem.* **2013**, *5*, 673-678.

9. Milios, C. J.; Vinslava, A.; Wernsdorfer, W.; Moggach, S.; Parsons, S.; Perlepes, S. P.; Christou, G.; Brechin, E. K., A record anisotropy barrier for a single-molecule magnet. *J. Am. Chem. Soc.* **2007**, *129*, 2754-2755.

10. Ako, A. M.; Hewitt, I. J.; Mereacre, V.; Clerac, R.; Wernsdorfer, W.; Anson, C. E.; Powell, A. K., A ferromagnetically coupled Mn_{19} aggregate with a record *S*=83/2 ground spin state. *Angew. Chem. Int. Ed.* **2006**, *45*, 4926-4929.

11. Zhang, S.; Li, H.; Duan, E.; Han, Z.; Li, L.; Tang, J.; Shi, W.; Cheng, P., A 3D Heterometallic Coordination Polymer Constructed by Trimeric {$NiDy_2$} Single-Molecule Magnet Units. *Inorg. Chem.* **2016**, *55*, 1202-1207.

12. Ganivet, C. R.; Ballesteros, B.; de la Torre, G.; Clemente-Juan, J. M.; Coronado, E.; Torres, T., Influence of peripheral substitution on the magnetic behavior of single-ion magnets based on homo- and heteroleptic Tb^{III} bis(phthalocyaninate). *Chem. Eur. J.* **2013**, *19*, 1457-1465.

13. Liu, J. L.; Wu, J. Y.; Chen, Y. C.; Mereacre, V.; Powell, A. K.; Ungur, L.; Chibotaru, L. F.; Chen, X. M.; Tong, M. L., A heterometallic Fe^{II}-Dy^{III} single-molecule magnet with a record anisotropy barrier. *Angew. Chem. Int. Ed.* **2014**, *53*, 12966-12970.

14. Ephraim, F., Über ein neues Reagens zur qualitativen und quantitativen Bestimmung des Kupfers. *Ber. Dtsch. Chem. Ges.* **1930**, *63*, 1928-1930.

15. Cox, E. G.; Pinkard, F. W.; Wardlaw, W.; Webster, K. C., The planar configuration for quadricovalent nickel, palladium, and platinum. *J. Chem. Soc.* **1935**, 459.

16. Stevens, J. R.; Plieger, P. G., Anion-driven conformation control and enhanced sulfate binding utilising aryl linked salicylaldoxime dicopper helicates. *Dalton Trans.* **2011**, *40*, 12235-12241.

17. Pannu, A. P.; Stevens, J. R.; Plieger, P. G., Aryl-linked salicylaldoxime-based copper(II) helicates and "boxes": synthesis, X-ray analysis, and anion influence on complex structure. *Inorg. Chem.* **2013**, *52*, 9327-9337.

18. Wenzel, M.; Knapp, Q. W.; Plieger, P. G., A bis-salicylaldoximato-copper(II) receptor for selective sulfate uptake. *Chem. Comm.* **2011**, *47*, 499-501.

19. De Silva, D. N.; Jameson, G. B.; Pannu, A. P.; Pouhet, R.; Wenzel, M.; Plieger, P. G., Piperazine linked salicylaldoxime and salicylaldimine-based dicopper($_{II}$) receptors for anions. *Dalton Trans.* **2015**, *44*, 15949-15959.

20. Milios, C. J.; Raptopoulou, C. P.; Terzis, A.; Lloret, F.; Vicente, R.; Perlepes, S. P.; Escuer, A., Hexanuclear manganese(III) single-molecule magnets. *Angew. Chem. Int. Ed.* **2004**, *43*, 210-212.

21. Inglis, R.; Milios, C. J.; Jones, L. F.; Piligkos, S.; Brechin, E. K., Twisted molecular magnets. *Chem. Comm.* **2012**, *48*, 181-190.

22. Milios, C. J.; Vinslava, A.; Wood, P. A.; Parsons, S.; Wernsdorfer, W.; Christou, G.; Perlepes, S. P.; Brechin, E. K., A single-molecule magnet with a "twist". *J. Am. Chem. Soc.* **2007**, *129*, 8-9.

23. Rowlands, G. J., The synthesis of enantiomerically pure [2.2]paracyclophane derivatives. *Org. Biomol. Chem.* **2008**, *6*, 1527-1534.

24. David, O. R. P., Syntheses and applications of disubstituted [2.2]paracyclophanes. *Tetrahedron.* **2012**, *68*, 8977-8993.

25. Paradies, J., [2.2]Paracyclophane Derivatives: Synthesis and Application in Catalysis. *Synthesis.* **2011**, 3749-3766.

26. Demissie, T. B.; Dodziuk, H.; Waluk, J.; Ruud, K.; Pietrzak, M.; Vetokhina, V.; Szymanski, S.; Jazwinski, J.; Hopf, H., Structure, NMR and Electronic Spectra of [*m*.n]Paracyclophanes with Varying Bridges Lengths (*m*, n = 2-4). *J. Phy. Chem. A.* **2016**, *120*, 724-736.

27. Wolf, H.; Leusser, D.; Mads, R. V. J.; Herbst-Irmer, R.; Chen, Y. S.; Scheidt, E. W.; Scherer, W.; Iversen, B. B.; Stalke, D., Phase transition of [2,2]-paracyclophane - an end to an apparently endless story. *Chem. Eur. J.* **2014**, *20*, 7048-7053.

28. Dikarev, E. V.; Filatov, A. S.; Clerac, R.; Petrukhina, M. A., Unligated diruthenium(II,II) tetra(trifluoroacetate): the first X-ray structural study, thermal compressibility, Lewis acidity, and magnetism. *Inorg. Chem.* **2006**, *45*, 744-751.

29. Jayasundera, K. P.; Kusmus, D. N. M.; Deuilhe, L.; Etheridge, L.; Farrow, Z.; Lun, D. J.; Kaur, G.; Rowlands, G. J., The synthesis of substituted amino[2.2]paracyclophanes. *Org. Biomol. Chem.* **2016**, *14*, 10848 - 10860.

30. Munakata, M.; Wu, L. P.; Ning, G. L.; Kuroda-Sowa, T.; Maekawa, M.; Suenaga, Y.; Maeno, N., Construction of metal sandwich systems derived from assembly of silver(I) complexes with polycyclic aromatic compounds. *J. Am. Chem. Soc.* **1999**, *121*, 4968-4976.

31. Pye, P. J.; Rossen, K.; Reamer, R. A.; Tsou, N. N.; Volante, R. P.; Reider, P. J., A New Planar Chiral Bisphosphine Ligand for Asymmetric Catalysis: Highly Enantioselective Hydrogenations under Mild Conditions. *J. Am. Chem. Soc.* **1997**, *119*, 6207-6208.

32. Ball, P. J.; Shtoyko, T. R.; Krause Bauer, J. A.; Oldham, W. J.; Connick, W. B., Binuclear rhenium(I) complexes with bridging [2.2]paracyclophane-diimine ligands: probing electronic coupling through pi-pi interactions. *Inorg. Chem.* **2004**, *43*, 622-632.

33. Richardson, D. E.; Taube, H., Electronic Interactions in Mixed-Valence Molecules as Mediated by Organic Bridging Groups. *J. Am. Chem. Soc.* **1983**, *105*, 40-51.

34. Creutz, C.; Taube, H., Direct approach to measuring the Franck-Condon barrier to electron transfer between metal ions. *J. Am. Chem. Soc.* **1969**, *91*, 3988-3989.

35. Hogue, R. W.; Dhers, S.; Hellyer, R. M.; Luo, J.; Hanan, G. S.; Larsen, D. S.; Garden, A. L.; Brooker, S., Self-Assembly of Cyclohelicate [M3 L3] Triangles Over [M4 L4] Squares, Despite Near-Linear Bis-terdentate L and Octahedral M. *Chem. Eur. J.* **2017**, *23*, 14193-14199.

36. Shen, F.; Huang, W.; Wu, D.; Zheng, Z.; Huang, X. C.; Sato, O., Redox Modulation of Spin Crossover within a Cobalt Metallogrid. *Inorg. Chem.* **2016**, *55*, 902-908.

37. Hausmann, J.; Brooker, S., Control of molecular architecture by use of the appropriate ligand isomer: a mononuclear "corner-type" versus a tetranuclear [2 x 2] grid-type cobalt(III) complex. *Chem. Comm.* **2004**, 1530-1531.

38. Pelter, A.; Kidwell, H.; Crump, R. A. N. C., N-methyl- and N-benzyl-4-amino[2.2]paracyclophanes as unique planar chiral auxiliaries. *J. Chem. Soc.* **1997**, 3137-3139.

39. Lahann, J.; Höcker, H.; Langer, R., Synthesis of Amino[2.2]paracyclophanes-Beneficial Monomers for Bioactive Coating of Medical Implant Materials. *Angew. Chem. Int. Ed.* **2001**, *40*, 726-728.

40. Schneider, J. F.; Frohlich, R.; Paradies, J., [2.2]Paracyclophane-Derived Planar-Chiral Hydrogen-Bond Receptors. *Isr. J. Chem.* **2012**, *52*, 76-91.

41. Hong, B.; Ma, Y.; Zhao, L.; Duan, W.; He, F.; Song, C., Synthesis of planar chiral imidazo[1,5-*a*]pyridinium salts based on [2.2]paracyclophane for asymmetric β-borylation of enones. *Tetrahedron.* **2011**, *22*, 1055-1062.

42. Marchand, A.; Maxwell, A.; Mootoo, B.; Pelter, A.; Reid, A., Oxazoline mediated routes to a unique amino-acid, 4-amino-13-carboxy[2.2]paracyclophane, of planar chirality. *Tetrahedron.* **2000**, *56*, 7331-7338.

43. Schneider, J. F.; Falk, F. C.; Fröhlich, R.; Paradies, J., Planar-Chiral Thioureas as Hydrogen-Bond Catalysts. *Eur. J. Org. Chem.* **2010**, *2010*, 2265-2269.

44. Zitt, H.; Dix, I.; Hopf, H.; Jones, P. G., 4,15-Diamino[2.2]paracyclophane, a Reusable Template for Topochemical Reaction Control in Solution. *Eur. J. Org. Chem.* **2002**, *2002*, 2298.

45. Cipiciani, A.; Fringuelli, F.; Mancini, V.; Piermatti, O.; Pizzo, F.; Ruzziconi, R., Synthesis of chiral (*R*)-4-hydroxy- and (*R*)-4-halogeno[2.2]paracyclophanes and group polarizability. Optical rotation relationship. *J. Org. Chem.* **1997**, *62*, 3744-3747.

46. Meyer-Eppler, G.; Sure, R.; Schneider, A.; Schnakenburg, G.; Grimme, S.; Lutzen, A., Synthesis, chiral resolution, and absolute configuration of dissymmetric 4,15-difunctionalized [2.2]paracyclophanes. *J. Org. Chem.* **2014**, *79*, 6679-6687.

47. Rieche, A.; Gross, H.; Höft, E., Über α-Halogenäther, IV. Synthesen aromatischer Aldehyde mit Dichlormethyl-alkyläthern. *Chem. Ber.* **1960**, *93*, 88-94.

48. Zhu, J. L.; Lee, F. Y.; Wu, J. D.; Kuo, C. W.; Shia, K. S., An efficient new procedure for the one-pot conversion of aldehydes into the corresponding nitriles. *Synlett.* **2007**, *2007*, 1317-1319.

49. Sharghi, H.; Sarvari, M. H., Graphite as an efficient catalyst for one-step conversion of aldehydes into nitriles in dry media. *Synthesis.* **2003**, *2003*, 243-246.

50. Zhang, X.; Sun, J.; Ding, Y.; Yu, L., Dehydration of Aldoximes Using PhSe(O)OH as the Pre-Catalyst in Air. *Org. Lett.* **2015**, *17*, 5840-5842.

51. Sengoden, M.; Bhowmick, A.; Punniyamurthy, T., Stereospecific Copper-Catalyzed Domino Ring Opening and sp(3) C-H Functionalization of Activated Aziridines with *N*-Alkylanilines. *Org. Lett.* **2017**, *19*, 158-161.

52. Kreis, M.; Friedmann, C. J.; Bräse, S., Diastereoselective Hartwig-Buchwald reaction of chiral amines with *rac*-[2.2]paracyclophane derivatives. *Chem. Eur. J.* **2005**, *11*, 7387-7394.

53. Markiewicz, J. T.; Wiest, O.; Helquist, P., Synthesis of primary aryl amines through a copper-assisted aromatic substitution reaction with sodium azide. *J. Org. Chem.* **2010**, *75*, 4887-4890.

54. Zhao, G. Y.; Li, H. L.; Lu, C. G.; Xiao, Y. M.; Fang, X. X.; Wang, P. X.; Fang, X. X.; Zhao, K.; Li, X. L.; Yin, S. G.; Xu, J. W.; Yang, W., Di-nuclear nonionic magnetic resonance contrast agents using pyrazinyl linking centers. *RSC Adv.* **2012**, *2*, 6404-6407.

55. Das, S. K.; Frey, J., Regioselective double Boekelheide reaction: first synthesis of 3,6-dialkylpyrazine-2,5-dicarboxaldehydes from DL-alanine. *Tetrahedron Lett.* **2012**, *53*, 3869-3872.

56. Seacome, R. J.; Coles, M. P.; Glover, J. E.; Hitchcock, P. B.; Rowlands, G. J., Planar-chiral imidazole-based phosphine ligands derived from [2.2]paracyclophane. *Dalton Trans.* **2010**, *39*, 3687-3694.

57. Rolla, F., Sodium-Borohydride Reactions under Phase-Transfer Conditions - Reduction of Azides to Amines. *Journal of Organic Chemistry* **1982**, *47*, 4327-4329.

58. Lin, F. L.; Hoyt, H. M.; van Halbeek, H.; Bergman, R. G.; Bertozzi, C. R., Mechanistic investigation of the staudinger ligation. *J. Am. Chem. Soc.* **2005**, *127*, 2686-2695.

59. Palacios, F.; Alonso, C.; Aparicio, D.; Rubiales, G.; de los Santos, J. M., The aza-Wittig reaction: an efficient tool for the construction of carbon–nitrogen double bonds. *Tetrahedron.* **2007**, *63*, 523-575.

60. Garcia, J.; Urpí, F.; Vilarrasa, J., New synthetic “tricks”. Triphenylphosphine-mediated amide formation from carboxylic acids and azides. *Tetrahedron Lett.* **1984**, *25*, 4841-4844.

61. Andrews, K. G.; Denton, R. M., A more critical role for silicon in the catalytic Staudinger amidation: silanes as non-innocent reductants. *Chem. Comm.* **2017**, *53*, 7982-7985.

62. Xie, H.; Ye, Z.; Ke, Z.; Lan, J.; Jiang, H.; Zeng, W., Rh(III)-catalyzed regioselective intermolecular *N*-methylene Csp(3)-H bond carbenoid insertion. *Chem. Sci.* **2018**, *9*, 985-989.

63. Friedmann, C. J.; Ay, S.; Bräse, S., Improved synthesis of enantiopure 4-hydroxy[2.2]paracyclophane. *J. Org. Chem.* **2010**, *75*, 4612-4614.

64. Aly, A. A.; Hopf, H.; Jones, P. G.; Dix, I., Cycloadditions of alpha-(4-[2.2]paracyclophanyl)-*N*-methyl nitrone. *Tetrahedron.* **2006**, *62*, 4498-4505.

65. Koser, G. F.; Wettach, R. H.; Troup, J. M.; Frenz, B. A., Hypervalent Organoiodine - Crystal-Structure of Phenylhydroxytosyloxyiodine. *Journal of Organic Chemistry* **1976**, *41*, 3609-3611.

66. Schneider, J. F.; Frohlich, R.; Paradies, J., Synthesis of Enantiopure Planar-Chiral Thiourea Derivatives. *Synthesis.* **2010**, *2010*, 3486-3492.

67. Nehra, A.; Hinge, V. K.; Rao, C. P., Phenylene-diimine-capped conjugate of lower rim 1,3-calix[4]arene as molecular receptor for Mg^{2+} via arm conformational changes followed by aggregation and mimicking the species by molecular mechanics. *J. Org. Chem.* **2014**, *79*, 5763-5770.

68. Wang, Q.; Wilson, C.; Blake, A. J.; Collinson, S. R.; Tasker, P. A.; Schroder, M., The one-pot halomethylation of 5-substituted salicylaldehydes as convenient precursors for the preparation of heteroditopic ligands for the binding of metal salts. *Tetrahedron Lett.* **2006**, *47*, 8983-8987.

69. Braddock, D. C.; MacGilp, I. D.; Perry, B. G., Improved Synthesis of (±)-4,12-Dihydroxy[2.2]paracyclophane and Its Enantiomeric Resolution by Enzymatic Methods: Planar Chiral (*R*)- and (*S*)-Phanol. *J. Org. Chem.* **2002**, *67*, 8679-8681.

6. Additional Information

This section includes the ^{1}H and ^{13}C NMR spectroscopic information of the previously unreported compounds synthesized in this project.

^{1}H NMR of 4-(benzylideneamino)[2.2]paracyclophane ($CDCl_3$)

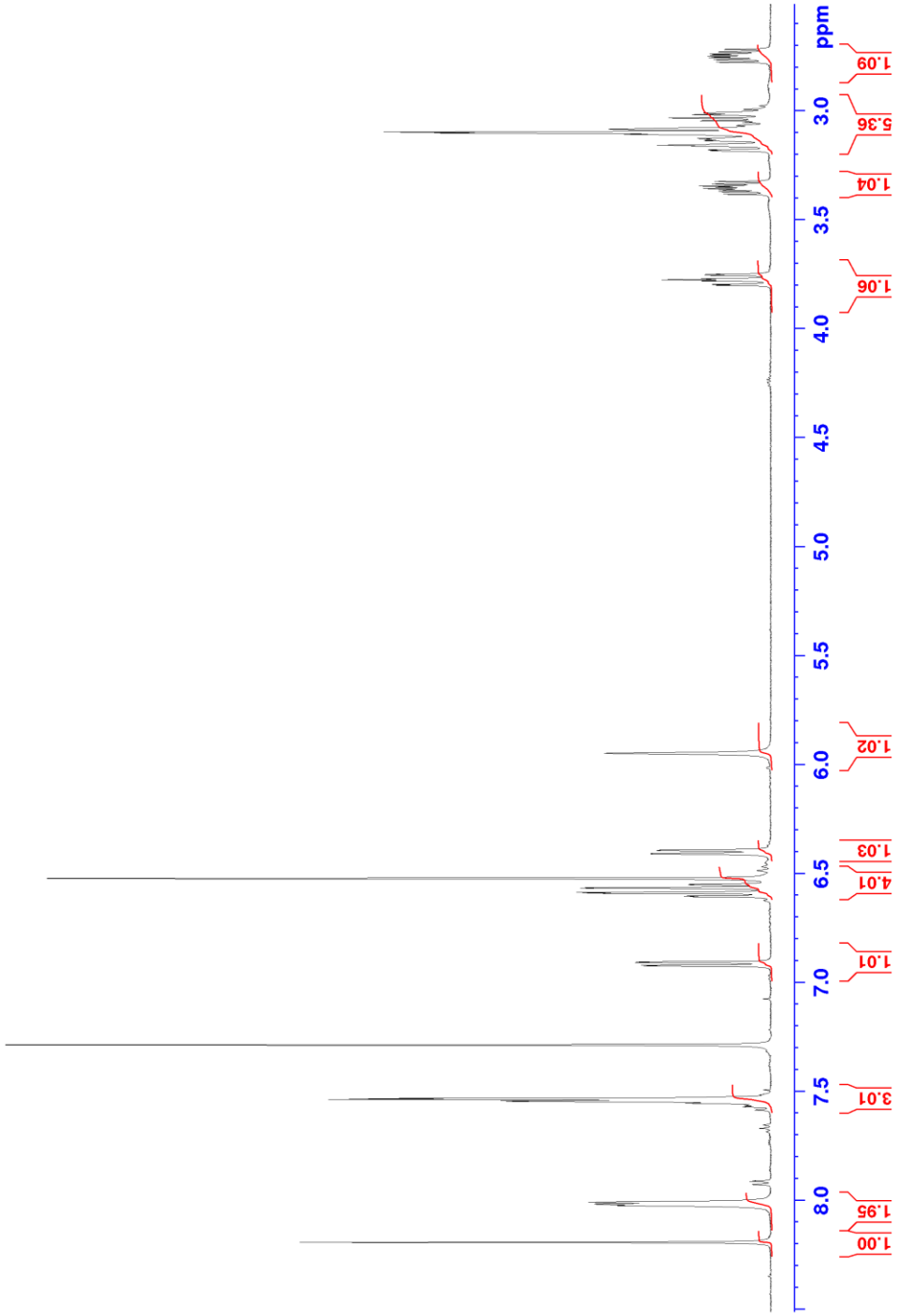

^{13}C NMR of 4-(benzylideneamino)[2.2]paracyclophane ($CDCl_3$)

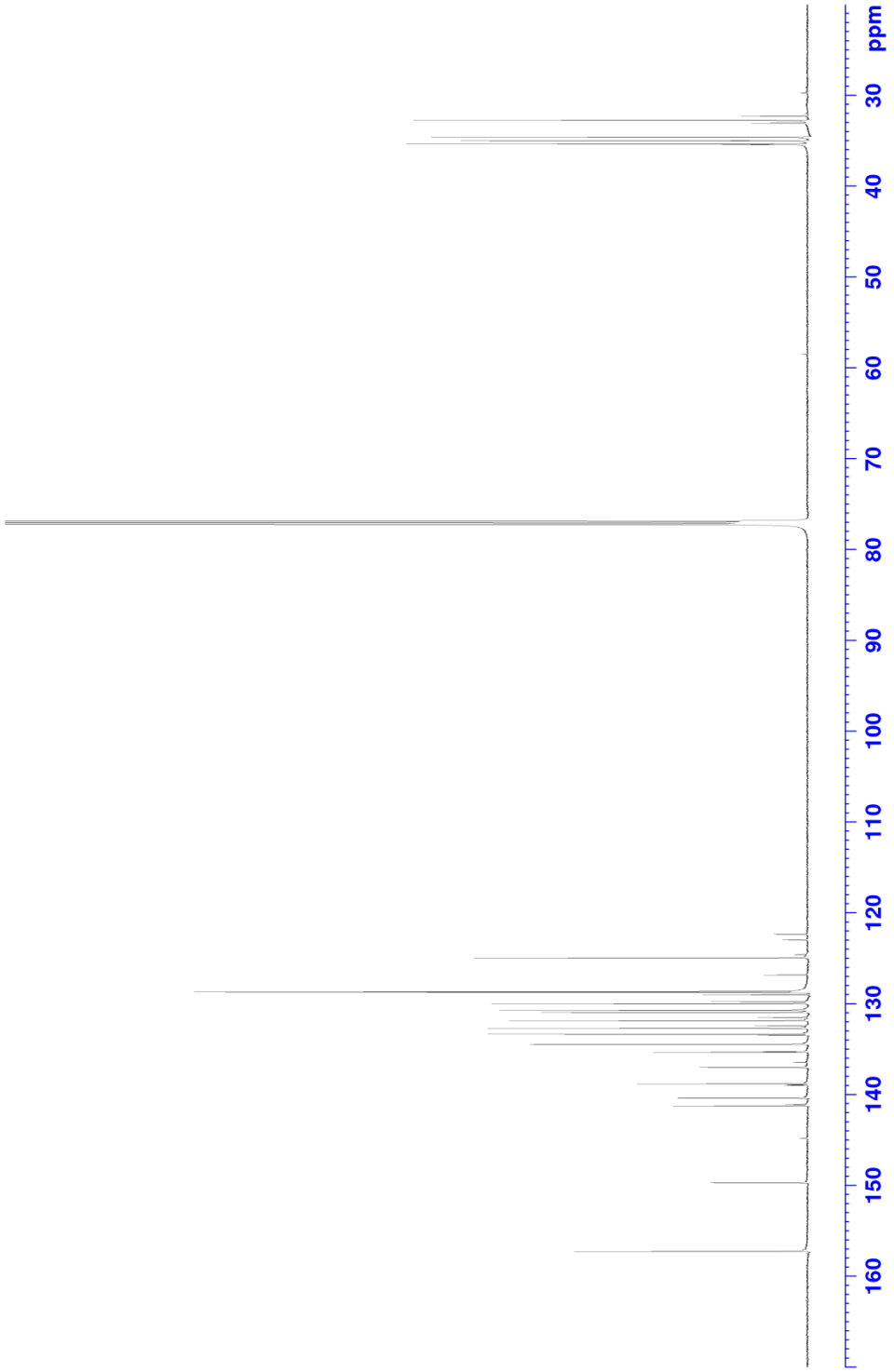

^{1}H NMR of (E)-5-(*tert*-butyl)-3-(benzyl[2.2]paracyclophan-4-yl methylamino)-2-hydroxy benzaldehyde ($CDCl_3$)

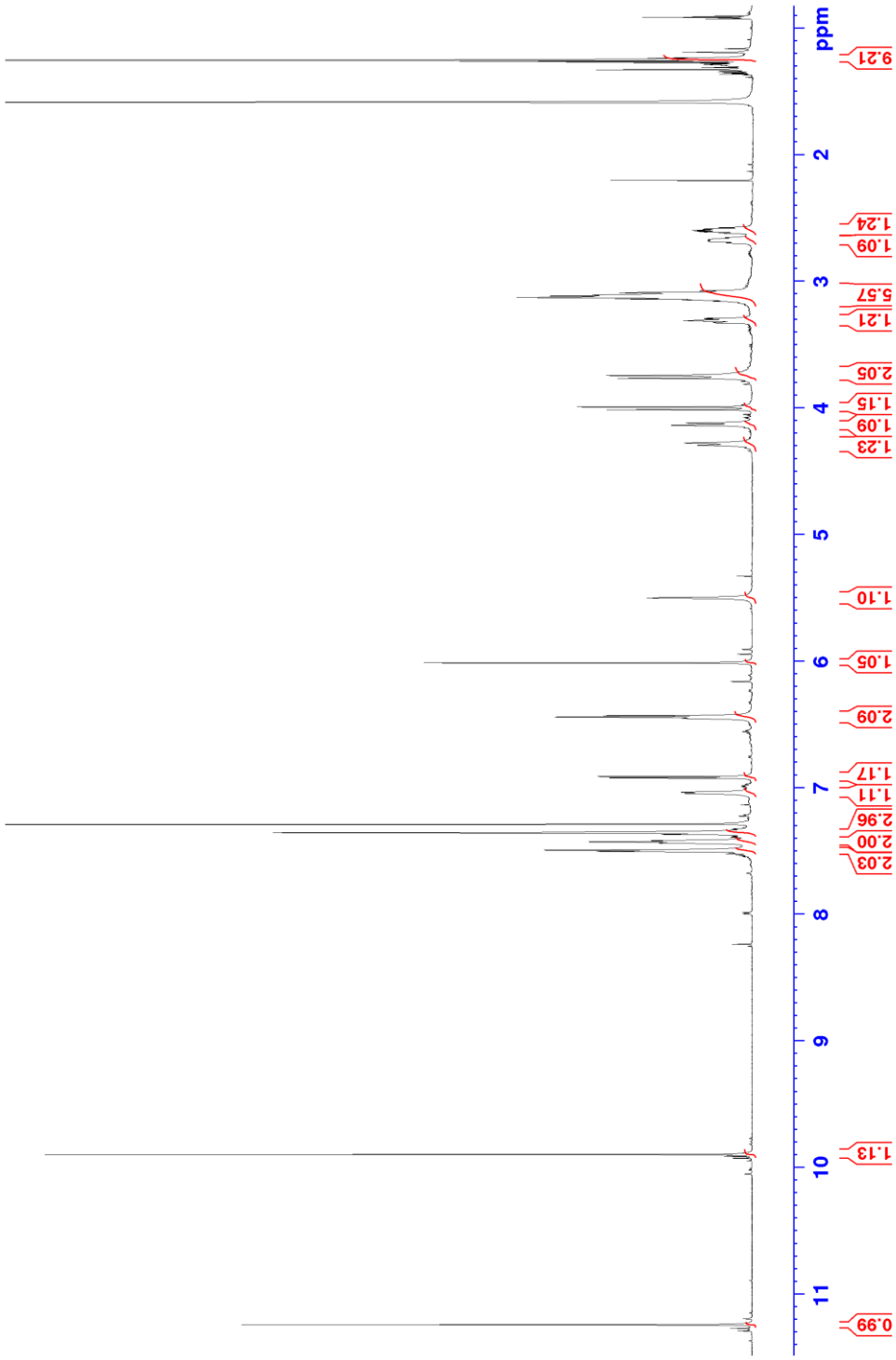

^{13}C NMR of (E)-5-(*tert*-butyl)-3-(benzyl[2.2]paracyclophan-4-yl methylamino)-2-hydroxy benzaldehyde ($CDCl_3$)

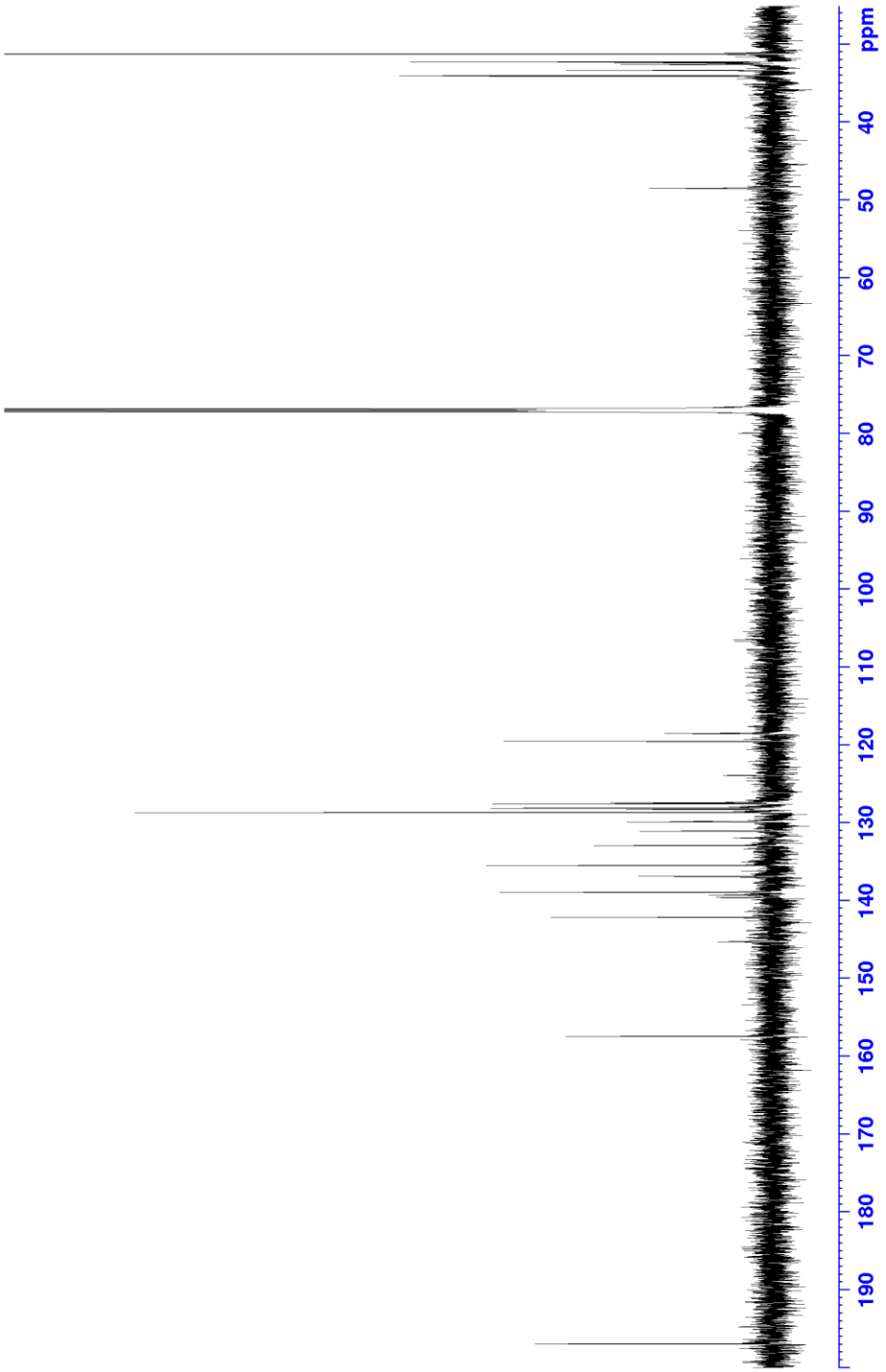

^{1}H NMR of (E)-5-(*tert*-butyl)-3-(benzyl[2.2]paracyclophan-4-yl methylamino)-2-hydroxy benzaldehyde oxime ($CDCl_3$)

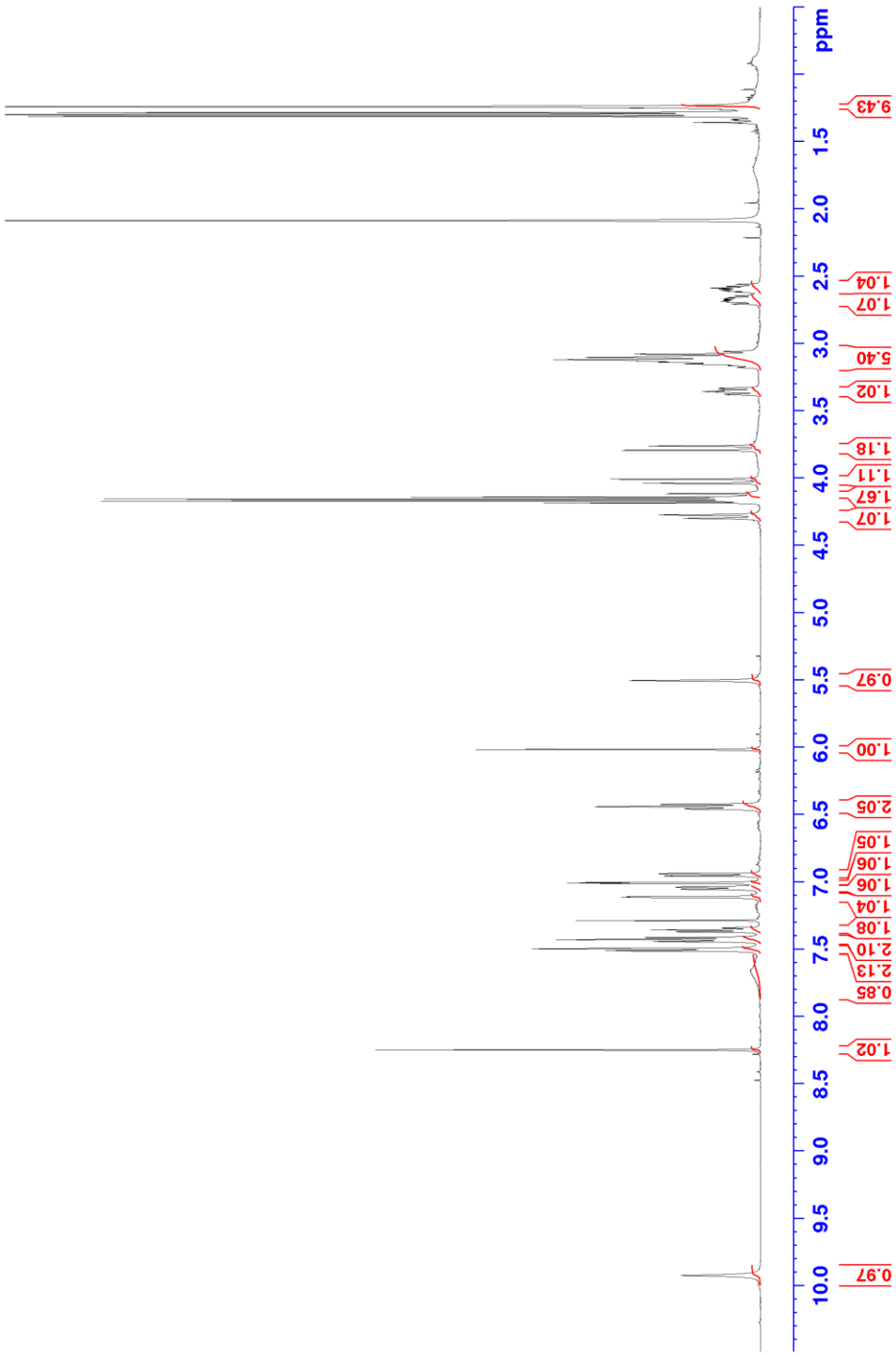

^{13}C NMR of (E)-5-(*tert*-butyl)-3-(benzyl[2.2]paracyclophan-4-yl methylamino)-2-hydroxy benzaldehyde oxime ($CDCl_3$)

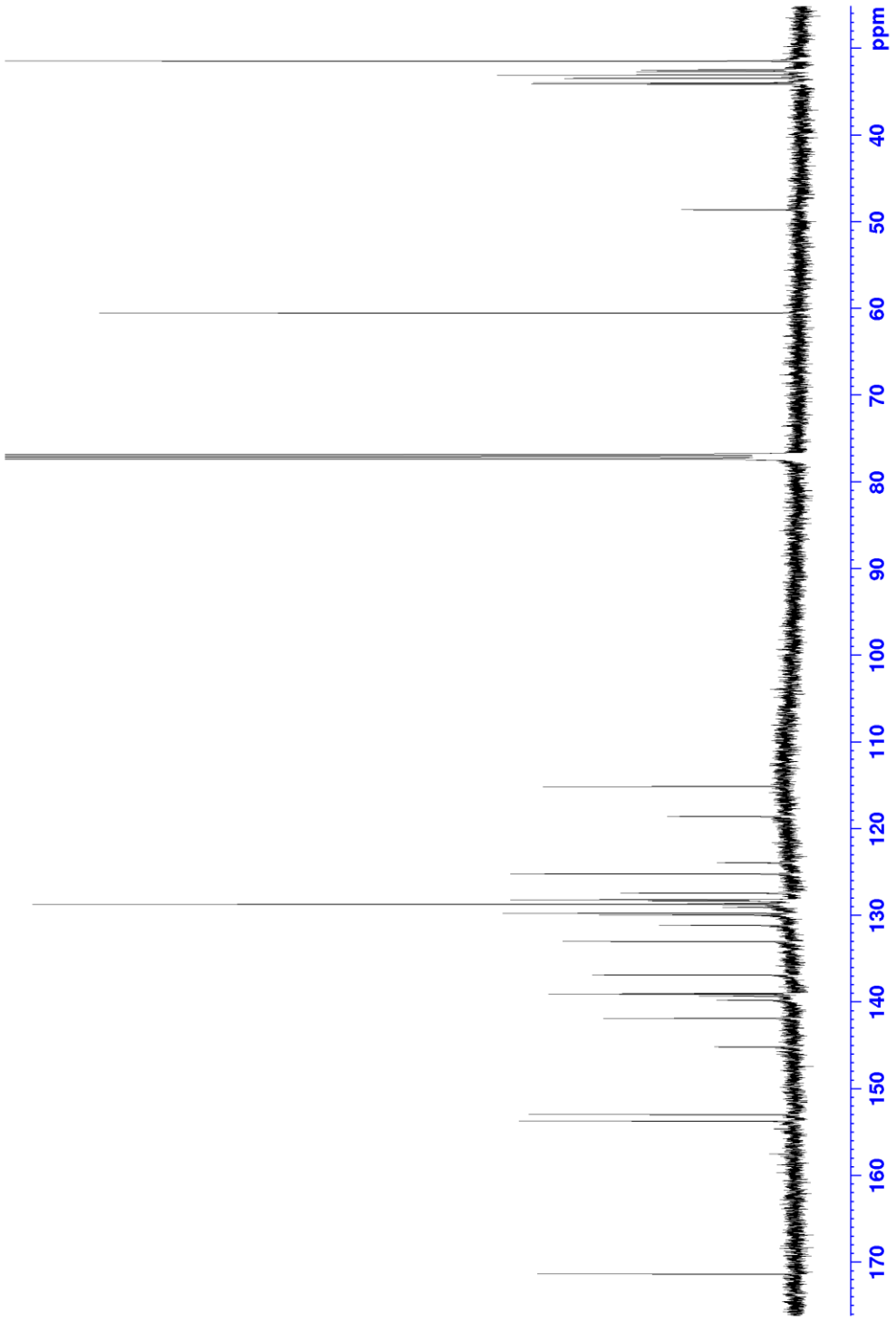

^{1}H NMR of pyrazine-2,5-diylbis(methylene) bis(tosylate) ($CDCl_3$)

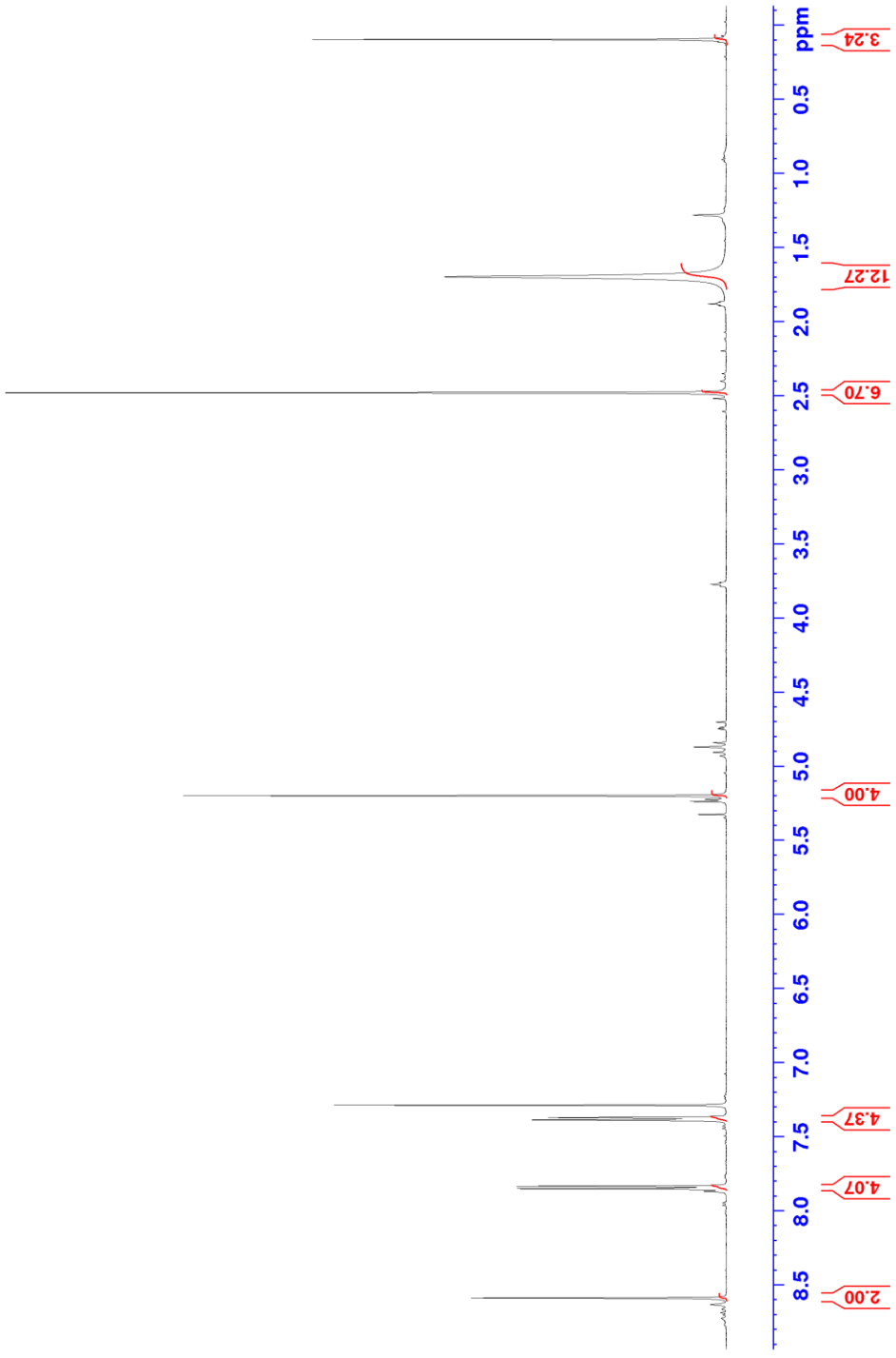

^{13}C NMR of pyrazine-2,5-diylbis(methylene) bis(tosylate) ($CDCl_3$)

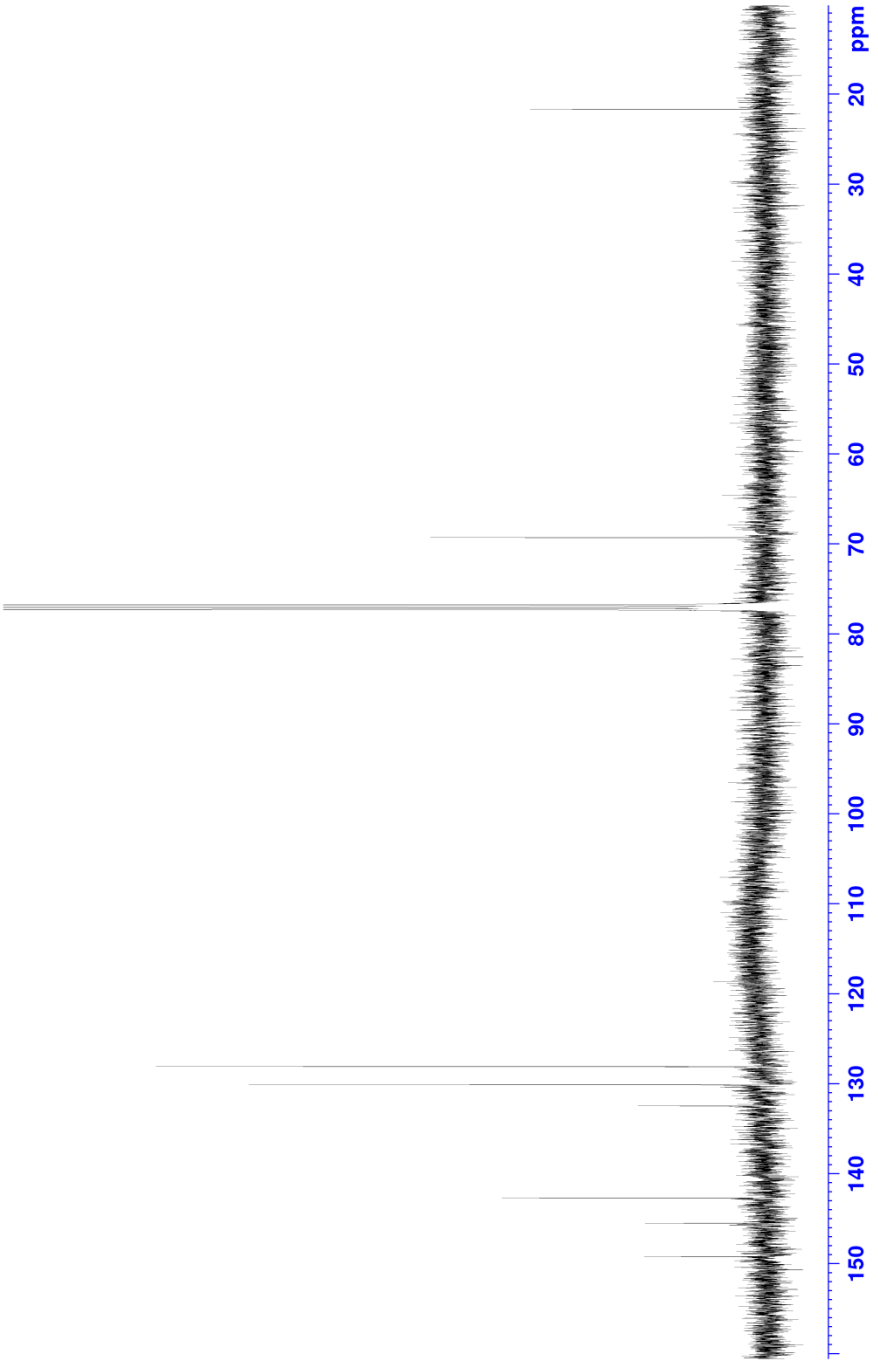

^{1}H NMR of 2,5-di(azidomethyl)pyrazine ($CDCl_3$)

^{1}H NMR of 2,5-di(azidomethyl)pyrazine ($CDCl_3$)

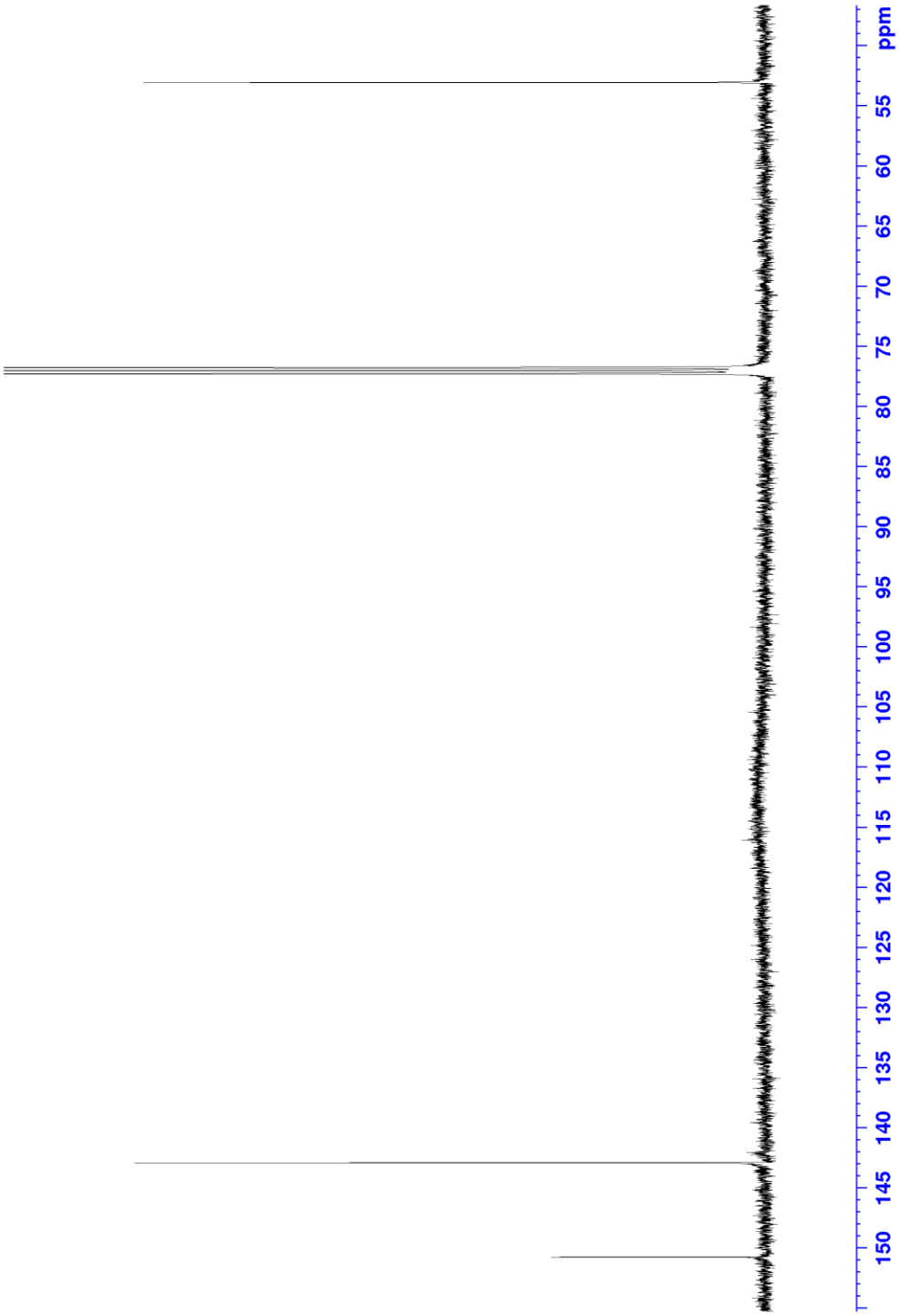

^{1}H NMR of 2,5-di(aminomethyl)pyrazine (D_2O)

^{1}H NMR of ((E)-2,5-bis((5-*tert*-butyl-2-hydroxybenzylideneamino)methyl))pyrazine ($CDCl_3$)

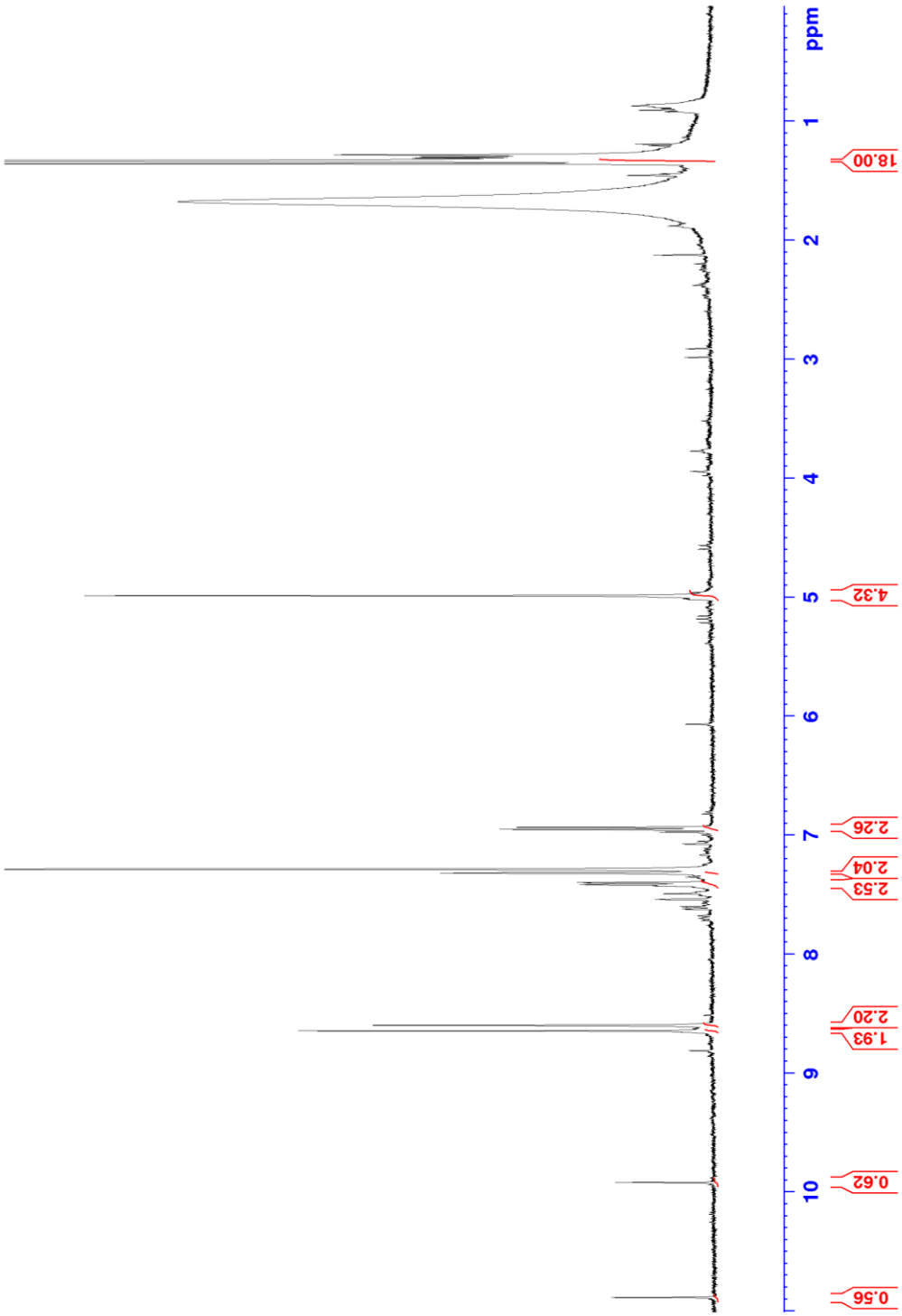

^{13}C NMR of ((E)-2,5-bis((5-*tert*-butyl-2-hydroxybenzylideneamino)methyl))pyrazine ($CDCl_3$)

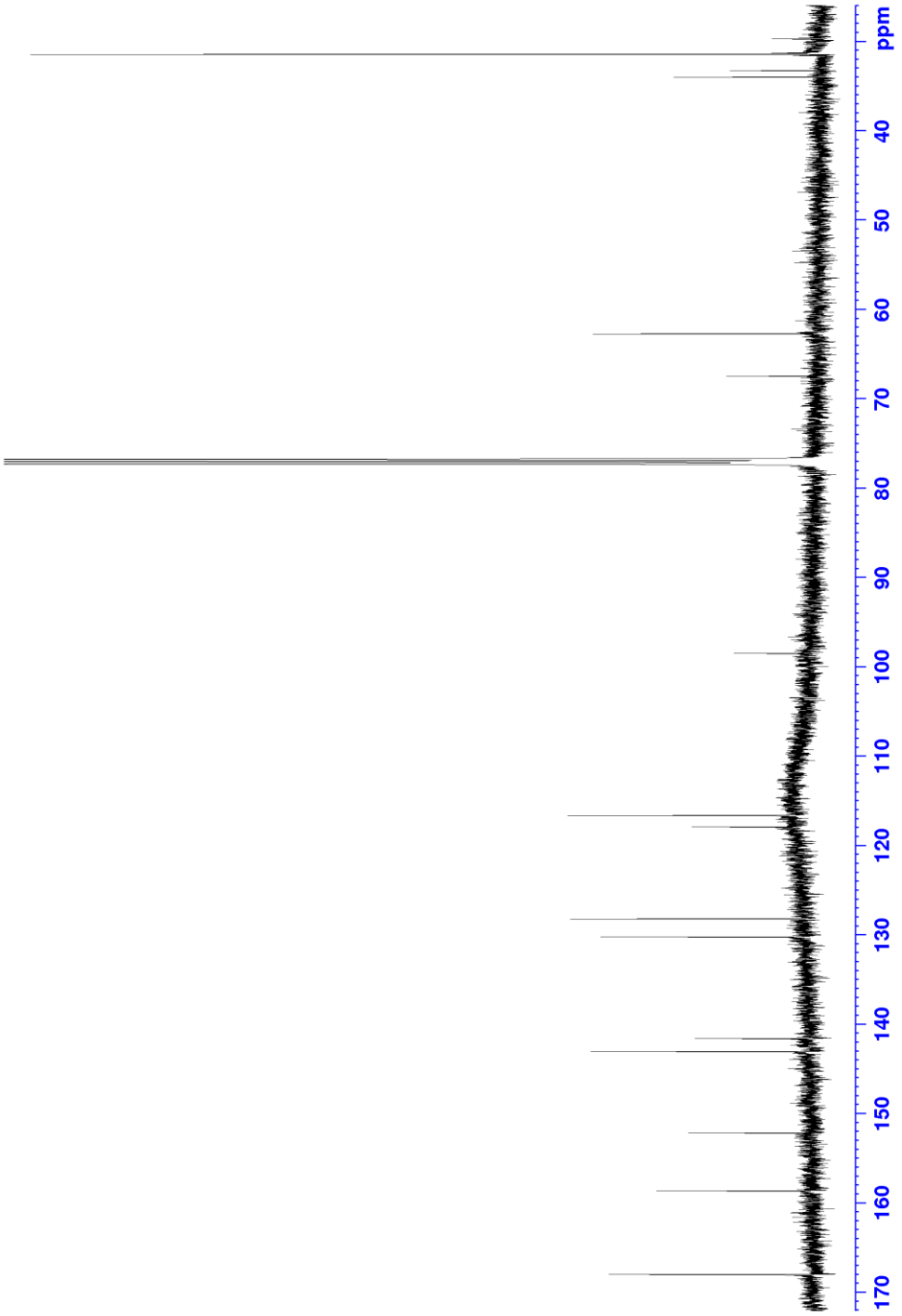

^{1}H NMR of (E)-2,5-bis((pyridine-2-ylmethyleneamino)methyl)pyrazine ($CDCl_3$)

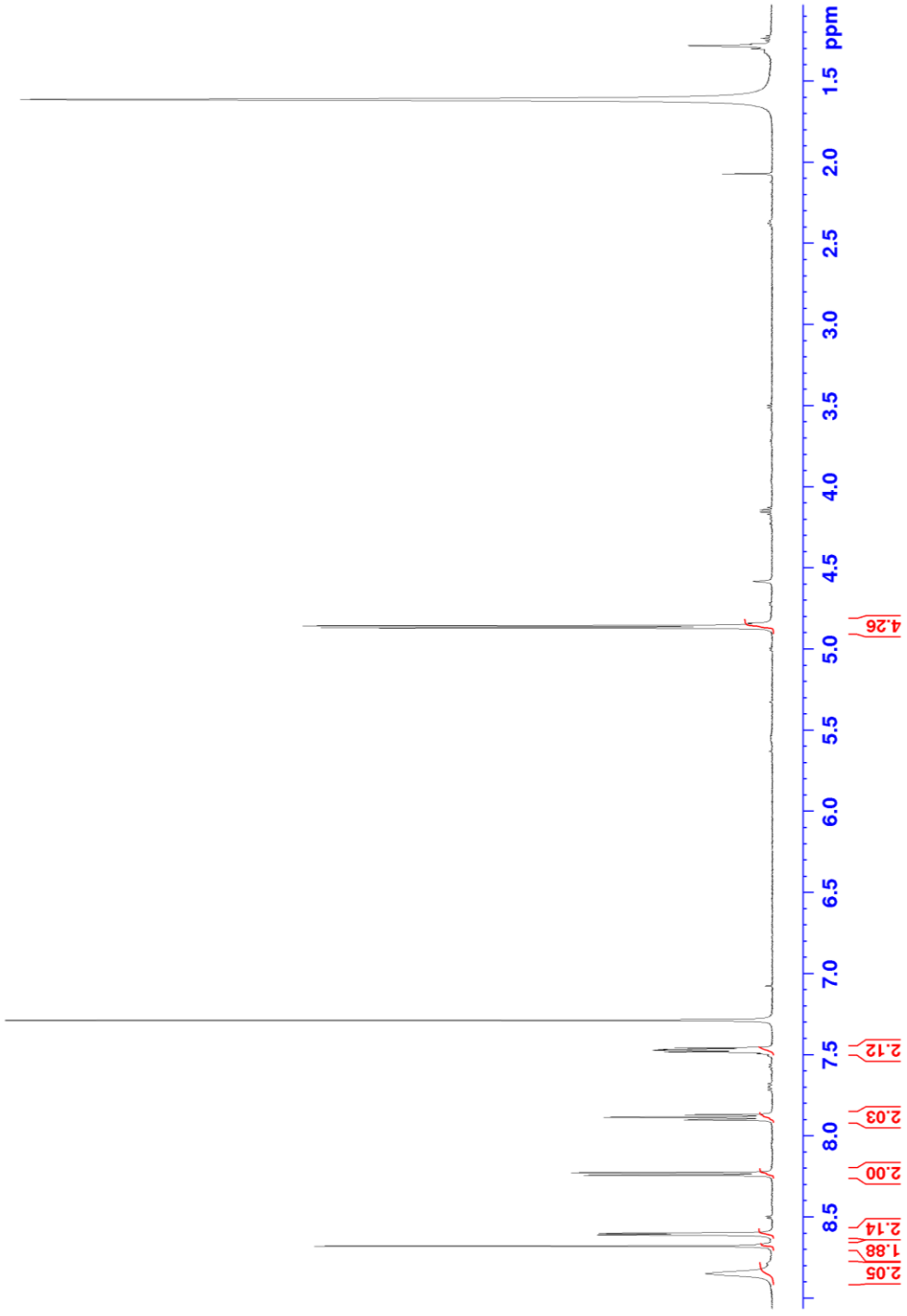

^{13}C NMR of (E)-2,5-bis((pyridine-2-ylmethyleneamino)methyl)pyrazine ($CDCl_3$)